DEPARTMENT OF BIOLOGICAL AND ECOLOGICAL SCIENCES (DEB)

XVII PhD COURSE IN GENETICS AND CELLULAR BIOLOGY

BIO/11

Importance of yeast metacaspase in metabolic pathways and in programmed cell death: an integrated "omics" approach

Tesi di dottorato di:

Dott.ssa Valentina Longo

Coordinatore del corso

Prof. Giorgio Prantera

Tutore

Prof. Lello Zolla

Index

ABSTRACT

This PhD work focuses on the effect of metacaspase gene deletion on W303-1B *Saccharomyces cerevisiae* metabolism and programmed cell death.

In the first section, we have analyzed the proteome and metabolome of wild type and *Δyca1* cells to better understanding physiological role of YCA1. Our results increased the knowledge about cellular process and proteins whose roles and function depend on YCA1 in yeast. The data obtained show a role of YCA1 in the modulation of central carbon metabolism as well as amino acid and nucleotide metabolism. YCA1 deletion appears to down-regulate glycolysis, TCA cycle and alcoholic fermentation as compared with WT cells. *Δyca1* cells also showed a down-regulation of PPP and an accumulation of pyruvate, correlated with higher levels of certain amino acids found in these cells. Accordingly, there is a decrease in protein biosynthesis and protein transport/folding, and accumulation of various stress response proteins like Ahp1p, which possibly provides these cells with a better protection against stress.

In the second part of this work, we have focused our attention on the apoptotic role of metacaspase, studying proteomic and metabolomic state during acetic acid-induced programmed cell death in wild type and *Δyca1* cells.

Although a common decrease in glycolytic cycle enzymes and shift towards the pentose phosphate pathway happened in both cases, WT cells seem to be more affected. Moreover, it could be in relation to the presence of metacaspases and its biochemical function, this allowed us to conclude that metacaspase could has a key role for the shift from glycolysis to pentose phosphate pathway during death.

We have also discussed a pro-apoptotic mechanism YCA1-indipendent that involve FAS2 protein. The activation of Ceramides (C18, C16, and 20), in our opinion, can trigger apoptosis. It is likely that the gene has a role on FAS2 regulation.

Furthermore, this study emphasized the central role of metacaspase gene in proteolysis, because its presence or absence influence the expression of ubiquitin proteasome pathway through the modulation of crucial proteins.

RIASSUNTO

Questo lavoro di dottorato si concentra sullo studio degli effetti della delezione del gene della metacaspase di lievito sui processi metabolici e sulla morte cellulare programmata di *Saccharomyces cerevisiae* W303-1B.

Nella prima sezione, abbiamo analizzato il proteoma e il metaboloma di cellule wild type e cellule *Δyca1* per comprendere meglio il ruolo fisiologico di YCA1. I nostri risultati hanno aumentato la conoscenza dei processi e delle proteine i cui ruoli e funzioni dipendono YCA1. I dati ottenuti mostrano un ruolo YCA1 nella modulazione del metabolismo centrale del carbonio, così come del metabolismo aminoacidico e nucleotidico. La delezione di YCA1 sembra down-regolare la glicolisi, il ciclo di Krebs e la fermentazione alcolica rispetto a quello che avviene nelle cellule wild type. Le cellule *Δyca1* hanno mostrato un down-regulazione del ciclo dei pentosi fosfato e un accumulo di piruvato, correlata con livelli più elevati di alcuni aminoacidi presenti in queste cellule. Di conseguenza, vi è una diminuzione della biosintesi delle proteine e di proteine di trasporto/folding, e l'accumulo di proteine di risposta allo stress come Ahp1p, che fornisce a queste cellule una migliore protezione contro lo stress.

Nella seconda parte di questo lavoro, abbiamo focalizzato la nostra attenzione sul ruolo apoptotico della metacaspase, studiando lo stato proteomico e metabolomico durante la morte cellulare programmata indotta da acido acetico cellule wild type e cellule *Δyca1*.

Sebbene si abbia una diminuzione degli enzimi del ciclo glicolitico e uno spostamento verso la via dei pentosi fosfati in entrambi i casi, le cellule WT sembrano essere più proni a questo cambiamento. Siccome questo evento potrebbe essere in relazione con la presenza della metacaspasi e la sua funzione biochimica, questo permette di concludere che la metacaspase potrebbe ha un ruolo chiave per il passaggio dalla glicolisi alla via dei pentosi fosfati durante la morte.

Abbiamo anche ipotizzato un meccanismo pro-apoptotico YCA1-indipendente che coinvolge la proteina FAS2. L'attivazione di ceramidi (C18, C16, e 20), a nostro avviso, può innescare l'apoptosi. È probabile che il gene abbia un ruolo nella regolazione di FAS2.

Inoltre, questo studio ha sottolineato il ruolo centrale del gene della metacaspase nella proteolisi, perché la sua presenza o assenza influenza l'espressione del pathway di ubiquitinazione attraverso la modulazione di proteine chiave di questo meccanismo.

Aim of the thesis

The yeast *Saccharomyces cerevisiae,* unlike mammalian, expresses only one member of the caspase-like proteins, called metacaspase, encoded by the YCA1 gene.
Deletion of this gene imply several change in cell metabolism and in death pathways, suggesting that this protein have both non-death roles and apoptotic function.
During programmed death cell (PCD) , the rate of survival of knock-out cells are higher of wild type cells. When metacaspase is not presence, a different PCD occurs. These pathway is cytochrome c independent.
Is not clear, what happen in cell as a result of YCA1 gene deletion.

In my PhD thesis, we have combined proteomics and metabolomics data to value:

1. In the first section, the implication of metacaspase in carbohydrate, amino acidic and nucleotide metabolism, in stress response and in protein biosynthesis, analyzing wild type cells and YCA1-knock-out cells.

2. In the second part, the role of Yca1p in yeast programmed death cell induced by adding of acetic acid. We have studies proteome and metabolome of two cell genotype, before and after the induction of acetic acid.

INTRODUCTION

1.1 *Saccharomyces cerevisiae* as a study model

Saccharomyces cerevisiae represent a valid model in several studies focused on superior eukaryote physiology and pathology. This is true in particular for the study of human diseases. In fact, the use of yeast for human physiopathology studies has various benefit:

a. It has a structure more similar to superior eukaryote organism: it hold all intracellular organelles like the other eukaryote cells, including mitochondria (Botstein, 1991).

b. Despite this important aspect, it has some advantage typical of unicellular organism. First of all, it grows very quickly in minimal medium, so its study is economic and rapid. Furthermore, there are two forms in which *S.cerevisiae* can survive and grow: haploid and diploid. Because of this, it's possible to study both dominant and recessive mutations.

c. Yeast is first eukaryotic organism to have its genome completely sequenced and published (Goffeau et al., 1996). *Genome project* have identified 6300 genes in *S.cereviasiae*: this number is 1/5 of human genes (Venter et al., 2001). Yeast genome is very compact with few introns. Comparative analysis of amino acidic sequences obtained by *S.cerevisiae* genome sequencing have suggested that more basic function of eukaryote are performed by ortholog proteins. For this reason, protein analysis conducted on yeast can be useful to better understand superior eukaryote. In particular, is more interesting that 46% of human proteins have homolog proteins in yeast. There are proteins involved in replication, DNA repair, transcription and traslation, more metabolic enzyme, transport proteins and proteins of mitochondrial biogenesis (Venter et al., 2001). The knowledge of genome and genetic engineering have allowed to complete large-scale analysis on yeast genome and proteome (Foury and Kucej, 2001). Thanks to this, an international

consortium have constructed 5943 strains knock-out for a specific gene (Winzeler et al., 1999).

Yeast has been widely used to study biological processes involved in cell stress, aging and cell death. In particular, after the discovery of yeast apoptosis, in 1997, by Madeo and coworkers (Madeo et al., 1997) several studies has led to identification multiple orthologs of crucial mammalian apoptotic proteins, delineating conserved cell death pathaways (Carmona-Gutierrez et al., 2010).

S.cerevisiae is also the only known organism in which mitochondrial genetic transformation is possible (Tuppen et al., 2010). This is important to evaluate the role of mitochondria in different cell processes and makes yeast a valid experimental platform for analyzing both cell response to mitochondrial dysfunction and mitochondrial role in pro-death and pro-survival signaling pathways. The best known intracellular pathway to mitochondrial dysfunctions are programmed cell death (PCD).

For all these reasons, *S.cerevisiae* was named "honorary mammal" (Resnick et al., 2000).

1.2 Apoptosis, caspases and cancer

Mammalian apoptosis and yeast PCD share a variety of features including reactive oxygen species (ROS) production, protease activity and a major role played by mitochondria (Guaragnella et al., 2012).

Alterations in mitochondrial structure and function, during PCD, depend on a variety of specific triggers, respiratory or fermentative growth conditions, and on overall cell metabolism.

In addition to their role as cell powerhouse mitochondria are key organelles in the processes deciding about cell life or death that are crucial for tumor cell growth and survival, as well as for tumor cell ability to metastasize. In fact, alterations in mitochondrial structure and functions have long been observed in cancer cells. Thus targeting mitochondria as an anticancer therapeutic strategy has gained momentum recently (Giannattasio et al., 2013).

Since yeast shares with cancer cells the metabolic features identified as the underlying causes of the Warburg effect (shift from aerobic respiration to glycolysis and

lactic acid fermentation) (Ruckenstuhl et al., 2009; Diaz-Ruizetal et al., 2010), it is a suitable model organism to identify cell compounds responsible for tumorigenesis for development of targeted cancer drugs.

Chromatin condensation, nuclear DNA fragmentation and phosphatidylserine externalization onto the cell surface are general markers of both mammalian and yeast PCD cells. A characteristic feature of mammalian apoptosis is the activation of caspases, proteases that initiate and execute cell death through degradation of cell components. Deregulations in the expression or activity of these proteases can lead to the development of several human apoptotic diseases, including cancer and neurodegenerative disorders. The high complexity of mammalian caspase-signalling pathways led several research groups to investigate simpler eukaryotic systems as complementary cell models (Pereira et al., 2012). Yeast contains only one gene homolog of caspases, named YCA1, encoding for yeast metacaspase (Madeo et al., 2002) which has substrate specificity different from caspases (Wilkinson and Ramsdale, 2011). YCA1 shares structural homology and mechanistic features with mammalian caspases, but major differences in the primary cleavage specificity have lead to the questioning of its classification as a 'true' caspase. However, although mammalian caspases specifically cleave their substrates after aspartic acid residues, metacaspases specifically cleave substrates after an arginine or lysine (basic residues) (Vercammen et al., 2004). Furthermore, yeast PCD mechanisms occurring both in YCA1-dependent and –independent manner as well as the role of other proteases in yeast PCD remain to be established (Madeo et al., 2009; Wilkinson and Ramsdale et al., 2011).

The study of yeast metacaspase and the role of mitochondria in *S.cerevisiae* PCD pathway can be help to development of targeted cancer drugs.

1.3 Yeast Programmed Cell Death

In yeast, like in mammal cells, all three major PCD (apoptosis, autophagy and necrosis) happen: these can be activated in response to different intra- and extracellular stress.

Autophagy refers to a group of processes that involve degradation of cytoplasmic components including cytosol, macromolecular complexes, and organelles, within the vacuole or the lysosome of higher eukaryotes (Reggiori et al., 2013). Many

aspects of autophagy are conserved from yeast to human; in particular, this applies to the gene products mediating these pathways as well as some of the signaling cascades regulating it, so that the information we relate is relevant to higher eukaryotes.

Necrosis was long regarded as an accidental cell death process resulting from overwhelming cellular injury such as chemical or physical disruption of the plasma membrane. Really, mitochondria, aging and a low pH are positive regulators of this process while cellular polyamines (e.g. spermidine) and endonuclease G as well as homeostatic organelles like the vacuole or peroxisomes are potent inhibitors of necrosis. Physiological necrosis may stimulate intercellular signaling via the release of necrotic factors that promote viability of healthy cells and, thus, assure survival of the clone. Together, the data obtained in yeast argue for the existence of a necrotic program, which controls longevity and whose physiological function may thus be aging (Einsenberg et al., 2010).

In the last decade, yeast apoptosis has been more investigated than the other two programmed deaths. It has been shown most of morphological and biochemical hallmarks of mammalian apoptosis, such as phosphatidylserine externalization to the outer layer of the plasma membrane, DNA fragmentation, chromatin condensation, ROS production and involvement of specific pro-apoptotic proteins, including cytochrome c, Aif1p and BH3-containing protein (Ludovico et al., 2002; Wissing et al., 2004; Buttner et al., 2011).

These similar events between unicellular yeast and mammalians are due to conserved suicide programme during evolution in which there are an high coordination. In fact, yeast population can be seen like a multicellular community of interacting individuals, rather than a group on single individual that do not communicate among each other (Carmona-Gutierrez et al., 2010).

It’s known that the altruistic death of single cell in promoting the long-term survival of population is very common in older and damaged cells during aging (Laun et al., 2001; Herker et al., 2004; Vachova and Palkova, 2005), in infertile or damaged cells during failed mating (Severin and Hyman, 2002) and in diploid cells during meiosis (Ahn et al., 2005, Knorre et al., 2005).

For individual cells or uniform cell suspension can be used the term "phenoptosis", but also the term "apoptosis" is generally related both phenoptosis and death of individual cells in biofilms and cell colonies (Sukhanova et al., 2012).

Numerous stimuli can induce yeast apoptosis (**Figure 1**). A wild-type yeast population promotes its own long-term survival and spreading of the clone by eliminating infertile or otherwise damaged cells (failed mating), or genetic recombinants not adapted to the surroundings (meiosis and sporulation). In addition, death of old cells within the colony center feeds the young cells at the colony margin (colony differentiation). The death of chronologically old cells preserves resources, releases nutrients, and allows adaptive regrowth (chronological aging), whereas replicatively old cells die for the good of young cells, which inherit the undamaged cellular material upon cellular division (replicative aging). However, death in the population may also be triggered by toxins from either non-clonal enemy strains in competition for nutrients (killer strain attack), or higher eukaryotes in their defense against pathogenic fungi (plant or animal attack). In these cases of external cell death induction, the endogenous apoptotic machinery is hijacked (Carmona-Gutierrez et al., 2010).

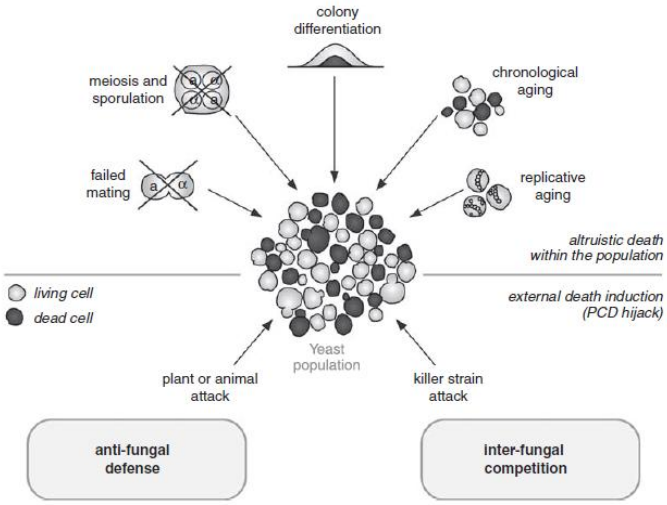

Figure 1. Physiological scenarios of yeast apoptosis

Such stimuli can be provided externally in the form of chemical or physical stress, via heterologous expression of human proapoptotic proteins (exogenous triggers)

or by the yeast cells themselves, as part of lethal signal transduction pathways (endogenous triggers) (Carmona-Gutierrez et al., 2010).

External stresses reported to induce apoptosis in yeast can be physical agents like UV radiation or heat or chemical agents like ethanol, hypochlorous acid, high concentration of salt and the most commonly used triggers hydrogen perodixe (H_2O_2) and acetic acid (AA).

Yeast PCD can also be caused by natural signal substance such as α-factor pheromone produced by α-type haploid cells of *S.cerevisiae* (Severin and Hyman et al., 2002).

Instead, endogenous trigger of cell death in yeast include defects in chromatin cohesion, mRNA stability and ubiquitination (Mazzoni et al., 2005; Ren et al., 2005; Bettiga et al., 2006). Furthermore, several cellular processes like inositol starvation, lipid toxicity and the inhibition of N-glycosylation have been connected to ER-stress associated cell death (Austriaco, 2012). Yeast secretes toxins that induce apoptosis in competing yeast cells in the fight for nutrients (Reiter et al., 2005).

Finally, the yeast death can be provoked by superior eukaryotes (plants and animals) as a result of activation of immunological defense against pathogenic fungi (Narasimhan et al., 2005; Morton et al., 2007).

Several mitochondrial proteins are involved in yeast PCD and in its regulation. In particular, in this complex mechanism play an important role proteins involved in electronic transfer along the respiratory chain and oxidative phosphorylation, in mitochondrial dynamics and permeabilization and in trafficking from mitochondria to cytosol and vice versa.

Yeast were reported to externalize phosphatidylserine on the outer leaflet of their plasma membrane (Martin et al., 1995), and to undergo DNA degradation and chromatin condensation (Clifford et al., 1996), all characteristics of apoptotic mammalian cells (Madeo et al. 1997; Madeo et al., 1999). Yeast also encode orthologs of the DNA endonuclease EndoG that is involved in cell death of mammals and *Caenorhabditis elegans* (Ikeda and Kawasaki, 2001; Li et al., 2001; Parrish et al., 2001; Wang et al., 2002), and mammalian Beclin, a Bcl-2-interacting factor that is homologous to the autophagy regulator Apg6/Vps30 in yeast (Liang et al., 1999). Despite these analogies, yeast appear to lack the Bcl-2 family proteins and caspases that

constitute the core cell death machinery in mammals. However, the cell death-promoting function of plant and yeast metacaspases fuel the idea that yeast possess a protease-mediated death pathway analogous to mammals (Madeo et al., 2002b; Hoeberichts et al., 2003; Suarez et al.,2004).

Yeast apoptosis shares several processes with mammalian intrinsic apoptotic pathway, such as ROS acting as second messengers in the death cascade, the alteration of mitochondrial outer membrane permeability and the release of mitochondrial apoptogenic factors (Eisenberg et al., 2007; Pereira et al., 2008; Guaragnella et al., 2012).

Reactive oxygen species which are formed in any organism exposed to molecular oxygen, appear to be crucial players in apoptosis (Ghibelli et al., 1995). ROS or H_2O_2 can act as primary triggers of apoptosis (Hockenbery et al., 1993; Kane et al., 1993; Greenlund et al., 1995; Slater et al., 1995). The anti-apoptotic effect of Bcl-2 appears to be at least partly due to its antioxidant properties (Saraiva et al., 2006). These results allowed the identification of ROS production as a key cellular event common to the known scenarios of apoptosis in yeast and animal cells (Madeo et al., 1999).

However, many questions regarding the role of mitochondrial proteins in apoptotic process, as well as the regulation of yeast apoptotic pathway still need to be answered. In particular, is not clear if the release of cytochrome c (cyt c) is due to damaged mitochondria and what is the role of the released cyt c *en route* to yeast PCD. There is no evidence of the existence of a functional homolog of the apoptosome in yeast, accordingly, yeast cyt c is unable to activate caspases in cytosolic extracts from metazoan cells, so its role in PCD remains to be clarified (Kluck et al., 2000; Huttemann et al., 2011; Bender et al., 2012).

1.4. Acetic acid-induced PCD in yeast

Acetic acid is one of most used chemical agents to induce PCD.

Acetic acid is a normal end product of the alcoholic fermentation carried out by *S.cerevisiae*. This compound is not metabolized by glucose-repressed yeast cells and enters the cell in the undissociated form by simple diffusion. Inside the cell, the acid dissociates and if the extracellular pH is lower than the intracellular pH, this will lead to

intracellular acidification, anion accumulation and inhibition of the metabolic cell activity (Leão and van Uden, 1986; Cássio et al., 1987; Pampulha and Loureiro, 1989).

Under certain conditions, acetic acid compromises cell viability and ultimately results in two types of cell death, high and low enthalpy (Pinto et al., 1989). However, the process by which the yeast cell dies when injured by acetic acid is unknown (Ludovico et al., 2001). Since acetic acid is a normal product of glucose fermentation in *S.cerevisiae,* is important validate a model of this death and investigate on cell components and mechanisms involved in yeast PCD triggered by acetic acid (AA-PCD).

Ludovico and collaborates (Ludovico et al., 2001) have shown that acetic acid (20–80 mM, pH 3.00) induces death in exponential cells of *S.cerevisiae* which displays the most common PCD hallmarks:

- Chromatin condensation along the nuclear envelope
- Exposure of phophatidylserine on the surface of cytoplasmic membrane
- Occurrence of DNA strand breaks

Mitochondria are important players in AA-PCD. Regarding the mitochondrial pathway, two main events have been proposed as integral control elements in the cell's decision to dye: the release of apoptogenic factors such as cytochrome c and the production of reactive oxygen species (Liu et al., 1996; Kluck et al., 1997; Pham et al., 2000). Release of cyt c to the cytosol drives the assembly of a high-molecular-weight complex, the mitochondrial apoptosome that activates caspases (Adrian and Martin, 2001). Translocation of cyt c to the cytosol is, therefore, a pivotal event in apoptosis. Cyt c is a soluble protein loosely bound to the outer face of the inner mitochondrial membrane, and its release is associated with an interruption of the normal electron flow at the complex III site of the respiratory chain, with the accumulation of reducing equivalents in the middle portion of the electron transfer chain, and thus directing one-electron transfer to O_2, resulting in the production of superoxide (Cai and Jones, 1998). The mechanism by which cyt c is released from mitochondria during apoptosis remains unknown.

S.cerevisiae mutant strains, lacking mitochondrial DNA, hemelyase or ATPase were more resistant to AA-PCD compared to wild-type strains. This data showing that mitochondrial respiration is essential for death of yeast induced by acetic acid.

Acid acetic-induced apoptosis induces a severe amino acid starvation, involving the general amico acid-control (GAAC) system and TOR pathway (Almeida et al., 2009). Silva and coworkers (Silva et al., 2013) have demonstrated the up-regulation of two Heat Shock Protein 90 (Hsp90), important chaperone family isoforms, that are involved in cell response to acetic acid stress.

Recent genome-wide analysis identified genes involved in AA-PCD regulation and elects metabolism as a main regulator (Sousa et al., 2013). Deficiency in carbohydrate, lipid, amico acid and vitamin metabolism that induced a decrease in cell death, suggesting that these process play an important role in PCD.

This study has led to conclusion that mitochondrial function, transcription of glucose-repressed genes, protein biosynthesis and modifications and vesicular traffic from Golgi to the endosome and the vacuole are more important for AA-PCD protection, while amino acid biosynthesis, oxidative stress, cell growth and differentiation, protein phosphorylation, autophagosomes formation and histone deacetylation are fundamental for AA-PCD execution (Sousa et al., 2013).

In my PhD research, the experimental model system, W303-1B *S.cerevisiae*, is exponentially growing in glucose in which PCD is induced adding 80 mM acetic acid.

80 mM acetic acid-induced programmed cell death is an adequate experimental set up to further investigate the different molecular events, such as bioenergetical processes and related gene expression regulation, leading to yeast cell demise (Giannattasio et al., 2005). Acetic acid-treatment induced a progressive loss of cell viability that is complete at 200 min after the start induction.

Recent studies have shown that in this strain more key biochemical process occur *en route* to AA-PCD and, in particular, that mutant stains lacking or overespressing PCD regulatory genes evince different response to AA induction, like ROS generation, cyt c release, mitochondrial function and proteolytic activities (Giannattasio et al., 2008).

For example, yeast cells lacking the metacaspase-encoding gene YCA1 (*Δyca1*) show a reduced rate of death. This prove that YCA1 contributes to AA-PCD not only in a manner related to caspase-like activity (Guagnarella et al., 2006).

1.5. Yeast metacaspase (Yca1p)

Caspases are a conserved family of cysteine proteases. They play different roles in inflammatory responses and apoptotic pathways. Among the caspases is a subgroup whose primary function is to initiate apoptosis. Despite sharing some common features, other aspects of the biochemistry, substrate specificity, regulation and signaling mechanisms differ between initiator apoptotic caspases. Defects in expression or activity of these caspases are related to certain pathological conditions including neurodegenerative disorders, autoimmune diseases and cancer (Ho et al., 2005).

In mammalian apoptosis, caspases play a major role. However, there is now accumulating evidence indicating that cell death can occur in a programmed fashion but in complete absence and independent of caspase activation (Broker et al., 2005).

Uren at coworkers (Uren et al., 2000) have identified two families of caspase-like proteins: paracaspases (found in metazoans and Dictyostelium) and metacaspases (found in plants, fungi, and protozoa).

Unlike traditional caspases which contain a C-terminal caspase domain (empty box) and in some cases a prodomain with CARD or DED oligomerization motifs, metacaspases from yeast contain a proline-rich region at their N terminus (**Figure 2**). In *S.cerevisiae*, metacaspase, a protein belonging to the superfamily of caspase-related proteases, are codes by YCA1 gene (Uren et al., 2000).

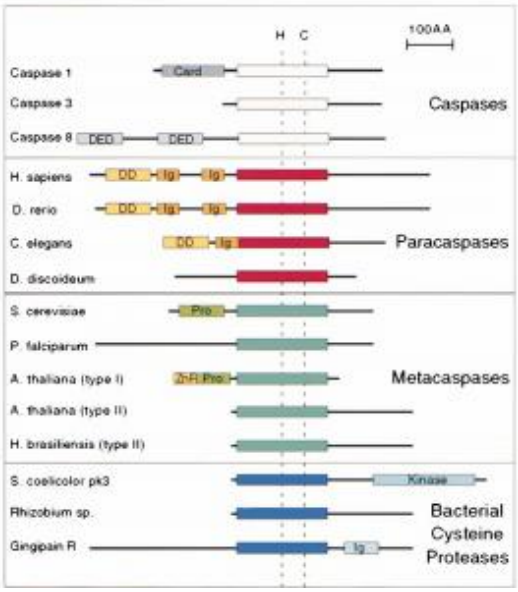

Figure 2. Domain structure of caspases, paracaspases, and metacaspases.

Metacaspase (**Figure 3**) is involved in *S.cerevisiae* PCD triggered by different stimuli. In addition, disruption of YCA1 attenuated the stimulation of apoptosis due to apoptosis-inducing factor (AIF) overexpression (Wissing et al., 2004) or hydrogen peroxide (Khan et al., 2005). However, yeast metacaspase-independent PCD has also been reported (Ivanovska and Hardwich, 2005, Hauptmann et al., 2006).

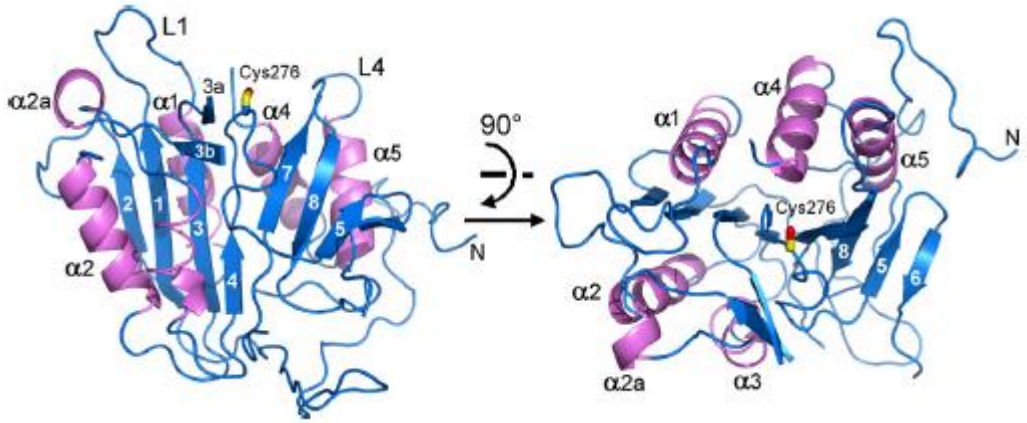

Figure 3. Crystal Structure of the Yeast Metacaspase Yca1

The role of YCA1 in AA-PCD is still controversial although Yca1p has been indicated as an executor of AA-PCD in *S.cerevisiae* (Madeo et al., 2002). More recently, a minor role for YCA1 in AA-PCD was proposed by Saraiva and collaborators (Saraiva et al., 2006). The results of this study suggest that stimulation by PKC isoforms, which modulate apoptotic proteins, is not associated with an enhancement of Yca1p activity. These results are consistent with an apoptotic pathway induced by acetic acid, in which the role of yeast caspase seems less relevant compared with other apoptotic stimuli like oxidative (Madeo et al., 2002) or hyperosmotic (Silva et al., 2005) stresses. Therefore, stimulation of *S.cerevisiae* AA-PCD by PKC isoform expression seems to involve an Yca1p-independent pathway (Saraiva et al., 2006).

Guaragnella et coworkers (Guaragnella et al., 2006) have done a comparison between wild type (WT) and YCA1-lacking (*Δyca1*) W303-1B yeast cells with respect to the occurrence, nature and time course of the death process and have shown that YCA1 contributes to AA-PCD is not as a conventional caspase.

First, they have compared WT and *Δyca1* yeast cells in exponential phase with respect to their viability up to 200 min after PCD induction (**Figure 4**).

In both cases the yeast cells died but the cell death patterns were different. After 30 min of acetic acid treatment (**Figure 4A**), WT (white bars) and *Δyca1* (black bars) cells showed about 74% and 83% cell viability, respectively. This progressively decreased to 0% for WT and 7% for *Δyca1* cells at 200 min. *Δyca1* cell viability was significantly higher ($P < 0.001$) than that of WT cells from 60 to 120 min after acetic acid challenge with death rates of $\mu d = 0.015 \pm 0.0021$ min−1 and 0.0074 ± 0.0002 min−1 for WT and *Δyca1* cells, respectively.

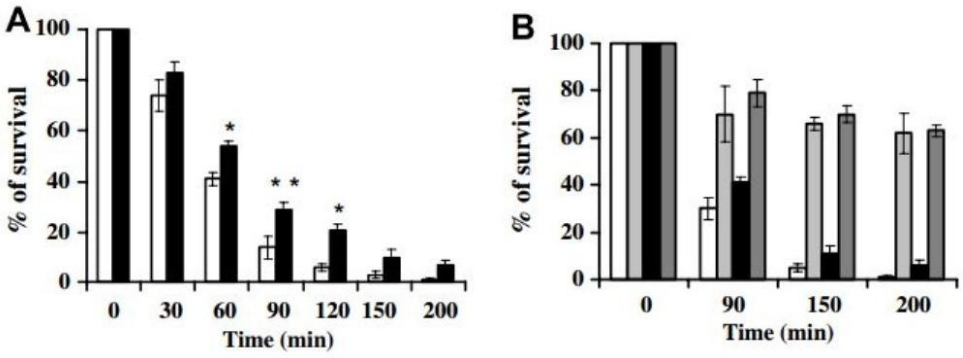

Figure 4. **Effect of YCA1 deletion and/or cycloheximide on viability of *S.cerevisiae* W303-1B exponential cells exposed to acetic acid**. WT and *Δyca1* cell death was induced with 80 mM acetic acid in the absence (A and B, white and black bars, respectively) or in the presence of cycloheximide (B, light and dark grey bars, respectively) and cell viability analyzed at indicated times

To determine whether death of *Δyca1* cells occurs via PCD, given that AA-PCD is dependent on *de novo* protein synthesis (Ludovico et al., 2001), the effect of cycloheximide, an inhibitor of protein biosynthesis, on survival of *Δyca1* and WT cells was investigated. In both cases cycloheximide prevented cell death in a similar way (**Figure 4B**).

Another PCD hallmark was also analyzed during AA-PCD of both WT and *Δyca1* cells is chromatin condensation, through analysis of nuclear morphology and plasma membrane integrity by co-staining cells with DAPI and PI (**Figure 5**).

With both cell types chromatin condensation along the nuclear envelope was detectable after 60, 120 and 200 min of acetic acid treatment in cells with an integral plasma membrane as shown by lack of staining with PI.

Thus, yeast cells lacking the metacaspase YCA1 gene undergo the process of AA-PCD in a manner similar to that of the WT cells but at a lower rate.

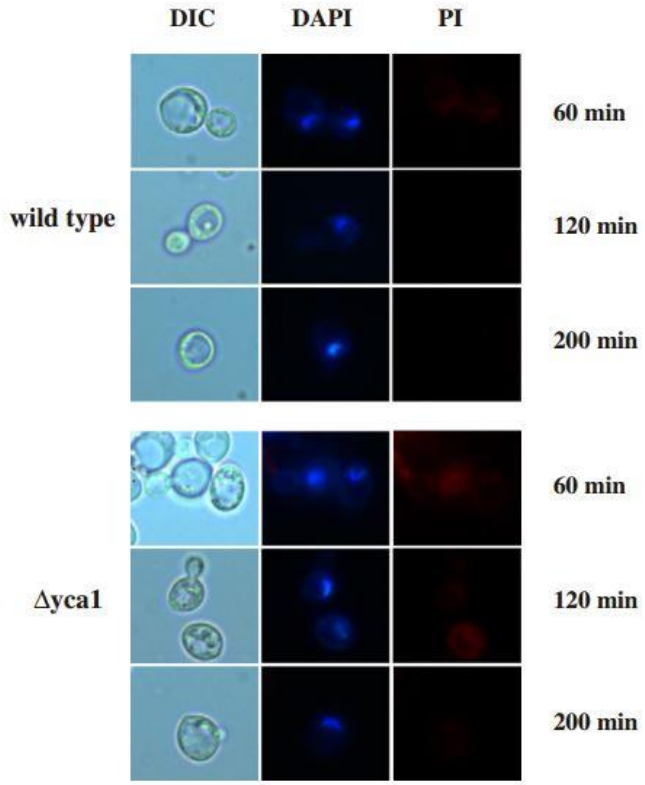

Figure 5. **DAPI/PI staining of WT and *Δyca1 S.cerevisiae* W303-1B exponential cells exposed to 80 mM acetic acid**

In the light of the above results, to ascertain whether and how caspase activity is involved in yeast AA-PCD, Guaragnella and coworkers (Guaragnella et al., 2006) have monitored caspase-like activity by simultaneous staining of cells with FITC-VAD-fmk (carbobenzoxy-valyl-alanyl-aspartyl-[O-methyl]-fluoromethylketone) (Madeo et al., 2002; Silva et al., 2005) and with PI to differentiate between FITC-VAD-fmk specific and unspecific staining (Vachova et al., 2005). (**Figure 6**).

Cells treated with 60% (w/w) of glucose, which die via PCD (Silva et al., 2005) were used as a control for positive staining with FITC-VAD-fmk. About 36.9% of WT cells displayed FITC-VAD-fmk positive and PI negative staining (specific staining); after acetic acid treatment the corresponding percentage was 11.8%. Pre-incubation with

the pan-caspase inhibitor z-VAD-fmk, before staining with FITC-VAD-fmk, caused a reduction in the percentage of FITC-VAD-fmk positive cells both in acetic acid and 60% glucose treated cells.

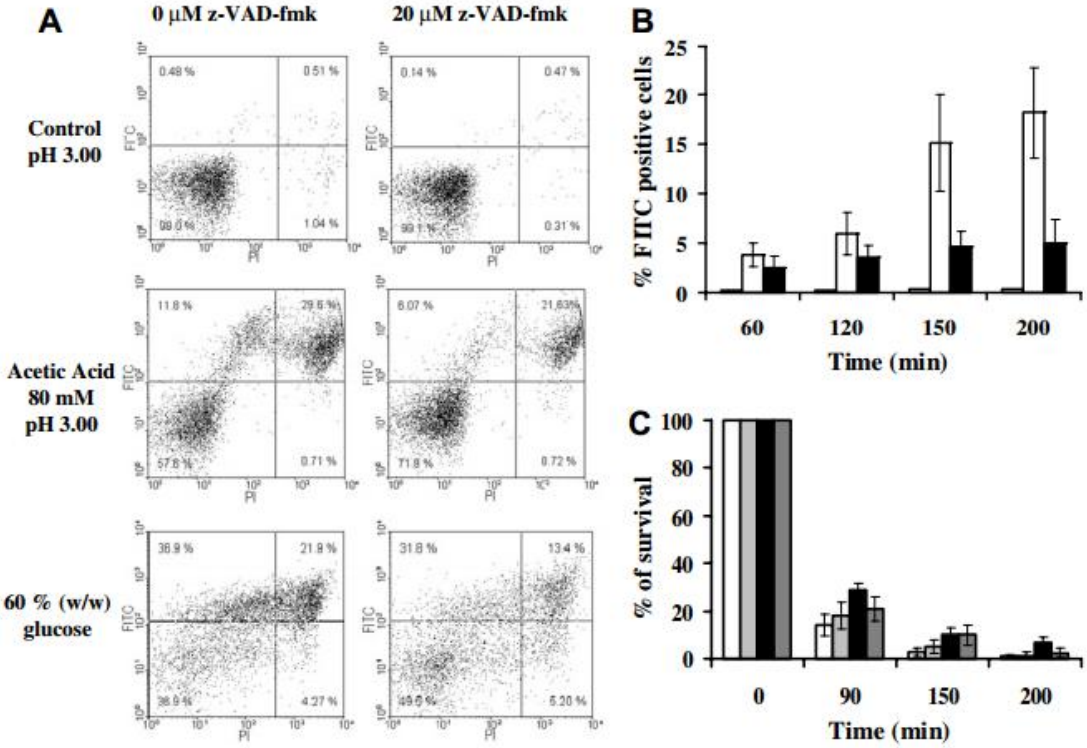

Figure 6. Caspase-like activity in *S.cerevisiae* W303-1B exponential cells upon treatment with acetic acid and effect of z-VAD-fmk on cell viability

Staining with FITC-VAD-fmk was very low in WT cells held at pH 3 but without acetic acid (**Figure 6A**) and did not increase with time (**Figure 6B**). In WT cells treated with acetic acid the staining with FITC-VAD-fmk increased progressively up to about 20% at 200 min after induction of PCD. By contrast, with *Δyca1* cells the percentage of FITC-VAD-fmk staining remained virtually constant at about 5% between 60 and 200 min of PCD. These results are consistent with YCA1 acting as a z-VAD-fmk sensitive caspase-like protease and/or as a protease activator. In parallel, cell survival was monitored either in the absence or presence of z-VAD-fmk.

Furthemore, WT and *Δyca1* cell death induced with 80 mM acetic acid in the absence (white and black bars, respectively) and in the presence of 20 μM z-VAD-fmk (light and dark grey bars, respectively) was no difference in AA-PCD time-course (**Figure 6C**).

Guaragnella and coworkers (Guaragnella et al., 2006) have shown that as with the WT, *Δyca1* cells die via PCD. Moreover, they have demonstrated that AA-PCD in WT and *Δyca1* cells differ from one another essentially in the reduced rate of death. That is, the characteristics of the death process are the same for both cell types except that YCA1 disruption increases cell survival.

In WT cells treated with acetic acid there is a time-dependent increase in caspase-like activity, as revealed by flow cytometry with FITC-VAD-fmk, which is inhibited by z-VAD-fmk. This does not occur in *Δyca1* cells, thus strongly suggesting a role for YCA1 in promoting caspase-like activity. Nonetheless, z-VAD-fmk addition did not result in death prevention (**Figure 6C**). Given that this substance can inhibit caspase-like activity, as indicated by the experiments with flow cytometry, we conclude that yeast can die in a manner independent of caspase activity and consequently that YCA1 participates in AA-PCD in a manner unrelated to its putative caspase-like activity.

At present, the explanation of the reduced rate of death in yeast cells lacking YCA1 can only be speculative. In addition to the possibility that YCA1 is a caspase-like protein, the possibility that YCA1 could be associated with other function different from caspase activity, perhaps protease activity must be taken into consideration. This is supported by findings which show that recombinant Yca1p exhibits arginine/lysine-specific cysteine endopeptidase activity, which is not inhibited by z-VAD-fmk (Watanabe et al., 2005). Thus, it cannot be excluded that Yca1p, acting as a protease, activates other caspase-like activities (Guaragnella et al., 2006).

To better understand the mechanism of AA-PDC in *S.cerevisiae* and the involvement of metacaspase in key events of this pathway, an important study was carried out by Doctor Giannattasio's group (Guaragnella et al., 2010). They have compared WT and *Δyca1* cells with the respective mutant cells lacking cytochrome c isoforms for the occurrence of AA-PCD, H_2O_2 level and caspase activation and have shown that AA-PCD can occur without cyt c release, which itself requires YCA1.

Furthermore, they have conducted a western blot analysis of cytochrome c in AA-PCD *Δyca1* cells in comparison with wild type cells (**Figure 7**).

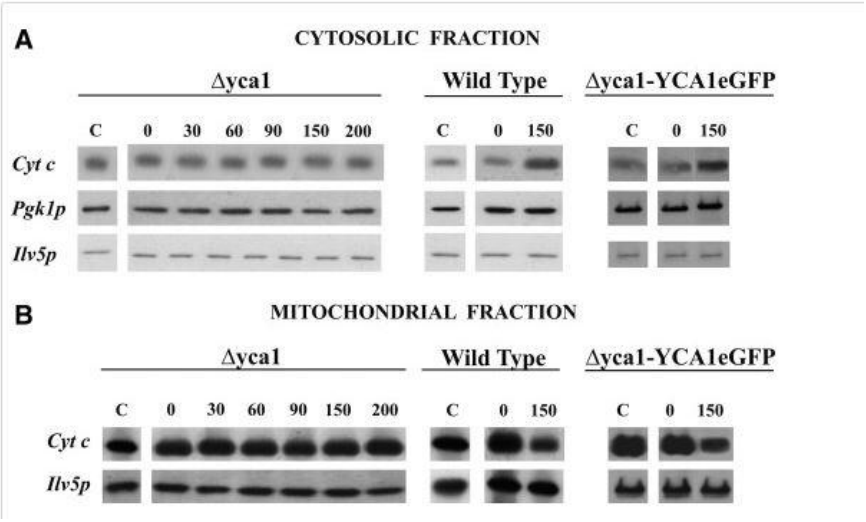

Figure 7. Western blot analysis of cytochrome c in AA-PCD *Δyca1* and wild type cells

In distinction with WT cells in which at 150 min after AA-treatment the cytosolic cyt c amount increases up to 140% of the control (**Figure 7A**), no cyt c release was found in *Δyca1* cells. Consistently, no change in the mitochondrial cyt c amount was found in *Δyca1* cells, as opposed to WT cells in which it decreased (**Figure 7B**). Since *Δyca1* cells were shown to accumulate deleterious mutations with time (Severin et al., 2008) they tried to ascertain whether YCA1 deletion *per se* is responsible for the lack of cyt c release. Thus, they over-expressed in *Δyca1* cells a YCA1-eGFP fusion gene under the control of MET17 inducible promoter (Szallies et al., 2002), and induced cell death with AA. Similarly to wt cells a higher cyt c level was found in the cytosol with respect to control untreated cells after 150 min (**Figure 7A**). Consistently, a decrease in mitochondrial cyt c was found in AA-treated *Δyca1*-YCA1eGFP cells at the same time (**Figure 7B**). These data demonstrate that the lack of the cyt c release is dependent on YCA1.

As a loading control they have used two monoclonal antibodies against Pgk1p and Ilv5p, cytosolic and mitochondrial matrix protein markers, respectively. A low but constant amount of Ilv5p was found in the cytosolic fraction of both control and AA-

PCD cells up to 200 min, resulting from mitochondrial damage during the isolation procedure (Giannattasio et al., 2008).

Furthermore, in YCA1-lacking cells, AA-PCD is characterized by an early burst of H_2O_2 (Guagnarella et al., 2010a). An important evidence is that antioxidant N-acetyl-L-cysteine (NAC) did not prevent AA-PCD occurrence in *Δyca1* cells, as opposed to its effect on WT AA-PCD, showing that knock-out cells die in ROS-indipendent manner (Guaragnella et al., 2010 b).

As results of all these data, can be delineated two different AA-PCD pathways in relation with YCA1 implication (**Figure 8**) (Guaragnella et al., 2011).

In the first phase, acetic acid enters in yeast cells and dissociates into acetate and protons causing intracellular acidification. H_2O_2 accumulates, superoxide dismutase (SOD) activity increases, while catalase activity is undetectable.

En route to AA-PCD, in WT cells, cyt c is released in YCA1- and ROS-dependent manner, and works as an electron donor (c_{red}) to mitochondrial respiratory chain and as superoxide anion ($O_2^{-\bullet}$) scavenger (c_{ox}). In a late phase, cyt c is degraded by unidentified proteases. Mitochondrial functions progressively decline with decrease in mitochondrial membrane potential ($\Delta\Psi$), respiratory control index (RCI) and cyclooxygenase (COX) activity. Caspase-like activity increases in a late phase and fragment DNA occurs. This way is NAC-sensitive.

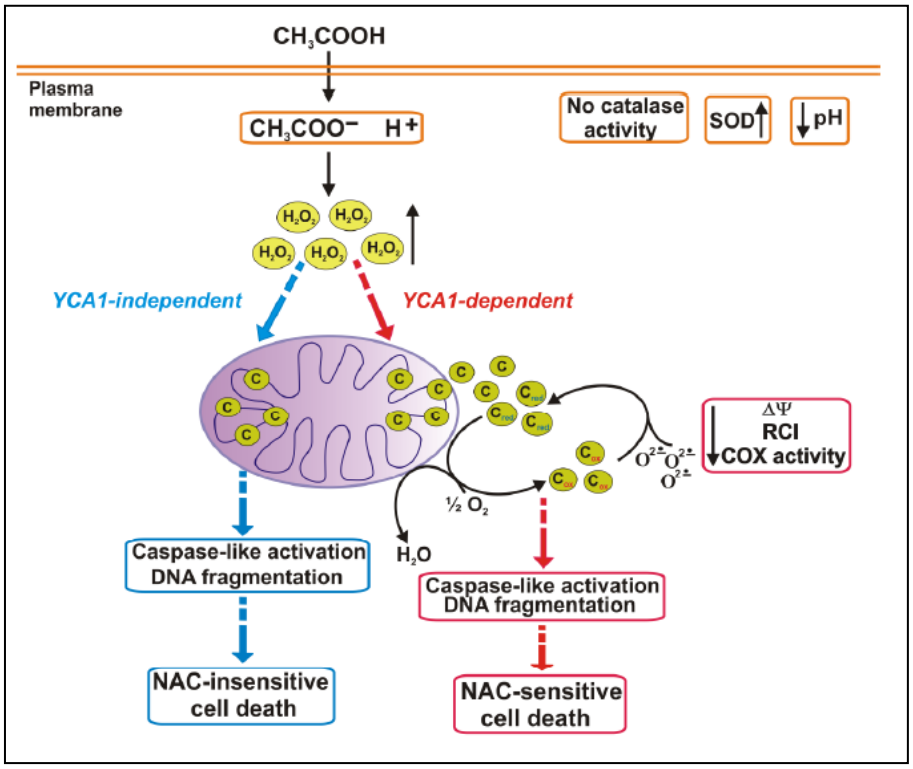

Figure 8. Yeast AA-PCD pathways in glucose-grown cells

Alternatively, AA-PCD pathway can occur in manner independent of YCA1 and in this case not seeing cyt c release. Only in late phase caspase-like activity is observed. This YCA1-indipendent way is not affected by NAC treatment (Guagnarella et al., 2011).

In conclusion, we can affirm that there are two different alternative compensatory pathways that can be activated in death inducted by acetic acid: one is physiologic and one occurs when the main route is blocked in certain steps, like as the release of cyt c. In this equilibrium, metacaspase plays a key role.

1.6. Importance of proteomics in yeast study

Since completion of the genome sequence of *S.cerevisiae* in 1996 (Goffeau et al., 1996), yeast has been the lead organism for post-genomic analysis. Large-scale methods are being used to study the mutant phenotype of deletion of each gene (Bettiga et al., 2004), to monitor the expression level of the genes (Griffin et al., 2002), to detect the protein–protein interactions (Jeong et al., 2001), and to measure directly the abundance, localization and modification of the proteins (Ghaemmaghami et al., 2003).

Proteomics regards the study of the structure, function and location of all proteins expressed in a biological system.

The latter is the field of the "proteome". The term proteome was coined by Wilkins and colleagues in 1996 to indicate the "PROTeins expressed by a genOME" (Wilkins et al., 1996), that are dynamic and changing based on the type and functional state of a cell.

S.cerevisiae proteome characterization has been more important to build a Yeast Protein Database (YPD). YPD is a curated proteome database that seeks to compile, organize and present in a convenient format the current knowledge of yeast protein functions (Garrels et al., 1996; Payne et al., 1997). This database is continually updated with new information derived from the various investigations.

The primary mean using in proteomic studies is proteome maps generated by two-dimensional gel electrophoresis (2-DE).

Since the advent of the 2-DE methodology, numerous improvements have been introduced to develop the full potential of 2-DE and to make it an indispensable tool in biological research. Particularly fruitful was the establishment of annotated 2-D protein maps where proteins of model organisms separated on 2-D gels are identified.

Hence a great deal of effort has been spent in the development of a reference protein map of the yeast *S.cerevisiae*. Since this pioneering work, a large number of annotated yeast reference maps have been reported. They include proteins from total cell extracts (Maillet et al., 1996; Garrels et al., 1997; Gygi et al., 1999; Perrot et al., 2006; Kobi et al., 2004; Yin et al., 2004), strongly alkaline (Wildgruber et al., 2002), mitochondrial (Ohlmeier et al., 2004; Sickmann et al., 2003) or vacuolar luminal proteins (Sarry et al., 2007). Several hundred proteins have been identified on these maps. These annotated maps have proved to be helpful in solving numerous biological problems (Kolkman et al., 2005).

The first yeast reference map was reported by McLaughlin's group in 1982 (Ludwig et al., 1982). After, Boucherie (Boucherie et al., 1996) have published onto *Electrophoresis* journal a manuscript in which show the identification of 250 protein spots. In later years, Perrot and coworkers have published 3 update of yeast proteome map. In 1999 (Perrot et al., 1999) their identification extended the number of protein spots identified on our yeast reference map to 401, in 2006 (Perrot et al., 2006) to 602 and, finally, in 2009 (Perrot et al., 2009) to 716 (**Figure 9**).

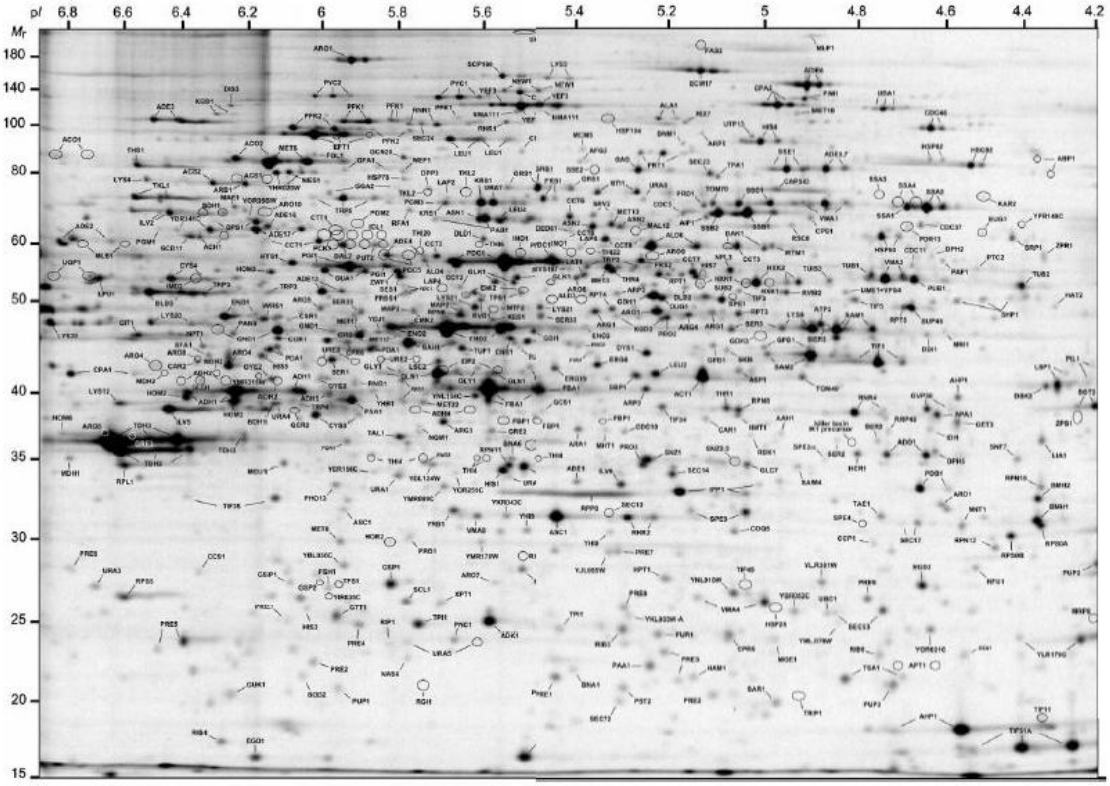

Figure 9. Standard yeast reference map with names of the identified spots

Hence proteomics represent a valid instrument to have an overview of what is happening when, for example, strain is knock out for a gene, such as in my PhD research for deletion of metacaspase gene YCA1.

REFERENCES

Adrian C. and Martin S.J. The mitochondrial apoptosome: a killer unleashed by the cytochrome seas. *Trends Biochem Sci*, (2001), 26:390–397.

Ahn S. H., Henderson K. A., Keeney S., Allis C. D. H2B (Ser10) phosphorylation is induced during apoptosis and meiosis in S. cerevisiae. *Cell Cycle*. (2005),4(6): 780-783.

Almeida B., OhlmeierS.,Almeida A.J., MadeoF., Leao C.,Rodrigues F., Ludovico P. Yeast protein expression profile during acetic acid-induced apoptosis indicates causal involvement of the TOR pathway. *Proteomics*.(2009), 9:720–732.

Austriaco, N. Endoplasmic reticulum involvement in yeast cell death. *Front Oncol. (*2012), 2: 87.

Bender C. E., Fitzgerald P., Tait S. W., Llambi F., McStay G. P., Tupper D. O., Pellettieri J., Sanchez Alvarado A., Salvesen G. S., Green D. R. Mitochondrial pathway of apoptosis is ancestral in metazoans. *Proc Natl Acad SciUSA* (2012) 109(13): 4904-4909.

Bettiga M., Calzari L., Orlandi I., Alberghina L., Vai M. Involvement of the yeast metacaspase Yca1 in ubp10Delta-programmed cell death. *FEMS Yeast Res*. (2004), 5(2):141-7.

Botstein D. Why yeast? *Hosp Pract (Off Ed).* (1991), 26(10):157-61, 164.

Boucherie H., Sagliocco F., Joubert R., Maillet I., Labarre J., Perrot M. Two-dimensional gel protein database of *Saccharomyces cerevisiae*. *Electrophoresis*. (1996), 17(11):1683-99.

Bröker L.E., Kruyt F.A., Giaccone G. Cell death independent of caspases: a review. *Clin Cancer Res.* (2005), 11(9):3155-62. Review.

Buttner S., Ruli D., Vogtle F. N., Galluzzi L., Moitzi B., Eisenberg T., Kepp O., Habernig L., Carmona-Gutierrez D., Rockenfeller P., Laun P., Breitenbach M., Khoury C., Frohlich K. U., Rechberger G., Meisinger C., Kroemer G., Madeo F. A

yeast BH3-only protein mediates the mitochondrial pathway of apoptosis. *Embo J.*(2011), 30(14): 2779-2792.

Cai J. and Jones D.P. Superoxide in apoptosis. Mitochondrial generation triggered by cytochrome c loss. *J. Biol. Chem.* (1998), 273:11401–11404.

Carmona-Gutierrez D., Eisenberg T., Buttner S., Meisinger C., Kroemer G., Madeo F. Apoptosis in yeast: triggers, pathways, subroutines. *Cell Death Differ*. (2010), 17(5): 763-773.

Cássio F., Leão C., van Uden N. Transport of lactate and other short-chain monocarboxylates in the yeast *Saccharomyces cerevisiae*. *Appl Environ Microbiol* (1987), 53:509–513.

Clifford J., Chiba H., Sobieszczuk D., Metzger D., Chambon P. RXRa-null F9 embryonal carcinoma cells are resistant to the differentiation,anti-proliferative and apoptotic effects of retinoids. *EMBO (Eur. Mol. Biol.Organ.) J.* (1996), 15:4142–4155.

Diaz-Ruiz R., Rigoulet M., Devin A. The Warburg and Crab-tree effects: on the origin of cancer cell energy metabolism and of yeast glucose repression. *Biochim. Biophys. Acta* (2010), 1807, 568–576.

Eisenberg T., Büttner S., Kroemer G., Madeo F. The mitochondrial pathway in yeast apoptosis. *Apoptosis* (2007) , 12(5):1011-23.

Eisenberg T., Carmona-Gutierrez D., Büttner S., Tavernarakis N., Madeo F. Necrosis in yeast. *Apoptosis* (2010), 15(3): 257-68. Review.

Foury F. and Kucej M. Yeast mitochondrial biogenesis: a model system for humans? *Curr Opin Chem Biol* (2001), 6, 106-111.

Garrels J.I. YPD-A database for the proteins of *Saccharomyces cerevisiae*. *Nucleic Acids Res.* (1996), 24(1):46-9.

Garrels J.I., McLaughlin C.S., Warner J.R., Futcher B., Latter G.I., Kobayashi R., Schwender B., Volpe T., Anderson D.S., Mesquita-Fuentes R., Payne W.E.

Proteome studies of *Saccharomyces cerevisiae*: identification and characterization of abundant proteins. *Electrophoresis.* (1997), 18(8):1347-60.

Ghaemmaghami S., Huh W.K., Bower K., Howson R.W., Belle A., Dephoure N., O'Shea E.K., Weissman J.S. Global analysis of protein expression in yeast. *Nature.* (2003), 425(6959):737-41.

Ghibelli L., Coppola S., Rotilio G., Lafavia E., Maresca V., Ciriolo M.R. Non-oxidative loss of glutathione in apoptosis via GSH extrusion. *Biochem. Biophys. Res. Commun* (1995), 216:313–320.

Giannattasio S., Atlante A., Antonacci L., Guaragnella N., Lattanzio P., Passarella S., Marra E. Cytochrome c is released from coupled mitochondria of yeast en route to acetic acid-induced programmed cell death and can work as an electron donor and a ROS scavenger. *FEBS Lett*.(2008), 582(10): 1519-1525.

Giannattasio S., Guaragnella N., Arbini A.A., Moro L. Stress-related mitochondrial components and mitochondrial genome as targets of anticancer therapy. *Chem Biol Drug Des.* (2013), 81(1):102-12.

Giannattasio S., Guaragnella N., Corte-Real M., Passarella S., Marra E. Acid stress adaptation protects *Saccharomyces cerevisiae* from acetic acidinduced programmed cell death. *Gene.* (2005), 354: 93-98.

Goffeau A., Barrell B.G., Bussey H., Davis R.W., Dujon B., Feldmann H., Galibert F., Hoheisel J.D., Jacq C., Johnston M., Louis E.J., Mewes H.W., Murakami Y., Philippsen P., Tettelin H., Oliver S.G. Life with 6000 genes. *Science* (1996), 74(5287):546, 563-7.

Greenlund L.J.S., Deckwerth T.L., Johnson E.M.Jr. Superoxide dismutase delays neuronal apoptosis: a role for reactive oxygen species in programmed neuronal death. *Neuron.* (1995), 14:303–315.

Griffin T.J., Gygi S.P., Ideker T., Rist B., Eng J., Hood L., Aebersold R. Complementary profiling of gene expression at the transcriptome and proteome levels in *Saccharomyces cerevisiae*. *Mol Cell Proteomics.* (2002), 1(4):323-33.

Guaragnella N., Antonacci L., Passarella S., Marra E., Giannattasio, S. Achievements and perspectives in yeast acetic acid-induced programmed cell death pathways. *Biochem Soc Trans*.(2011), 39(5): 1538-1543.

Guaragnella N., Bobba A., Passarella S., Marra E., Giannattasio S. Yeast acetic acid-induced programmed cell death can occur without cytochrome c release which requires metacaspase YCA1. *FEBS Lett*. (2010a), 584(1): 224-228.

Guaragnella N., Passarella S., Marra E., Giannattasio S. Knock-out of metacaspase and/or cytochrome c results in the activation of a ROS-independent acetic acid-induced programmed cell death pathway in yeast. *FEBS Lett*. (2010b), 584(16): 3655-3660.

Guaragnella N., Pereira C., Sousa M. J., Antonacci L., Passarella S., Corte-Real M., Marra E., Giannattasio S. YCA1 participates in the acetic acid induced yeast programmed cell death also in a manner unrelated to its caspase like activity. *FEBS Lett.* (2006), 580(30):6880-6884.

Guaragnella, N., Ždralević, M., Antonacci, L., Passarella, S., Marra, E. and Giannattasio, S. The role of mitochondria in yeast programmed cell death. *Front Oncol.*(2012), 2: 70.

Gygi S.P., Rochon Y., Franza B.R., Aebersold R. Correlation between protein and mRNA abundance in yeast. *Mol Cell Biol*. (1999), 19(3):1720-30.

Hauptmann P., Riel C., Kunz-Schughart L.A., Frohlich K.U, Madeo F., Lehle L. Defects in N-glycosylation induce apoptosis in yeast. *Mol Microbiol*. (2006), 59:765-778.

Herker E., Jungwirth H., Lehmann K. A., Maldener C., Frohlich K. U., Wissing S., Buttner S., Fehr M., Sigrist S., Madeo F. Chronological aging leads to apoptosis in yeast. *J Cell Biol.* (2004), 164(4): 501-507.

Ho P.K., Hawkins C.J. Mammalian initiator apoptotic caspases. *FEBS J.* (2005), 272(21):5436-53. Review.

Hockenbery D.M., Oltvai Z.N., Yin X.M., Milliman C.L., Korsmeyer S.J. Bcl-2 functions in an antioxidant pathway to prevent apoptosis. *Cell.* (1993), 75:241–251.

Hoeberichts F.A., ten Have A., Woltering E.J. A tomato metacaspase gene is upregulated during programmed cell death in Botrytis cinerea-infected leaves. *Planta* (2003), 217: 517–522.

Huttemann M., Pecina P., Rainbolt M., Sanderson T. H., Kagan V. E., Samavati L., Doan J. W., Lee I. The multiple functions of cytochrome c and their regulation in life and death decisions of the mammalian cell: From respiration to apoptosis. *Mitochondrion* (2011), 11(3): 369-381.

Ikeda S. and Kawasaki N. Isolation and characterization of the Schizosaccharomyces pombe cDNA encoding the mitochondrial endonuclease(1). *Biochim. Biophys. Acta* (2001), 1519: 111–116.

Ivanovska I. and Hardwick J.M. Viruses activate a genetically conserved cell death pathway in a unicellular organism. *J. Cell Biol.* (2005), 170:391–399.

Jeong H., Mason S.P., Barabási A.L., Oltvai Z.N. Lethality and centrality in protein networks. *Nature.* (2001), 411(6833):41-2.

Kane D.J., Sarafian T.A., Anton R., Hahn H., Gralla E.B., Valentine J.S., Örd T., Bredesen D.E. Bcl-2 inhibition of neural death: decreased generation of reactive oxygen species. *Science* (1993), 262:1274–1277.

Khan M.A., Chock P.B., Stadtman E.R. Knockout of caspase-like gene, YCA1, abrogates apoptosis and elevates oxidized proteins in *Saccharomyces cerevisiae*. *Proc NatlAcad Sci USA.* (2005), 102(48):17326-31.

Kluck R. M., Ellerby L. M., Ellerby H. M., Naiem S., Yaffe M. P., Margoliash E., Bredesen D., Mauk A. G., Sherman F., Newmeyer D. D. Determinants of cytochrome c pro-apoptotic activity. The role of lysine 72 trimethylation. *J BiolChem.*(2000), 275(21): 16127-16133.

Kluck R., Bossy-Wetzel E., Green D.R., Newmeyer D.D. The release of cytochrome c from mitochondria: a primary site for Bcl-2 regulation of apoptosis. *Science* (1997), 275:1132–1136.

Knorre D. A., Smirnova E. A., Severin, F. F. Natural conditions inducing programmed cell death in the yeast *Saccharomyces cerevisiae*. *Biochemistry (Mosc)*. (2005), 70(2): 264-266.

Kobi D., Zugmeyer S., Potier S., Jaquet-Gutfreund L. Two-dimensional protein map of an "ale"-brewing yeast strain: proteome dynamics during fermentation. *FEMS Yeast Res.* (2004), 5(3):213-30.

Kolkman A., Slijper M., Heck A. J. Development and application of proteomics technologies in *Saccharomyces cerevisiae*. *Trends Biotechnol*. (2005), 23:598–604.

Laun P., Pichova A., Madeo F., Fuchs J., Ellinger A., Kohlwein S., Dawes I., Frohlich K. U., Breitenbach M. Aged mother cells of *Saccharomyces cerevisiae* show markers of oxidative stress and apoptosis. *Mol Microbiol*. (2001), 39(5): 1166-1173.

Leão C. and van Uden N. Transport of lactate and other monocarboxylates in the yeast Candida utilis. *Appl Microbiol Biotechnol* (1986), 23:389-393.

Li L.Y., LuoX., Wang X. Endonuclease G is an apoptotic DNase when released from mitochondria. *Nature* (2001), 412: 95–99.

Liang X.H., Jackson S., Seaman M., Brown K., Kempkes B. Hibshoosh H., Levine B. Induction of autophagy and inhibition of tumorigenesis by beclin 1. *Nature* (1999), 402:672–676.

Liu X., Kim C.N., Yang J., Jemmerson R., Wang X. Induction of apoptotic program in cell-free extracts: requirement for dATP and cytochrome c. *Cell* (1996), 86:147–157.

Ludovico P., Rodrigues F., Almeida A.,Silva M.T., Barrientos A., Corte- Real M. Cytochrome c release and mitochondria involvement in programmed cell death induced by acetic acid in *Saccharomyces cerevisiae*. *Molecular Biology of the Cell.* (2002), 13, 2598–2606.

Ludovico P., Sousa M.J., Silva M.T., Leão C., Côrte-Real M. *Saccharomyces cerevisiae* commits to a programmed cell death process in response to acetic acid. *Microbiology* (2001), 147: 2409-2415.

Ludwig J.R. 2nd, Foy J.J., Elliott S.G., McLaughlin C.S. Synthesis of specific identified, phosphorylated, heat shock, and heat stroke proteins through the cell cycle of *Saccharomyces cerevisiae*. *Mol Cell Biol*. (1982), 2(2):117-26.

Madeo F, Fröhlich E, Ligr M, Grey M, Sigrist SJ, Wolf DH, Fröhlich KU. Oxygen stress: a regulator of apoptosis in yeast. *J Cell Biol.* (1999), 145(4):757-67.

Madeo F., Carmona-Gutierrez D., Ring J., Büttner S., Eisenberg T., Kroemer G.. Caspase-dependent and caspase- independent cell death pathways in yeast. *Biochem.Biophys.Res.Commun.* (2009), 382:227–231.

Madeo F., Frohlich, E., Frohlich, K. U. A yeast mutant showing diagnostic markers of early and late apoptosis. *J Cell Biol*.(1997), 139(3): 729-734.

Madeo F., Herker E., Maldener C., Wissing S., Lachelt S., Herlan M., Fehr M., Lauber K., Sigrist S.J., Wesselborg S., Frohlich K.U. A caspase-related protease regulates apoptosis in yeast. *Mol.Cell* (2002), 9: 911–917.

Maillet I., Lagniel G., Perrot M., Boucherie H., Labarre J. Rapid identification of yeast proteins on two-dimensional gels. *J Biol Chem*. (1996), 271(17):10263-70.

Martin S.J., Reutelingsperger C.P.M., McGahon A.J., Rader J.A., van Schie R.C.A.A.,. LaFace D.M, Green D.R. Early redistribution of plasma membrane phosphatidylserine is a general feature of apoptosis regardless of the initiating stimulus: inhibition by overexpression of Bcl-2 and Abl. *J. Exp. Med*. (1995), 182:1545–1556.

Mazzoni C., Herker E., Palermo V., Jungwirth H., Eisenberg T., Madeo F., Falcone C. Yeast caspase 1 links messenger RNA stability to apoptosis in yeast.*EMBO Rep.* (2005), 6(11): 1076-1081.

Morton C. O., Dos Santos S. C., Coote P. An amphibian-derived, cationic, alpha-helical antimicrobial peptide kills yeast by caspase-independent but AIFdependent programmed cell death. *Mol Microbiol.* (2007), 65(2): 494-507.

Narasimhan M. L., Coca M. A., Jin J., Yamauchi T., Ito Y., Kadowaki T., Kim K. K., Pardo J. M., Damsz B., Hasegawa P. M., Yun D. J., Bressan R.A. Osmotin is a homolog of mammalian adiponectin and controls apoptosis in yeast through a homolog of mammalian adiponectin receptor. *Mol Cell*. (2005),17(2): 171-180.

Ohlmeier S., Kastaniotis A. J., Hiltunen J. K., Bergmann U. The yeast mitochondrial proteome, a study of fermentative and respiratory growth. *J. Biol. Chem*. (2004), 279: 3956–3979.

Pampulha M.A. and Loureiro-Dias M.C. Combined effect of acetic acid, pH and ethanol on intracellular pH of fermenting yeast. *Appl Microbiol Biotechnol* (1989), 31: 547–550.

Parrish J., Li L., Klotz K., Ledwich D., Wang X., Xue D. Mitochondrial endonuclease G is important for apoptosis in C. elegans. *Nature* (2001),412: 90–94.

Payne W.E., Garrels J.I. Yeast Protein database (YPD): a database for the complete proteome of *Saccharomyces cerevisiae*. *Nucleic Acids Res*. (1997), 25(1):57-62.

Pereira C., Coutinho I., Soares J., Bessa C., Leão M., Saraiva L. New insights into cancer-related proteins provided by the yeast model. *FEBS J.* (2012), 279(5):697-712.

Pereira C., Silva R.D., Saraiva L., Johansson B., Sousa M.J., Côrte-Real M. Mitochondria-dependent apoptosis in yeast. *Biochim Biophys Acta* (2008), 1783(7):1286-302.

Perrot M., Guieysse-Peugeot A.L., Massoni A., Espagne C., Claverol S., Silva R.M., Jenö P., Santos M., Bonneu M., Boucherie H. Yeast proteome map (update 2006). *Proteomics.* (2007), 7(7):1117-20.

Perrot M., Moes S., Massoni A., Jenoe P., Boucherie H. Yeast proteome map (last update). *Proteomics.* (2009), 9(20):4669-73.

Perrot M., Sagliocco F., Mini T., Monribot C., Schneider U., Shevchenko A., Mann M., Jenö P., Boucherie H. Two-dimensional gel protein database of *Saccharomyces cerevisiae* (update 1999). *Electrophoresis*. (1999), 20(11):2280-98.

Pham N., Robison B., Hedley D. Simultaneous detection of mitochondrial respiration chain activity and reactive oxygen in digitonin-permeabilized cells using flow cytometry. *Cytometry* (2000), 41:245–251.

Pinto I., Cardoso H., Leão C. High enthalpy and low enthalpy death in *Saccharomyces cerevisiae* induced by acetic acid. *Biotechnol Bioeng* (1989), 33:1350-1352.

Reggiori F. and Klionsky D.J. Autophagic processes in yeast: mechanism, machinery and regulation. *Genetics.* (2013), 194(2):341-61. Review.

Reiter J., Herker E., Madeo F., Schmitt M. J. Viral killer toxins induce caspase-mediated apoptosis in yeast. *J Cell Biol*. (2005), 168(3): 353-358.

Ren Q., Yang H., Rosinski M., Conrad M. N., Dresser M. E., Guacci V., Zhang Z. Mutation of the cohesin related gene PDS5 causes cell death with predominant apoptotic features in *Saccharomyces cerevisiae* during early meiosis. *Mutat Res*.(2005) 570(2): 163-173.

Resnick M.A. and Cox B.S. Yeast as an honorary mammal. *Mutat Res.* (2000), 451:1-11.

Ruckenstuhl C., Büttner S., Carmona-Gutierrez D., Eisenberg T., Kroemer G., Sigrist S.J., Fröhlich K.U., Madeo F. The Warburg effect suppresses oxidative stress induced apoptosis in a yeast model for cancer. *PLoS One* (2009), 4(2):e4592. doi: 10.1371.

Saraiva L., Silva R. D., Pereira G., Goncalves J. Corte-Real, M. Specific modulation of apoptosis and Bcl-xL phosphorylation in yeast by distinct mammalian protein kinase C isoforms. *J Cell Sci*.(2006), 119(Pt 15): 3171-3181.

Sarry J.E., Chen S., Collum R.P., Liang S., Peng M., Lang A., Naumann B., Dzierszinski F., Yuan C.X., Hippler M., Rea P.A. Analysis of the vacuolar luminal proteome of *Saccharomyces cerevisiae*. *FEBS J.* (2007), 274(16):4287-305.

Severin F. F. and Hyman A. A. Pheromone induces programmed cell death in S. cerevisiae. *Curr Biol*. (2002), 12(7): R233-235.

Severin F. F., V.Meer M., Smirnova E. A., Knorre D. A., P. Skulachev V. Natural causes of programmed death of yeast *Saccharomyces cerevisiae*," Biochimica et Biophysica Acta, vol. 1783, no. 7, pp. 1350–1353, 2008.N.

Sickmann A., Reinders J., Wagner Y., Joppich C., Zahedi R., Meyer H.E., Schönfisch B., Perschil I., Chacinska A., Guiard B., Rehling P., Pfanner N., Meisinger C. The proteome of *Saccharomyces cerevisiae* mitochondria. *Proc Natl Acad Sci USA.* (2003), 100(23):13207-12.

Silva A., Sampaio-Marques B., Fernandes A., Carreto L., Rodrigues F., Holcik M., Santos M. A., Ludovico P. Involvement of yeast HSP90 isoforms in response to stress and cell death induced by acetic acid. *PLoS One.* (2013), 8(8):e71294.

Silva R.D., Sotoca R., Johansson B., Ludovico P., Sansonetty F., Silva M.T., Peinado J.M., Côrte-Real M. Hyperosmotic stress induces metacaspase- and mitochondria-dependent apoptosis in *Saccharomyces cerevisiae*. *Mol Microbiol*, (2005), 58:824–834.

Slater A.F.G., Stefan C., Nobel I., van den Dobbelsteen D.J., Orrenius S. Signalling mechanisms and oxidative stress in apoptosis. *Toxicol.* (1995), Lett.82/83:149–153.

Sousa M., Duarte A. M., Fernandes T. R., Chaves S. R., Pacheco A., Leao C., Corte-Real M., Sousa M. J. Genome-wide identification of genes involved in the positive and negative regulation of acetic acid-induced programmed cell death in *Saccharomyces cerevisiae*. *BMC Genomics.* (2013), 14: 838.

Suarez M.F., Filonova L.H., Smertenko A., Savenkov E.I.,Clapham D.H., von Arnold S., Zhivotovsky B., Bozhkov P.V. Metacaspase-dependent programmed celldeath is essential for plant embryogenesis. *Curr. Biol.* (2004), 14:R339–R340.

Sukhanova E. I., Rogov A. G., Severin F. F., Zvyagilskaya R. A. Phenoptosis in yeasts. *Biochemistry (Mosc).* (2012), 77(7): 761-775.

Szallies A., Kutaba B.K., Duszenko M. A metacaspase of Trypanosoma brucei causes loss of respiration competence and clonal death in the yeast *Saccharomyces cerevisiae*. FEBS Lett., 517 (2002), pp. 144–150

Tuppen, H. A., Blakely, E. L., Turnbull, D. M., Taylor, R. W. Mitochondrial DNA mutations and human disease. *Biochim Biophys Acta*. (2010), 1797(2): 113-128.

Uren A.G., O'Rourke K., Aravind L.A., Pisabarro M.T., Seshagiri S., Koonin E.V., Dixit V.M. Identification of paracaspases and metacaspases: two ancient families of caspase-like proteins, one of which plays a key role in MALT lymphoma. *Mol Cell.* (2000), 6(4):961-7.

Vachova L. and Palkova Z. Physiological regulation of yeast cell death in multicellular colonies is triggered by ammonia. *J Cell Biol*. (2005), 169(5): 711-717.

Venter J.C., Adams M.D., Myers E.W., Li P.W., Mural R.J., Sutton G.G.; Smith H.O., Yandell M., Evans C.A., Holt R.A., et al. The Sequence of the Human Genome. *Science* (2001), 291:1304-51.

Vercammen D., van de Cotte B., De Jaeger G., Eeckhout D., Casteels P., Vandepoele K., Vandenberghe I., Van Beeumen J., Inzé D., Van Breusegem F. Type II metacaspases Atmc4 and Atmc9 of Arabidopsis thaliana cleave substrates after arginine and lysine. *J Biol Chem.* (2004) , 279(44):45329-36.

Wang X., Yang C., Chai J., Shi Y., Xue D. Mechanisms of AIF-mediated apoptotic DNA degradation in Caenorhabditis elegans. *Science* (2002), 298: 1587–1592.

Watanabe N., Lam E. Two Arabidopsis metacaspases AtMCP1b and AtMCP2b are arginine/lysine-specific cysteine proteases and activate apoptosis-like cell death in yeast. *J. Biol. Chem.* (2005), 280:14691–14699.

Wildgruber R., Reil G., Drews O., Parlar, H., Görg A. Web-based two-dimensional database of *Saccharomyces cerevisiae* proteins using immobilized pH gradients from

pH 6 to pH 12 and matrix-assisted laser desorption/ionization- time of flight mass spectrometry. *Proteomics* (2002), 2:727–732.

Wilkins M.R., Pasquali C., Appel R. D., Ou K., Golaz O., Sanchez J. C., Yan J. X., Gooley A. A., Hughes G., Humphery Smith I., Williams K. L., Hochstrasser D. F., From proteins to proteomes: Large scale protein identification by two-dimensional electrophoresis and amino acid analysis. *Bio-Technology* (1996), 14:61-65.

Wilkinson D., Ramsdale M. Proteases and caspase-like activity in the yeast *Saccharomyces cerevisiae*. *Biochem.Soc.Trans.* (2011), 39: 1502–1508.

Winzeler E. A., Shoemaker D. D., Astromoff A., Liang H., Anderson K., Andre B., Bangham R., Benito R., Boeke J. D., Bussey H. et al. Functional characterization of the *S.Cerevisiae* Genome by Gene Deletion and Parallel Analysis." *Science* (1999), 285:901-6.

Wissing S., Ludovico P., Herker E., Buttner S., Engelhardt S. M., Decker T., Link A., Proksch A., Rodrigues F., Corte-Real M., Frohlich K. U., Manns J., Cande C., Sigrist S. J., Kroemer G., Madeo F. An AIF orthologue regulates apoptosis in yeast. *J Cell Biol*. (2004), 166(7): 969-974.

Yin Z., Stead D., Selway L., Walker J., Riba-Garcia I., McLnerney T., Gaskell S., Oliver S.G., Cash P., Brown A.J. Proteomic response to amino acid starvation in Candida albicans and *Saccharomyces cerevisiae*. *Proteomics.* (2004), 4(8):2425-36.

CHAPTER 2
Non-death roles of Yca1p

Differential proteome-metabolome profiling of Yca1-knock-out and wild type cells reveals novel metabolic pathways and cellular processes dependent on the yeast metacaspase

2.1 Introduction

Mammalian caspases are the best studied of a large family of multifunctional proteases sharing a common caspase-haemoglobinase fold (CHF) (Aravind and Koonin, 2002). Caspases have a cysteine-dependent aspartate-specific protease activity with a central role in apoptosis, the major form of programmed cell death (PCD), and inflammation (Nicholson and Thornberry,1997; Earnshaw et al., 1999; Salvesen and Dixit, 1997). Proper regulation of apoptosis is critical for both development and tissue homeostasis, and malfunction of apoptosis contributes to the development of human diseases (Hanahan and Weinberg, 2000; Fulda, 2009; Fadeel et al., 1999). Caspase-mediated cleavage of specific substrates is responsible for most of the visible changes that characterize apoptotic cell death (Thornberry and Lazebnik, 1998). Caspases are synthesized as catalytically inactive zymogens that can be activated by a proteolytic cleavage by a processing caspase, or by holoenzyme formation (Earnshaw et al., 1999, Pop and Salvesen, 2009). Paracaspases, found in animals and slime molds, and metacaspases, from plants, fungi and protozoa, are two other classes of multifunctional CHF proteases, phylogenetically related to mammalian caspases (Aravind and Koonin, 2002; Uren et al., 2000) whose biochemistry and function are still poorly characterized (for refs see Tsiatsiani et al., 2011).

The discovery that the yeast *Saccharomyces cerevisiae* can undergo a form of PCD sharing several morphological and biochemical features with mammalian apoptosis (Carmona-Gutierrez et al., 2010) has further confirmed this unicellular eukaryote as an ideal model to study the molecular pathways regulating cell stress response and PCD (Portt et al., 2011; Ždralević et al., 2012). With this respect, it is of note that *S. cerevisiae* expresses a single metacaspase encoded by YCA1 gene. Yca1p undergoes caspase-like autocatalytic activation, similar to mammalian caspases (Madeo

et al., 2002). YCA1 was first implicated in PCD regulation in yeast: its overexpression coupled with oxidative stress or prolonged culture triggers cell death while its deletion decreases H_2O_2- or age-induced PCD (Madeo et al., 2002). However, metacaspase-dependent and –independent PCD pathways have been shown in yeast (Madeo et al., 2009). Interestingly, although YCA1 can modulate somehow a z-VAD-fmk-inhibited caspase-like activity (Madeo et al., 2002; Guaragnella et al., 2006), its protein product lacks Asp specificity and cleaves its targets preferentially after Arg or Lys residues (for refs see Tsiatsiani et al., 2011).

Recent investigations have also revealed a number of non-apoptotic cellular processes in which YCA1 is involved. YCA1 is implicated in cell cycle control; its deletion or catalytic inactivation was shown to alter cell cycle dynamics (Lee et al., 2008). In addition, YCA1 contributes to the fitness and adaptability of growing yeast through clearance of insoluble protein aggregates in an Hsp104 disaggregase and proteasome-dependent manner (Lee et al., 2010; Shrestha et al., 2013; Hill et al., 2014). Finally, YCA1 was reported to be implicated in the regulation of antioxidant status and mitochondrial respiration (Khan et al., 2005; Lefevre et al., 2012). Yet, both Yca1p biochemistry and physiological function in yeast are still elusive.

For the past decade, considerable effort has been invested in maturing proteomic technology to deliver information at a rate and cost commensurate to transcriptomic technologies. Proteomics technologies offer considerable opportunities for improved biological understanding and biomarker discovery. The central platform for proteomics is tandem mass spectrometry (MS) but a number of other technologies, resources, and expertise are absolutely required to perform meaningful experiments. The combination of complementary approaches on the protein and on the peptide level provided an almost complete overview of the proteome of entire cell like yeast or organelles by countervailing mutual drawbacks. Washburn and co-workers reported the first large-scale yeast proteome study in 2001 with the identification of 1483 proteins following ≈ 68 h of mass spectral analysis, i.e. 0.4 proteins were identified per minute (Washburn et al., 2001). Relative proteomic changes induced by YCA1 ablation in BY4741 background identified proteins involved in vacuolar catabolism, stress response, mitochondria-associated factors, the 20S proteasome and DNA repair proteins as species unique to YCA1-knock-out (*Δyca1*) strain (Lee et al., 2008; Lee et al., 2010).

In addition, a proteomic approach was used to understand the role of YCA1 in protein aggregate formation and dissolution (Shrestha et al., 2013). Nevertheless, the only specific substrate of yeast metacaspase identified to date is the enzyme glyceraldehyde-3-phosphate dehydrogenase (GAPDH) (Silva et al., 2011).

For a better understanding of physiological role of YCA1 in yeast cell, we combine proteomic and metabolomic data in order to provide valuable insight into conditional changes in the metabolic activity. While transcriptomics and proteomics provide important insights into the hierarchical regulation of metabolic flux, metabolomics shed light on the actual enzyme activity through metabolic regulation and mass action effects. Metabolomics is a comprehensive tool for monitoring processes within biological systems (Meyer et al., 2012). In fact, in a systemic viewpoint relevant biological information on living systems can be grasped from the study of small, albeit pivotal molecules, which constitute the fundamental bricks of metabolic pathways. Thus, proteomics and metabolomics offer a nonbiased suite of tools to address physiologic mechanisms from various levels by integrating signal transduction, cellular metabolism, and phenotype analysis.

In this context to better understand the physiological role of YCA1 in yeast cell, the total cellular proteomic analysis of wild type and *Δyca1* yeast cell was performed. By combining proteomics and metabolomics techniques, we linked alterations of protein expression to metabolism. Technical aspects of rapid-resolution reversed-phase HPLC on-line with mass spectrometry are hereby described. Finally, our results revealed that YCA1 is crucial in regulation of carbohydrate, amino acid and nucleotide metabolism and confirmed that its deletion causes a general decrease in protein synthesis and transport with an increase in cell stress response.

2.2. Materials and methods

2.2.1. *Yeast strains, growth conditions and protein extraction*

The *S.cerevisiae* strain used in this study were W303-1B (MATα ade2 leu2 his3 trp1 ura3) (X.J. Chen's lab§) and *Δyca1* (W303-1B yca1*Δ*::KanMX4)17. Cells were streaked out freshly on a YPD plate from the -80 ºC stock and incubated for two days at 30 ºC. Cells were inoculated from starter cultures in YPD medium (1% yeast extract,

2% bactopeptone, and 2% glucose) and grown at 26 °C with 150-rpm orbital rotation up to the mid-logarithmic phase (OD600 = 0.7 – 0.8). For the extraction of proteins from yeast cells YPX™ Yeast Protein Extraction Kit (Expedeon) was used. Cells were harvested (5000 × g, at 4 ºC for 5 min), and proteins were solubilized with extraction buffers provided in the kit, which contain SDS and reducing agents, providing unbiased extraction of proteins from cells. The buffers are designed to maximize the protein extraction and are compatible with downstream proteomics applications. Protease Inhibitor Cocktail (Sigma) was added to the cell lysate to improve the yield of intact proteins. The samples were denaturated at 100 ºC for 3 min, cooled down at 4 ºC for 10 min, harvested at 20000 × g for 10 min to pellet the cellular debris and the supernatant was collected for the analysis. For accurate determination of total protein concentration, Bradford Ultra (Expedeon) assay, compatible with the presence of detergents was used.

2.2.2. *2D-SDS-PAGE*

For each sample, 600 µg of proteins were precipitated for 90 min at 4 °C with a cold mix of tri-n-butylphosphate/acetone/methanol (1:12:1) in ratio 1:4. This step is useful also to remove lipid component of the samples. After centrifugation, the pellets were solubilized in the buffer containing 7 M urea, 2 M thiourea, 4% (w/v) CHAPS, 40 mM Tris-HCl and were reduced and alkylated. Subsequently to a second precipitation, the samples were resuspended in rehydration solution (7M urea, 2M thiourea, 4% CHAPS and 1.25% v/v 3-10 carrier ampholyte (Bio-rad, CA, USA) and used to carry out passive rehydration of IPG strips (pH 3-10, non linear, 17 cm; Bio-Rad, CA, USA) over night. Isoelectrofocusing (IEF) was performed on an Protean IEF Cell (Bio-Rad, CA, USA) at 20 °C constant temperature and the total product time×voltage applied was 80,000 V-h. SDS-PAGE was done in polyacrylamide gels (12% T, 2.6% C) at 35 mA per gel. The spots resulting by two dimensional separation were stained by sensitive Coomassie brilliant blue G-250 stain. To ensure protein pattern reproducibility, three technical replicates were performed.

2.2.3. *Image analysis and statistics*

Image analysis was carried out with computer software (Progenesis SameSpots, Version 2.0, Nonlinear Dynamics, Newcastle upon Tyne, UK). For each protein spot,

the average spot quantity value and its variance coefficient in each group was determined. One-way analysis of variance (ANOVA) was carried out at $p < 0.05$ to assess for absolute protein changes among the different treatments. The statistically significant spots with fold ≥ 2 were cut by EXQuest Spot Cutter (Bio-Rad, CA, USA) and subjected to in-gel trypsin digestion.

2.2.4. *Tryptic digestion*

Protein spots observed in 2D-SDS-PAGE were carefully excised from Comassie-stained polyacrylamide gels and subjected to in-gel trypsin digestion according to Shevchenko and coworkers (Shevchenko et al., 1996) with minor modifications. The supernatant containing tryptic peptides was dried by vacuum centrifugation. Prior to mass spectrometric analysis, the peptide mixtures were redissolved in 10 μL of 5% Formic Acid (FA).

2.2.5. *LC–ESI–CID–MS/MS (proteomic analysis)*

Samples were analyzed using a split-free nano-flow liquid chromatography system (EASY-nLC II, Proxeon, Odense, Denmark) coupled to a 3D-ion trap (model AmaZon ETD, Bruker Daltonik, Germany) equipped with an online ESI nano-sprayer (the spray capillary was a fused silica capillary, 0.090 mm o.d., 0.020 mm i.d.). For all experiments a sample volume of 15μL was loaded by the autosampler onto a homemade 2 cm fused silica precolumn (100 μm I.D.; 375 μm O.D.; Reprosil C18-AQ, 5 μm, Dr. Maisch GmbH, Ammerbuch-Entringen, Germany). Sequential elution of peptides was accomplished using a flow rate of 300 nL/min and a linear gradient from Solution A (2% acetonitrile; 0.1% formic acid) to 50% of Solution B (98% acetonitrile; 0.1% formic acid) in 40 min over the precolumn on-line with a homemade 15 cm resolving column (75 μm I.D.; 375 μm O.D.; Reprosil C18-AQ, 3 μm, Dr. Maisch GmbH, Ammerbuch-Entringen, Germany). The acquisition parameters for the mass spectrometer were as follows: dry gas temperature, 220 °C; dry gas, 4.0 L/min; nebulizer gas, 10 psi; electrospray voltage, 4000 V; high-voltage end-plate offset, − 200 V; capillary exit, 140 V; trap drive: 63.2; funnel 1 in, 100 V out 35 V and funnel 2 in, 12 V out 10 V; ICC target, 200 000; maximum accumulation time, 50 ms. The sample was measured with the “Enhanced Resolution Mode at 8100 *m/z* per second (which

allows mono isotopic resolution up to four charge stages) polarity positive, scan range from *m/z* 300 to 1500, 5 spectra averaged, and rolling average of 1. The "Smart Decomposition" was set to "auto". Acquired CID spectra were processed in DataAnalysis 4.0, and deconvoluted spectra were further analyzed with BioTools 3.2 software and submitted to Mascot search program (in-house version 2.2, Matrix Science, London, UK). The following parameters were adopted for database searches: NCBInr database (release date 22/09/2012; 20543454 sequences; 7050788919 residues); taxonomy=All entries; peptide and fragment mass tolerance of ± 0.3 Da; enzyme specificity trypsin with 2 missed cleavages considered; fixed modifications: carbamidomethyl (C); variable modifications: oxidation (M).

2.2.6. *Sample preparation for metabolomic analysis*

Wild type and *Δyca1* W303-1B yeast cells, grown in YPD medium up to exponential phase (OD600 about 0.7). $2x10^7$ cells were collected and used for metabolomic analysis. The yeast cells were resuspended in 100 µl of ice cold ultra-pure water (18 MΩ) to lyse the cells and then the tubes were plunged alternatively into a water bath at 37 °C for 0.5 minutes and at 4 °C for 0.5 minutes. To be sure that the cells are lysed, the samples were sonicated for 10 minutes. Samples were mixed with 400µl of −20 °C methanol and then with 600 µL of −20 °C chloroform. The tubes were stored at -20 °C over night. After centrifugation, we have taken the top fraction (methanol fraction) which contained metabolites.

2.2.7. *Rapid Resolution Reversed-Phase HPLC (metabolite separation)*

An Ultimate 3000 Rapid Resolution HPLC system (DIONEX, Sunnyvale, USA) was used to perform metabolite separation. The system featured a binary pump and vacuum degasser, well-plate autosampler with a six-port micro-switching valve, a thermostated column compartment. A Phenomenex Luna 3µm HILIC 200A (150 x 2.0 mm), protected by a guard column HILIC 4 x 2.0mm ID (Phenomenex) was used to perform metabolite separation over a phase B to phase A gradient lasting 35 minutes. For HILIC separation, 50 mM ammonium acetate was prepared by dissolving ammonium acetate in deionized water. The aqueous ammonium acetate was mixed with

acetonitrile (95:5, v/v). This was used for mobile phase 'A'. Eluent 'B' was composed of mixture of 50 mM aqueous ammonium acetate: water and acetonitrile (95:5), v/v).

Samples were loaded onto a Reprosil C18 column (2.0 mm × 150 mm, 2.5 µm Dr Maisch, Germany) for metabolite separation. Chromatographic separations were achieved at a column temperature of 30 °C; and flow rate of 0.2 mL/min.. For downstream positive ion mode (+) MS analyses, a 0–100% linear gradient of solvent A (ddH2O, 0.1% formic acid) to B (acetonitrile, 0.1% formic acid) was employed over 30 min, returning to 100% A in 2 min and a 6-min post-time solvent A hold. Acetonitrile, formic acid, and HPLC-grade water and standards (≥98% chemical purity) were purchased from Sigma Aldrich.

2.2.8. *Mass spectrometry: Q-TOF settings*

Due to the use of linear ion counting for direct comparisons against naturally expected isotopic ratios, time-of-flight instruments are most often the best choice for molecular formula determination. Thus, mass spectrometry analysis was carried out on an electrospray hybrid quadrupole time-of flight mass spectrometer MicroTOF-Q (Bruker-Daltonik, Bremen, Germany) equipped with an ESI-ion source. Mass spectra for metabolite extracted samples were acquired both in positive and in negative ion modes. ESI capillary voltage was set at 4500 V (+) (−) ion mode. The liquid nebulizer was set to 27 psi and the nitrogen drying gas was set to a flow rate of 6 L/min. Dry gas temperature was maintained at 200 °C. Data were stored in centroid mode. Data were acquired with a stored mass range of *m/z* 50–1200. Calibration of the mass analyzer is essential in order to maintain a high level of mass accuracy. Instrument calibration was performed externally every day with a sodium formate solution consisting of 10 mM sodium hydroxide in 50% isopropanol: water, 0.1% formic acid. Automated internal mass scale calibration was performed through direct automated injection of the calibration solution at the beginning and at the end of each run by a 6-port divert-valve.

2.2.9. *Untargeted metabolomics analysis*

Replicates were exported as mzXML files and processed through MAVEN.52 Mass spectrometry chromatograms were elaborated for peak alignment, matching and

comparison of parent and fragment ions, and tentative metabolite identification (within a 10 ppm mass-deviation range between observed and expected results against the imported KEGG database53). MAVEN is an open-source software that could be freely downloaded from the official project websites (http://genomics-pubs.princeton.edu/mzroll/index.php?show=download). Scatter plot are obtained from MAVEN.

2.2.10. *Bioinformatics analysis*

Protein sequences of all identified proteins were analyzed for the presence of tripeptide metacaspase substrates (ARR, GRR, VKKR, GGR, VLK)35 by Yeast Genome Pattern Matching tool (http://www.yeastgenome.org/cgi-bin/PATMATCH/nph-patmatch). Genome of *S. cerevisiae* strain W303 was chosen for the analysis and translation of all *S. cerevisiae* strain W303 ORFs was chosen as a sequence database.

2.3. Results and Discussion

2.3.1. *Differential proteomic and metabolomic analysis of WT and Δyca1 W303-1B cells*

In order to get an insight into the function of yeast metacaspase gene YCA1 the effect of its deletion on protein abundance was analyzed by comparative proteomic and metabolomic analysis between WT and knock-out W303-1B strain growing in mid-exponential phase. The total cellular proteomes of WT and *Δyca1* cells were obtained by 2-DE, and a total of 23 spots with altered amount of proteins in *Δyca1* cells (5 with increased and 18 with decreased amount) were successfully identified by using mass spectrometry analysis (**Figure 10**). To maximize performance we used a cellular lysis approach, employed trypsin digestion, and used dimethyl sulfoxide (DMSO, 5%) as an LC additive to increase abundance of acidic peptides and unify charge state in agreement to (Meyer et al., 2012; Hahne et al., 2013). In our case DMSO improved performance, as reported by Herbert and coworkers (Herbert et al., 2014), thus we included it in all subsequent experiments.

MS analysis showed that these spots corresponded to 26 proteins, which were classified into functional groups (**Table 1**).

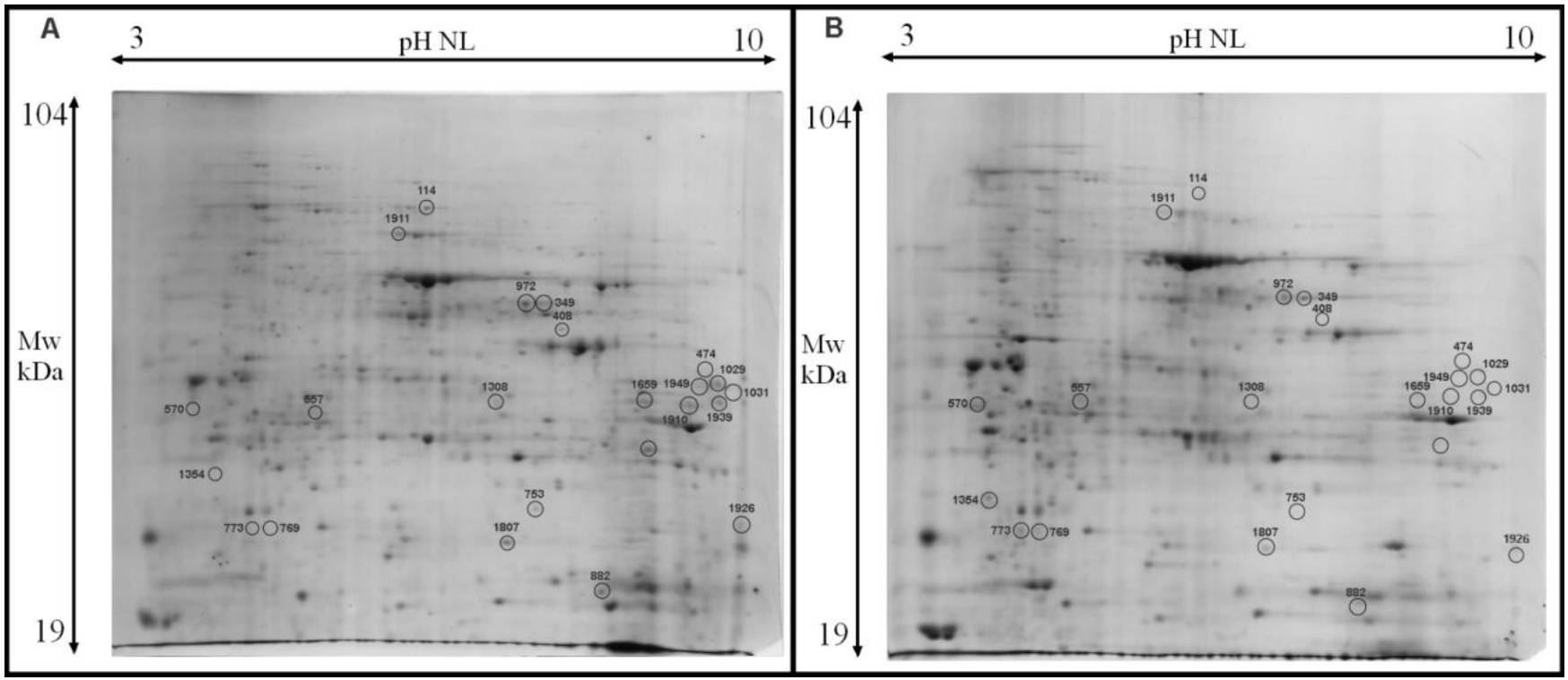

Figure 10. Representative 2-DE Coomasie-stained gels of total protein extract of W303-1B wild type and *Δyca1 S. cerevisiae* cells. Statistically significant differential spots (p value < 0.05 and fold change > 2) for WT (panel A) vs *Δyca1* (panel B) analysis are reported in both panels. Molecular weight (MW) and pI range of the first dimension strips (3-10 NL) are indicated on the appropriate axis. Numbers identify proteins with altered expression between the two gels, given as in Table 1. All experiments were performed in triplicate.

Table 1. Relative proteomic changes between WT and *Δyca1* cells

Spot number	*Theoretical Mr (Da)*	*Theoretical pI*	*N. of peptides identified*	*Mascot score*	*Proteins identified*	*Function*	*NCBI accession number*	*Fold change*	*Expression level*
Carbohydrate metabolism									
1911	39811	5.51	8	174	**Fba1**	*Fructose 1,6-bisphosphate aldolase*	gi|6322790	2.2	Down
882 *753*	35938 35938	6.46 6.46	24 7	427 58	**Tdh2**	*Glyceraldehyde-3-phosphate dehydrogenase, isozyme 2*	gi|6322468 gi|6322468	2.2 2.3	Down Down
1910	27461	8.86	37	600	**Gpm1**	*Glycerate PhosphoMutase*	gi|2624630	2.1	Down
114	46942	5.67	36	826	**Eno2**	*Enolase II*	gi|6321968	2.0	Down
1911	61685	5.8	27	593	**Pdc1**	*Pyruvate DeCarboxylase*	gi|6323073	2.2	Down
972 *349*	37282 37282	6.21 6.21	55 46	943 827	**Adh1**	*Alcohol dehydrogenase*	gi|6324486 gi|6324486	2.5 2.2	Down Down
408	37127	6.09	10	311	**Tal1**	*Transaldolase*	gi|6323386	2.1	Down
Amino acid metabolism									
408	38347	6.84	38	724	**Hom6**	*Homoserine dehydrogenase (L-homoserine:NADP oxidoreductase)*	gi|7245384	2.1	Down
649	37283	6.21	38	632	**Sfa1**	*Bifunctional alcohol dehydrogenase and formaldehyde*	gi|480311017	2.0	Down

						dehydrogenase			
Nucleic acid metabolism									
474	35387	8.51	5	133	**Prs3**	*PhosphoRibosylpyrophosphate Synthetase*	gi|6321776	3.3	Down
Translation machinery									
1031 *1029* *1939* *1926* *1949*	41542 41545 41542 50400 50400	8.36 8.36 8.36 9.14 9.14	27 33 19 7 11	359 505 415 149 199	**Tef1/2**	*Translation elongation factor*	gi|32563240 gi|32693297 gi|32563240 gi|6319594 gi|6319594	4.6 2.5 4.0 2.8 3.0	Down Down Down Down Down
1308	13685	5.91	3	99	**Rpl22a**	*Ribosomal 60S subunit protein L22A*	gi|6323090	2.1	Down
1659	28852	10.02	7	247	**Rps1b**	*Ribosomal protein 10 (RP10) of the small (40S) subunit*	gi|6323577	2.6	Down
1031 *649* *1949*	26543 26518 26543	9.42 9.44 9.42	22 4 24	555 106 575	**Rps3**	*Ribosomal protein of the small subunit*	gi|398364505 gi|468426 gi|398364505	4.6 2.0 3.0	Down Down Down
1910 *1659*	29449 29449	10.09 10.09	36 16	675 653	**Rps4b**	*Protein component of the small (40S) ribosomal subunit*	gi|6321997 gi|6321997	2.1 2.6	Down Down
882	15992	10.7	2	64	**Rps15**	*Ribosomal protein of the small subunit*	gi|6324533	2.2	Down
882	15838	10.26	4	92	**Rps16b**	*Ribosomal protein of the small subunit*	gi|6320120	2.2	Down
1354	18786	4.41	5	102	**Tma19**	*Translation machinery-associated protein 19*	gi|6322794	2.6	Up

Protein transport and folding									
1807	17010	6.1	12	253	**Egd1**	*Enhancer of Gal4 DNA binding*	gi|6325220	2.0	Down
1939	56630	9.42	2	51	**Nup57**	*FG-nucleoporin component of central core of the nuclear pore complex*	gi|1945327	4.0	Down
Stress response									
769 *773*	19274 19274	5.01 5.01	6 6	336 336	**Ahp1**	*Alkyl HydroPeroxide reductase*	gi|6323138 gi|6323138	2.8 2.1	Up Up
Cell wall biosynthesis									
570	29216	5.14	6	129	**Sec53**	*Phosphomannomutase*	gi|14318474	2.0	Up
408	39684	5.95	3	63	**Psa1**	*GDP-mannose pyrophosphorylase*	gi|894204	2.1	Down
Vacuolar acidification									
570	26568	5.48	6	136	**Vma4**	*Vacuolar H^+-Atp-ase*	gi|173169	2.0	Up
Unknown									
557	27541	5.10	15	210	**Hri1**	*HRr25 Interacting*	gi|6323332	2.1	Up
Other									
882	15956	9.07	3	124	**Mmf1**	*Mitochondrial Matrix Factor*	gi|151943108	2.2	Down

Several cellular processes were altered in the YCA1-lacking strain, including: i) metabolism of carbohydrates, ii) amino acids and iii) nucleotides, iv) transcription/translation machinery, v) protein transport and folding, vi) stress response, vii) cell wall biosynthesis and viii) vacuolar acidification. Relative expression changes of proteins altered in *Δyca1* cells are represented in **Figure 11**. The number and the corresponding name(s) of the identified proteins are indicated for each spot.

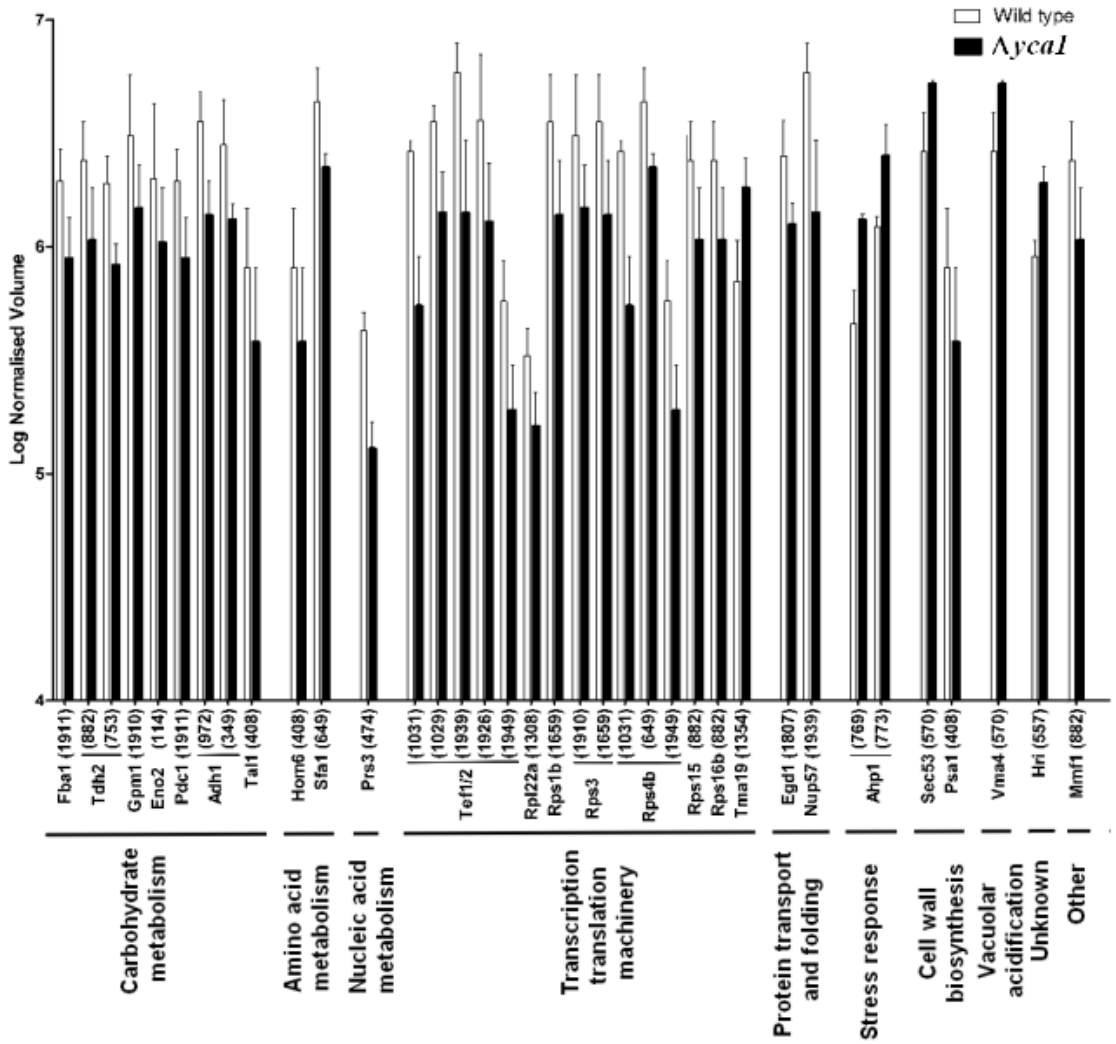

Figure 11. Relative protein expression changes of *Δyca1* with respect to the wild type cells. Black bars (*Δyca1*) and white bars (WT) represent the mean of normalized volume of single spot from 3 different replicates (in logarithmic scale) with correspondent standard deviation (SD), calculated by Progenesis SameSpots software Version 2.0, (Nonlinear Dynamics, Newcastle upon Tyne,UK).

Spots 753, 474, 1031, 1029, 1939, 1926 and 1949 (corresponding to Tdh2, Prs3, Tef 1/2, Rps3 and Nup57) were detected only in wild type cells, whereas two spots 773 and 570 (corresponding to Ahp1 and Vma/Sec54) were present only in *Δyca1* cells. The details of triplicate 2-D gel images of these spots are shown in **Figure 12**.

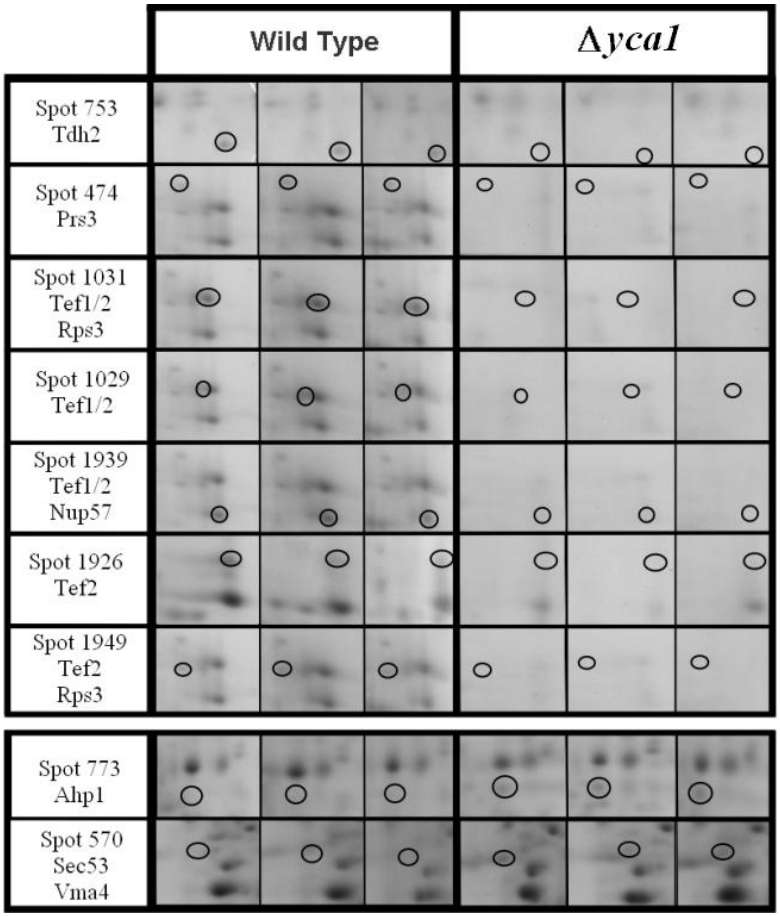

Figure 12. Magnified regions of triplicate 2-D gel images of protein spots detected exclusively in wild type or *Δyca1* cells. The number and the corresponding protein(s) are indicated for every spot. Spots 753, 474, 1031, 1029, 1939, 1926 and 1949 were detected only in wild type cells (corresponding to Tdh2, Prs3, Tef 1/2, Rps3 and Nup57), whereas spots 773 and 570 were present only in *Δyca1* cells (corresponding to Ahp1, Vma and Sec54).

Our results, using W303-1B strain, significantly differ qualitatively and quantitatively from the *Δyca1* cell proteomic profile characterized in BY4741 yeast strain: 59 and 13 proteins were found in higher and lower amounts, respectively, in YCA-knock-out BY4741 cells 19. This is mainly due to differences in both strains and

growth conditions analysed in the two studies. Although W303-1B and BY4741 cells were grown in glucose rich medium, in the case of BY4741 cells the growth medium pH has been set to 3.5 with HCl. Thus, the *Δyca1* W303-1B proteome profile obtained in this study is the first analysed at normal growth conditions (pH ~ 6.8). In fact, although there is no significant difference in the growth rate of either strains between normal and low pH growth medium, the acid environment used in the BY4741 study changed the pattern of gene expression observed at normal pH, causing metabolic re-programming and cellular adaptation (Carmelo et al., 1996; Gasch et al., 2002).

Furthermore, to characterize the role of YCA1 in yeast cell metabolism, we have performed HPLC-MS analysis of selected metabolites related to metabolic pathways altered by YCA1 deletion. Our metabolomics approach allows to discriminate and quantify a wide array of metabolites with extreme specificity and sensitivity, thus enabling to perform complex investigations even on extremely low quantities of biological material. The advantages also include the possibility to perform targeted investigations on a single (or a handful of) metabolite(s) simultaneously through single (multiple) reaction monitoring, which further improves the dynamic range of concentrations to be monitored. Files have been processed through MAVEN, an open-source software program for interactive processing of LC-MS-based metabolomics data. MAVEN enables rapid and reliable metabolite quantisation from multiple reaction monitoring data or high-resolution full-scan mass spectrometry data. It automatically detects and reports peak intensities for isotope-labelled metabolites (Clasquin et al., 2012). Metabolite assignment was further elaborated in the light of the hydrophobicity/hydrophilicity of the compound and its relative retention time in the RP-HILIC-HPLC run. Quantification of metabolites from carbohydrate, amino acid and nucleic acid metabolism and cell wall biosynthesis is shown in **Figure 13**.

In the next sections an integration of metabolomics and proteomics results, with special attention to those most affected metabolisms, will be discussed separately from the other cellular processes found to be affected by YCA1 deletion.

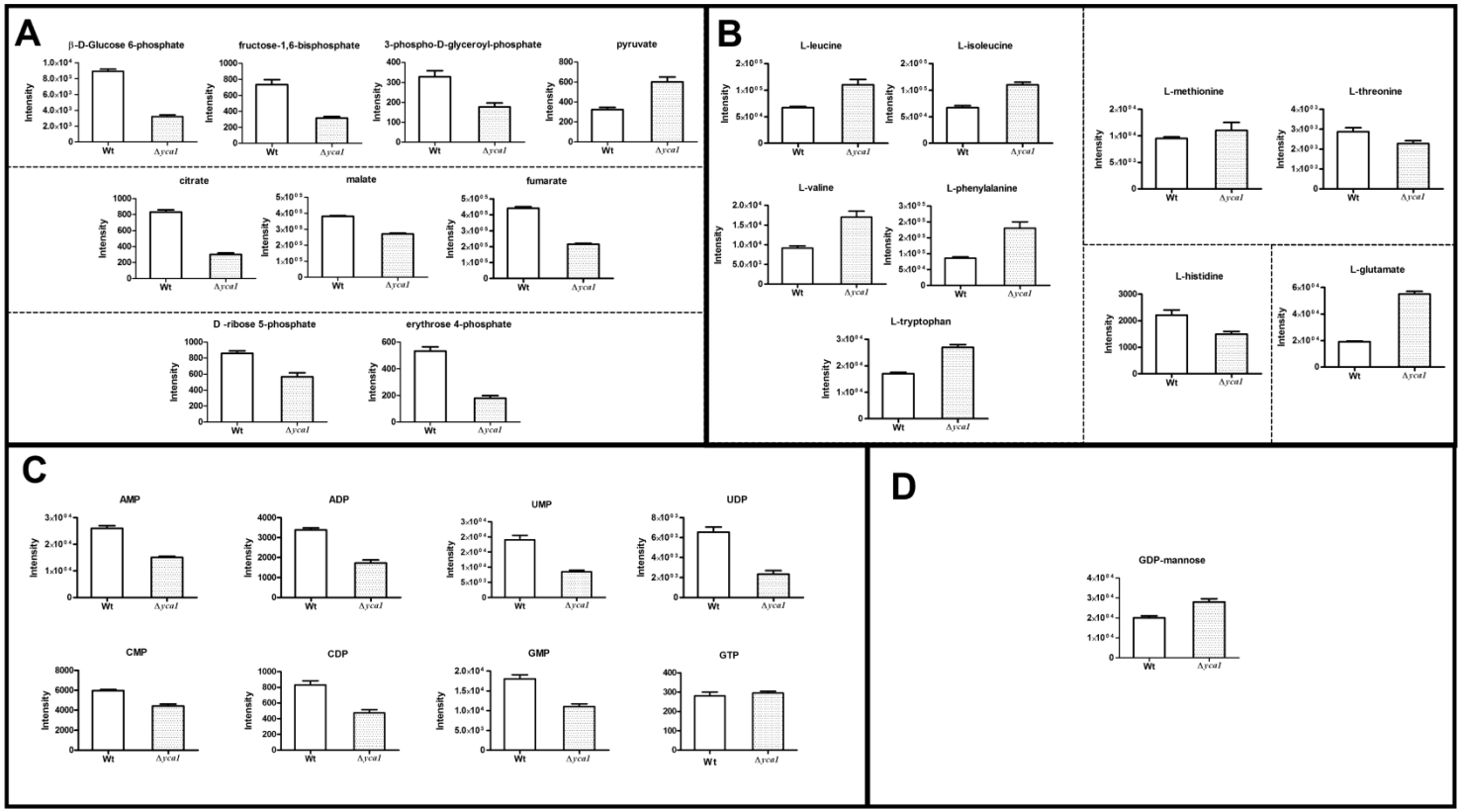

Figure 13. Absolute metabolomics quantification. Arbitrary ion counts of metabolites from carbohydrate metabolism (panel A) (glycolysis, citric acid cycle and pentose phosphate pathway), amino acid metabolism (panel B), nucleic acid metabolism (panel C) and cell wall biosynthesis (panel D) in W303-1B *S. cerevisiae* wild type (white bars) and *Δyca1* cells (dotted bars). Data are presented as mean ± SD.

2.3.2. *Δyca1 cells have altered carbohydrate, amino acid and nucleotide metabolism*

2.3.2.1. *Carbohydrate metabolism*

Glucose is the preferred carbon and energy source for yeast cells, but also an important primary messenger molecule, responsible for the down-regulation of respiration, gluconeogenesis and metabolism of other sugars (Rolland et al., 2002). In the exponential phase of growth, *S.cerevisiae* cells metabolize glucose mostly by fermentation to ethanol, despite the presence of oxygen (Diaz-Ruiz et al., 2011). We have found decreased amounts of all the seven proteins involved in carbohydrate metabolism in *Δyca1* cells. Fructose 1,6-bisphosphate aldolase (Fba1p), glyceraldehyde-3-phosphate dehydrogenase (Tdh2p/GAPDH), glycerate phosphomutase (Gpm1p) and enolase II (Eno2p) are glycolytic/gluconeogenetic enzymes; pyruvate decarboxylase (Pdc1p) and alcohol dehydrogenase (Adh1p) are involved in alcohol fermentation; and finally transaldolase (Tal1p) is a protein of pentose phosphate shunt.

GAPDH , already shown to be a specific target of metacaspase upon H_2O_2-induced apoptosis in yeast (Silva et al., 2011), was detected within two spots; 753 and 882, with significantly different MW both representing protein fragments. Silva and collaborators (Silva et al., 2011) showed by digestome analysis that GAPDH fragmentation is a biological phenomenon that occurs also independently on metacaspase activity, but additional protein fragments were detected under stressed-induced active metacaspase conditions (Silva et al., 2011). As shown in **Figure 12**, we detected spot 753 exclusively in WT cells, so this higher level of GAPDH fragmentation in WT cells is in agreement with the finding that specific GAPDH cleavage products occur only when metacaspase is active, that is in WT cells. Moreover, we performed bioinformatics analysis by analyzing GAPDH protein sequence for the presence of metacaspase-specific tripeptide cleavage sites with paired basic amino acid residues at P1 and P2 positions (Silva et al., 2005) , and identified the presence of Arg-specific cleavage site (GGR) at position 198 (**Table 2**). This is in agreement with first indications that GAPDH contains endopeptidase target-sequences distinct from the ones recognized by mammalian caspases (Silva et al., 2011). Yet, further biochemical and functional studies in physiological conditions are needed to identify the actual

metacaspase-specific cleavage site(s) in GAPDH. As a whole, these results confirm the validity of our experimental approach for exploring YCA1 function in yeast. We thus extended the bioinformatics analysis to all other differentially expressed proteins identified in our analysis as for the presence of putative metacaspase–specific cleavage sites. Seven proteins, beyond GAPDH were identified containing a metaspase-specific cleavage site and are reported in **Table 2**. Each protein identified will be discussed in the next sections with the relevant cellular process in which it is involved.

Sequence name (Protein ID)	Hit number	Match pattern	Match start position	Match stop position
YGR119C (Nup57p)	**1**	**VLK**	**293**	**295**
YOL086C (Adh1p)	**1**	**VLK**	**232**	**234**
YDL055C (Psa1p)	**1**	**VLK**	**96**	**98**
YLR301W (Hri1p)	**1**	**VLK**	**157**	**159**
YHR203C (Rps4bp)	**1**	**GGR**	**185**	**187**
YJR009C (Tdh2p)	**1**	**GGR**	**196**	**198**
YNL178W (Rps3p)	**1**	**GRR**	**63**	**65**
YHL011C (Prs3p)	**1**	**ARR**	**85**	**87**

Table 2. Proteins with altered expression between WT and *Δyca1* cells with putative metacaspase peptidyl substrates identified. All the proteins with altered expression between WT and *Δyca1* cells identified in our analysis were analyzed by Yeast Genome Pattern Matching (http://www.yeastgenome.org/cgi-bin/PATMATCH/nph-patmatch) for the presence of one or more peptide sequences for which recombinant Yca1p has been reported to display endopeptidase activity (Watanabe and Lam, 2005). Sequence pattern, together with its start and stop position in the protein sequence are reported.

Metabolomics analysis showed that the intracellular concentrations of glycolytic intermediates were significantly lower (about 56%) in *Δyca1* with respect to WT cells (**Figure 13**), which is consistent with the decreased amount of glycolytic enzymes determined by proteomic analysis. Thus, *Δyca1* cells showed decreased glycolysis with respect to the WT cells. The amount of tricarboxylic (TCA) acid cycle intermediates, citrate, malate and fumarate, also decreased in *Δyca1* cells, suggesting a down-regulation of respiratory activity, as already reported (Lefreve et al., 2012). Interestingly, pyruvate levels were found to be higher in *Δyca1* then in WT cells. This accumulation of pyruvate could be at least partially explained by decreased levels of the two enzymes of alcoholic fermentation, Pdc1p) and Adh1p, required for the reduction of acetaldehyde to ethanol. Finally, Adh1p was identified as a putative YCA1 substrate (**Table 2**), and it was detected in two spots (972 and 349) with different isoelectric points that could represent possible protein isoforms.

We have also found that Tal1p level decreased in *Δyca1* cells. Tal1p is a cytosolic transaldolase that converts sedoheptulose 7-phosphate and glyceraldehyde 3-phosphate to erythrose 4-phosphate and fructose 6-phosphate, important for the non-oxidative branch of the pentose phosphate pathway (PPP). Consistent with the lower amount of Tal1p found in these cells, erythrose 4-phosphate and D-ribose 5-phosphate had lower concentrations in *Δyca1* cells (**Figure 13**). By sharing some intermediate metabolites with glycolysis, Tal1p act as a bridge between glycolysis and PPP.

Altogether, these results showed a down-regulation of central carbon metabolism in *Δyca1* cells, including glycolysis, alcoholic fermentation and PPP with significant pyruvate accumulation. This in part could account for increased amount of amino acids induced by YCA1 deletion (see below).

2.3.2.2. *Amino acid metabolism*

Sfa1p, a bifunctional enzyme, containing both alcohol dehydrogenase and glutathione-dependent formaldehyde dehydrogenase activities, was found in lower amount in *Δyca1* cells. It is involved in the Ehrlich pathway for valine, isoleucine, phenylalanine, leucine and tryptophan degradation (Dickinson et al., 2003), as well as in detoxification of formaldehyde (Wehner et al., 1993). In fact, the concentrations of valine, leucine, isoleucine, phenylalanine and tryptophane were significantly higher in

Δyca1 than in the WT cells (**Figure 13**). Accordingly, Pdc1p and Adh1p, two other enzymes involved in Ehrlich pathway (Rinnerthaler et al., 2006), were down-regulated (see section 2.3.2.1). These results are also in agreement with the high levels of pyruvate observed in *Δyca1* cells, since pyruvate is a precursor of valine, leucine and isoleucine. Transcription of SFA1 is controlled by the HOG pathway, which controls cell response to osmotic shock (Guaragnella et al., 2010). In response to hyperosmotic stress yeast cells undergo PCD in a YCA1-dependent manner as shown by reduced cell death in *Δyca1* (Silva et al., 2005). Thus, whether and how YCA1 is related to HOG pathway deserves further investigation. It is of note that, differently from other aromatic amino acids, histidine levels were lower (37%) in *Δyca1* with respect to the WT cells.

Another enzyme of amino acid metabolism was found in lower amount to be down-regulated in the cells lacking YCA1 (**Figure 11**). The first enzyme is homoserine dehydrogenase (Hom6p), which catalyzes the third step in the common pathway for methionine and threonine biosynthesis from aspartate (Robichon-Szulmajster et al., 1966). Metabolomics analysis revealed that L-threonine concentration was lower in *Δyca1* with respect to WT cells, which is in agreement with proteomics data, while L-methionine concentration remains virtually unchanged (**Figure 13**).

2.3.2.3. *Nucleotide metabolism*

Beyond the relative proteomic changes identified in carbohydrate and amino acid metabolism, only one enzyme, 5-phospho-ribosyl-1(α)-pyrophosphate synthetase (Prs3p), involved into nucleotide metabolism, was detected exclusively in WT cells (**Figure 12**). Prs3p catalyzes biosynthesis of phosphoribosylpyrophosphate (PRPP). PRPP is an important biosynthetic intermediate, a precursor for the production of purine, pyrimidine, and pyridine nucleotides and the amino acids histidine and tryptophan, and is required for both de novo and the salvage pathways of nucleotide metabolism (Hazelwood et al., 2008). Accordingly, metabolomics analysis of the *Δyca1* cells showed a significant reduction in nucleotide content as compared with that of the WT cells, except for GTP content which remained virtually unchanged. Indeed, adenine nucleotides (AMP+ADP) were ~54% of the WT levels, GMP 60% of the WT levels and uridine nucleotides (UMP+UDP) 40% of the WT levels (**Figure 13**), consistent with the

down-regulation of Prs3p. The absence of Prs3p in YCA1-knock-out cells could also in part explain the decreased histidine content observed in these cells (see section 2.3.2.2). The apparent decrease in nucleotide content in *Δyca1* cells complies with a longer G1/S transition accompanied by slower growth of these cells in fermentation conditions (Lee et al., 2008).

Interestigly, Prs3p harbours a metacaspase-specific cleavage site (**Table 2**). We could speculate that YCA1 may have a role in Prs3p maturation, with Prs3p precursor protein being more susceptible to degradation in *Δyca1* cells, in which the protein is not detected.

2.3.3. *Protein biosynthesis, transport and folding are down-regulated in cells lacking YCA1*

The amount of eight proteins involved in protein biosynthesis and ribosome biogenesis was found to be altered in *Δyca1* cells. These proteins mainly showed a lower level (88%) than that in WT cells. Translation elongation factor (Tef1/2p) was detected in five different spots in WT cells. Spots 1031, 1029, 1939 and 1949 represent protein isoforms, whereas spot 1926 has a lower Mr and represent a putative protein fragment (**Figure 10**). However, none of the five spots was detected in *Δyca1* cells, as shown in **Figure 12**. Six ribosomal proteins were found to decrease their expression in *Δyca1* cells (**Table 1**). Ribosomal protein of the small (40S) subunit (Rps3p) was identified in three spots, two of which could represent protein isoforms (1031 and 1949) and spot 649 might represent a fragmented form. Spots 1031 and 1949 are detected exclusively in WT cells (**Figure 12**). Another ribosomal protein, Rps4b, was identified in two spots, that differed only by their pI, suggesting a possible additional PTM (**Figure 10**). In both Rps3p and Rps4b ribosomal subunits we have identified the presence of Arg-specific putative cleavage sites (**Table 2**). Thus, we could speculate that YCA1 is somehow involved in maturation of functional Rps4bp and Rps3p.

In agreement with the decreased level of proteins involved in the translation machinery observed in *Δyca1* cells, we have found decreased amount of proteins regulating co-translational protein folding and protein targeting to different subcellular locations. Two proteins (Egd1p and Nup57p) involved in protein transport and folding were found to be down-regulated in cells lacking YCA1. Egd1p is a subunit of the

nascent polypeptide-associated complex (NAC), involved in regulation of 'de novo' co-translational protein folding, post-translational protein targeting to membrane and unfolded protein binding. NAC complex is associated with cytoplasmic ribosomes and has a role in protein targeting to many subcellular locations, including mitochondria (Saito et al. 2012). Nup57p is an essential component of the central core of nuclear pore complex (NPC), responsible for the nucleocytoplasmic transport of macromolecules. Nup57p is one of the proteins identified as a potential YCA1 substrate (**Table 2**).

Altogether, these results suggest a lower efficiency of protein synthesis machinery in *Δyca1* cells, according to Shrestha and coworkers (Shrestha et al., 2013) that confirm a major role of YCA1 in cell stress response. Indeed, since YCA1 has a major role in proteostasis *Δyca1* cells may use a compensatory mechanism to limit protein production during stress (Shrestha et al., 2013). Ribosome biogenesis is energetically expensive to the cell; it utilizes ~90 % of the total cellular energy of exponentially growing yeast cells (Warner et al., 2001). Thus, down-regulation of the translation machinery is in agreement with the overall decrease in central carbon metabolism found in *Δyca1* cells.

Within this class of proteins, Tma19p (Mm1p) is the only protein found to be accumulated in *Δyca1* cells. Tma19p is the yeast orthologue of mammalian translationally-controlled tumor protein (TCTP), which has presumably anti-apoptotic functions in humans and interacts with translational machinery (Rinnerthaler et al., 2006). It has been shown that induction of apoptosis in *S cerevisiae* cells by oxidative stress, replicative ageing or mutation of CDC48 leads to translocation of Mmi1p from the cytoplasm to the mitochondria, and it also interacts with microtubules, stabilizing them (Rinnerthaler et al., 2006). The functional significance of Mmi1p transfer to mitochondria upon stress is still not clear, but the comparison with the mammalian system could offer an explanation of this transfer serving an anti-apoptotic function. Co-regulation of TCTP with ribosomal proteins has already been indicated by bioinformatics and experimental data (Rinnerthaler et al., 2006). Also, cells lacking MMI1 showed increased resistance to oxidative stress, as in YCA1-lacking cells (Khan et al., 2005; Rinnerthaler et al., 2006) but how MMI1 and YCA1 are interrelated deserves further investigations.

2.3.4. *Δyca1 cells are in oxidizing condition*

Genetic ablation of YCA1 caused accumulation of alkyl hydroperoxide reductase (Ahp1p), a thiol-specific peroxiredoxin, involved in cellular response to oxidative stress. Ahp1p was identified in *Δyca1* cells in two different spots with the same Mr, but slightly different pI, suggesting additional post-translational modification (PTM). Actually, one of the Ahp1p isoforms (spot 773) was detected exclusively in *Δyca1* cells (**Figure 12**). In fairly good agreement with our data, transcription of most of the genes involved in antioxidant defence mechanisms was shown to be repressed in *Δyca1* cells, except for an increase in AHP1 transcription (Lefevre et al., 2012). This result indicates a shift in *Δyca1* cell redox balance towards more oxidizing conditions. Although exponentially growing *Δyca1* cells have essentially unchanged ROS levels compared to WT cells (Lee et al., 2008; Guaragnella et al., 2010), these cells have been shown to have increased total and oxidized (GSSG) glutathione content in comparison with WT cells (Lefevre et al., 2012). YCA1 has already been implicated in the regulation of antioxidant defences; YCA1 deletion leads to a large H_2O_2-dependent accumulation of intracellular oxidized proteins and a compensatory increase in 20S proteasome activity, an essential part of the protein oxidation surveillance mechanism (Khan et al., 2005).

In addition, increased expression of molecular chaperones and activation of stress response pathways in *Δyca1* yeast cells has been already shown, in a different genetic background and environmental conditions (Lee et al., 2010). Those and our data further support the hypothesisthat *Δyca1* cells may be pre-conditioned to sudden insults. YCA1 deletion may induce compensatory changes in stress response proteins offering a better protection against apoptotic insults to *Δyca1* cells (Guaragnella et al., 2006; Lee et al., 2010), rather than a loss in a pro-apoptotic YCA1-associated activity (for Ref. Wilkinson and Ramsdale, 2011).

2.3.5. *Cell wall biosynthesis is altered in Δyca1 cells*

The expression of two enzymes involved in the cell wall biosynthesis, phosphomannomutase (Sec53p) and GDP-mannose pyrophosphorylase (Psa1p), was found to be altered by YCA1 deletion. Sec53p was present exclusively in *Δyca1* cells

(**Figure 12**). It is involved in synthesis of GDP-mannose and dolichol-phosphate-mannose and required for folding and glycosylation of secretory proteins in the ER lumen, as well as in protein targeting to ER. Sec53p catalyzes the conversion of mannose-6-phosphate to mannose-1-phosphate, an intermediate in the cell wall biosynthesis (Rinnerthaler et al., 2006). Psa1p, an enzyme catalyzing the next step in the pathway, the synthesis of GDP-mannose from mannose-1-phosphate and GTP, was found to be down-regulated in *Δyca1* cells. Psa1p was identified as a putative YCA1 substrate (**Table 2**). However, our metabolic analysis showed a 50% increase in the concentration of GDP-mannose in *Δyca1* cells (**Figure 13**), accordingly with Sec53p up-regulation. The yeast cell wall has diverse physiological functions: it maintains cell shape and integrity, and protects cell interior from environmental stresses. Proteins glycosylated by long chains of mannose residues represent 40-50 % of the cell wall mass (Francois et al., 2013). Thus, an increase in GDP-mannose levels in *Δyca1* cells could influence the capacity of dynamical remodelling of the cell wall upon environmental stresses (see section 2.3.4).

2.3.6. *Other cellular processes affected by YCA1 deletion*

Accumulation of other stress-related proteins has been observed in *Δyca1* cells. Subunit E of the V1 domain of the vacuolar H+-ATP-ase (Vma4p) was found exclusively in *Δyca1* cells (Fig. 3). Vacuolar ATP-ases are ATP-dependent proton pumps with a role in acidifying vacuolar compartments, which provides the driving force for secondary transport of variety of ions and metabolites (Plant et al., 1999). *Δyca1* BY4741 cells grown in low pH medium were shown to be enriched in vacuolar peptidases and to accumulate autophagic bodies, implying that a limited autophagic process occurs in these cells (Lee et al., 2010). In this study, *Δyca1* W303-1B cells are viable cells at normal pH, with the growth rate comparable to that of WT cells, and it has also been shown that basal macroautophagy levels in exponentially growing WT and *Δyca1* cells are essentially the same (Warner et al., 2001). Thus, YCA1 may have a role in intracellular pH homeostasis.

HRr25-interacting protein (Hri1p), whose function is unknown, showed increased amount in *Δyca1* cells. The function of Hri1p is still not completely understood, but in fission yeast Hri1p is known to function as a kinase of initiation

factor 2α (eIF2α), involved in the regulation of protein synthesis in response to various environmental stresses. Hri1p was shown to be activated by both nitrogen starvation and stationary phase entry stresses (Martin et al., 2013). Hri1p is the only protein accumulated in *Δyca1* cells harboring a putative metacaspase cleavage site (**Table 2**), suggesting that Hri1p may be degraded by YCA1.

Finally, the amount of mitochondrial protein Mmf1p, involved in maintenance of mitochondrial genome (Oxelmark et al., 2000), was found to decrease in cells lacking YCA1. Mmf1p is also required for transamination of isoleucine but not of valine or leucine and may regulate specificity of branched-chain transaminases Bat1p and Bat2p47. Accordingly, an increase in isoleucine content was found in *Δyca1* cells (see section 2.3.2.2).

2.4. Conclusions

In this section of work, we used a combination of proteomic and metabolomic analysis to identify metabolic pathways and cellular processes affected by YCA1 deletion in *S.cerevisiae* W303-1B genetic background under physiological growth conditions. Relevant information could be retrieved when performing both proteomics and metabolomics analysis simultaneously.

Our results increased the knowledge about cellular processes and proteins whose roles and functions depend on YCA1 in yeast. The data obtained show a role of YCA1 in the modulation of central carbon metabolism as well as amino acid and nucleotide metabolism. YCA1 deletion appears to down-regulate glycolysis, TCA cycle and alcoholic fermentation as compared with WT cells. *Δyca1* cells also showed a down-regulation of PPP and an accumulation of pyruvate, correlated with higher levels of certain amino acids found in these cells. Accordingly, there is a decrease in protein biosynthesis and protein transport/folding, and accumulation of various stress response proteins like Ahp1p, which possibly provides these cells with a better protection against stress.

We also identified eight proteins containing peptide sequences for which recombinant Yca1p has been shown to display endopeptidase activity (Watanabe and Lam,2005). However, in no case we found evidences of accumulation of uncleaved

polypeptides in *Δyca1* cells indicative of the presence of active metacaspase cleavage in WT cells. Thus, at least in our physiological growth conditions yeast metacaspase does not seem to cleave these sites.

To better understand the interactions between all proteins identified and metacaspase, we obtained a network pathway using STRING software (http://string-db.org) (**Figure 14**). It has been already demonstrated that Yca1p participates at different steps in cell cycle dynamics (Lee et al., 2008) and that has a role in proteostasis through regulation of the composition of insoluble proteins (Shrestha et al., 2013). Our combined proteome/metabolome approach added a new dimension to the non-apoptotic function of yeast metacaspase, which can specifically affect cell metabolism through as yet unknown mechanisms and possibly stress-response pathways, like HOG and cell wall integrity pathways.

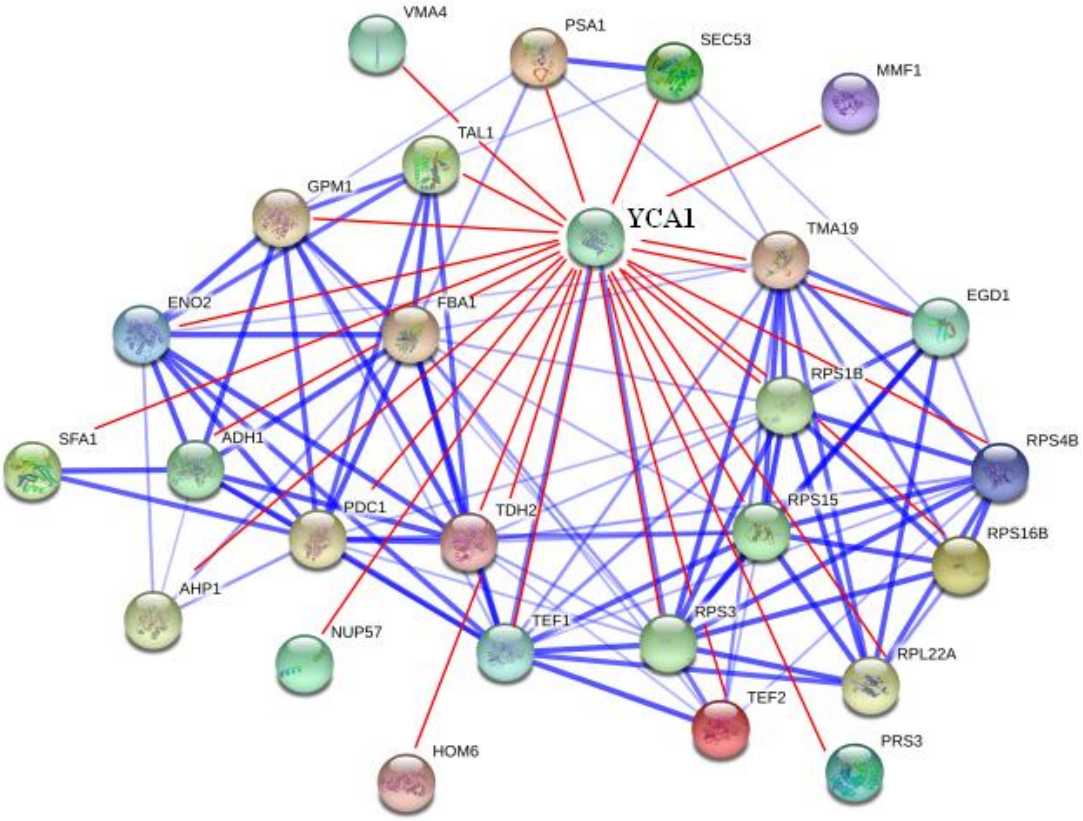

Figure 14. STRING Analysis (http://string-db.org). STRING Analysis of the proteins downn/up-regulated by metacaspase. Red and blue double lines represent known protein interactions of *YCA1*, red single lines are new *YCA1* interactors found and involved in cell metabolism and stress-response pathways.

REFERENCES

Antonacci L., Guaragnella N., Ždralevic M., Passarella S., Marra E., Giannattasio S. The N-acetylcysteine-insensitive acetic acid-induced yeast programmed cell death occurs without macroautophagy. *Curr Pharm Biotechnol.* (2012), 13(15):2705-11.

Aravind L. and Koonin E.V. Classification of the caspase-hemoglobinase fold: detection of new families and implications for the origin of the eukaryotic separins. *Proteins* (2002), 46(4): 355-67.

Carmelo V., Bogaerts P., Sá-Correia I. Activity of plasma membrane H+-ATPase and expression of PMA1 and PMA2 genes in *Saccharomyces cerevisiae* cells grown at optimal and low pH. *Arch Microbiol.* (1996), 166(5):315-20.

Carmona-Gutierrez D., Eisenberg T., Büttner S., Meisinger C., Kroemer G., Madeo F. Apoptosis in yeast: triggers, pathways, subroutines. *Cell Death Differ.* (2010), 17(5):763-73. Review.

Clasquin M.F., Melamud E., Rabinowitz J.D. LC-MS data processing with MAVEN: a metabolomic analysis and visualization engine. *Curr Protoc Bioinformatics.* (2012), Chapter 14:Unit14.11.

Diaz-Ruiz R., Rigoulet M., Devin A. The Warburg and Crabtree effects: On the origin of cancer cell energy metabolism and of yeast glucose repression. *Biochim Biophys Acta.* (2011), 1807(6):568-76.

Dickinson JR, Salgado LE, Hewlins MJ. The catabolism of amino acids to longchain and complex alcohols in *Saccharomyces cerevisiae*. *J Biol Chem.* (2003), 7;278(10):8028-34.

Earnshaw W.C., Martins L.M., Kaufmann S.H. Mammalian caspases: structure, activation, substrates, and functions during apoptosis. *Annu Rev Biochem.*(1999), 68:383-424. Review.

Fadeel B., Orrenius S., Zhivotovsky B. Apoptosis in human disease: a new skin for the old ceremony? *Biochem Biophys Res Commun.* (1999), 266(3):699-717.

Francois J.M., Formosa C., Schiavone M., Pillet F., Martin-Yken H., Dague E. Use of atomic force microscopy (AFM) to explore cell wall properties and response to stress in the yeast *Saccharomyces cerevisiae*. *Curr Genet*. (2013), 59(4):187-96. Review.

Fulda S. Tumor resistance to apoptosis. *Int J Cancer.* (2009), 124(3):511-5. Review.

Gasch A.P. and Werner-Washburne M. The genomics of yeast responses to environmental stress and starvation. *Funct Integr Genomics.* (2002), 2(4-5):181-92.

George R., Beddoe T., Landl K., Lithgow T. The yeast nascent polypeptide-associated complex initiates protein targeting to mitochondria in vivo. *Proc Natl Acad Sci U S A.* (1998), 3;95(5):2296-301.

Guaragnella N., Bobba A., Passarella S., Marra E., Giannattasio S. Yeast acetic acid-induced programmed cell death can occur without cytochrome c release which requires metacaspase YCA1. *FEBS Lett.* (2010), 4;584(1):224-8.

Guaragnella N., Pereira C., Sousa M.J., Antonacci L., Passarella S., Côrte-Real M., Marra E., Giannattasio S. YCA1 participates in the acetic acid induced yeastprogrammed cell death also in a manner unrelated to its caspase-like activity.*FEBS Lett.* (2006), 580(30):6880-4.

Hahne H., Pachl F., Ruprecht B., Maier S.K., Klaeger S., Helm D., Médard G., Wilm M., Lemeer S., Kuster B. DMSO enhances electrospray response, boosting sensitivity of proteomic experiments. *Nat Methods.* (2013), 10(10):989-91.

Hanahan D. and Weinberg R.A. The hallmarks of cancer. *Cell.* (2000), 100(1):57-70. Review.

Hazelwood L.A., Daran J.M., van Maris A.J., Pronk J.T., Dickinson J.R. The Ehrlich pathway for fusel alcohol production: a century of research on

Saccharomyces cerevisiae metabolism. *Appl Environ Microbiol*. (2008), 74(8):2259-66.

Hebert A.S., Richards A.L., Bailey D.J., Ulbrich A., Coughlin E.E., Westphall M.S., Coon J.J. The one hour yeast proteome. *Mol Cell Proteomics.* (2014), 13(1):339-47.

Hernando Y., Carter A.T., Parr A., Hove-Jensen B., Schweizer M. Genetic analysis and enzyme activity suggest the existence of more than one minimal functional unit capable of synthesizing phosphoribosyl pyrophosphate in *Saccharomyces cerevisiae. J Biol Chem.* (1999), 274(18):12480-7.

Hill S.M., Hao X., Liu B., Nyström T. Life-span extension by a metacaspase in the yeast *Saccharomyces cerevisiae*. *Science.* (2014),344(6190):1389-92.

Kepes F. and Schekman R. The yeast SEC53 gene encodes phosphomannomutase. *J Biol Chem.* (1988), 263(19):9155-61.

Khan M.A., Chock P.B., Stadtman E.R. Knockout of caspase-like gene, YCA1, abrogates apoptosis and elevates oxidized proteins in *Saccharomyces cerevisiae*. *Proc Natl Acad Sci U S A.* (2005), 102(48):17326-31.

Kim J.M., Yoshikawa H., Shirahige K. A member of the YER057c/yjgf/Uk114 family links isoleucine biosynthesis and intact mitochondria maintenance in *Saccharomyces cerevisiae*. *Genes Cells*. (2001), 6(6):507-17.

Lee R.E., Brunette S., Puente L.G., Megeney L.A. Metacaspase Yca1 is required for clearance of insoluble protein aggregates. *Proc Natl Acad Sci U S A.* (2010), 27;107(30):13348-53.

Lee R.E., Puente L.G., Kaern M., Megeney L.A. A non-death role of the yeast metacaspase: Yca1p alters cell cycle dynamics. *PLoS One.* (2008), 3;3(8):e2956.

Lefevre S., Sliwa D., Auchère F., Brossas C., Ruckenstuhl C., Boggetto N., Lesuisse E., Madeo F., Camadro J.M., Santos R. The yeast metacaspase is implicated in oxidative stress response in frataxin-deficient cells. *FEBS Lett.* (2012), 586(2):143-8.

Madeo F., Carmona-Gutierrez D., Ring J., Büttner S., Eisenberg T., Kroemer G. Caspase-dependent and caspase-independent cell death pathways in yeast. *Biochem Biophys Res Commun.* (2009), 1;382(2):227-31. Review.

Madeo F., Herker E., Maldener C., Wissing S., Lächelt S., Herlan M., Fehr M., Lauber K., Sigrist S.J., Wesselborg S., Fröhlich K.U. A caspase-related protease regulates apoptosis in yeast. *Mol Cell.* (2002), 9(4):911-7.

Martín R., Berlanga J.J., de Haro C. New roles of the fission yeast eIF2α kinases Hri1 and Gcn2 in response to nutritional stress. *J Cell Sci*. (2013), 126(Pt 14):3010-20.

Meyer J.G. and A Komives E. Charge state coalescence during electrospray ionization improves peptide identification by tandem mass spectrometry. *J Am Soc Mass Spectrom.* (2012), 23(8):1390-9.

Nicholson D.W. and Thornberry N.A. Caspases: killer proteases. *Trends Biochem Sci.*(1997), 22(8):299-306. Review.

Oxelmark E., Marchini A., Malanchi I., Magherini F., Jaquet L., Hajibagheri M.A., Blight K.J., Jauniaux J.C., Tommasino M. Mmf1p, a novel yeast mitochondrial protein conserved throughout evolution and involved in maintenance of the mitochondrial genome. *Mol Cell Biol.* (2000), 20(20):7784-97.

Plant P.J., Manolson M.F., Grinstein S., Demaurex N. Alternative mechanisms of vacuolar acidification in H(+)-ATPase-deficient yeast. *J Biol Chem.* (1999), 24;274(52):37270-9.

Pop C. and Salvesen G.S. Human caspases: activation, specificity, and regulation. *J Biol Chem.* (2009), 284(33):21777-81. Review.

Portt L., Norman G., Clapp C., Greenwood M., Greenwood M.T. Anti-apoptosis and cell survival: a review. *Biochim Biophys Acta*. (2011),1813(1):238-59. Review.

Rinnerthaler M., Jarolim S., Heeren G., Palle E., Perju S., Klinger H., Bogengruber E., Madeo F., Braun R.J., Breitenbach-Koller L., Breitenbach M., Laun P. MMI1 (YKL056c, TMA19), the yeast orthologue of the translationally

controlled tumor protein (TCTP) has apoptotic functions and interacts with both microtubules and mitochondria. *Biochim Biophys Acta.* (2006), 1757(5-6):631-8.

Robichon-Szulmajster H., Surdin Y., Mortimer R.K. Genetic and biochemical studies of genes controlling the synthesis of threonine and methionine in Saccharomyces. *Genetics*. (1966), 53(3):609-19.

Rolland F., Winderickx J., Thevelein J.M. Glucose-sensing and –signalling mechanisms in yeast. *FEMS Yeast Res*. (2002), 2(2):183-201. Review.

Saito H and Posas F. Response to hyperosmotic stress. *Genetics.* (2012), 192(2):289-318. Review.

Salvesen G.S. and Dixit V.M. Caspases: intracellular signaling by proteolysis. *Cell.* (1997), 91(4):443-6. Review.

Shevchenko A., Wilm M., Vorm O., Mann M. Mass spectrometric sequencing of proteins silver-stained polyacrylamide gels. *Anal Chem.* (1996), 68(5):850-8.

Shrestha A., Puente L.G., Brunette S., Megeney L.A. The role of Yca1 inproteostasis. Yca1 regulates the composition of the insoluble proteome. *J Proteomics.* (2013), 9;81:24-30.

Silva A., Almeida B., Sampaio-Marques B., Reis M.I., Ohlmeier S., Rodrigues F., Vale Ad., Ludovico P. Glyceraldehyde-3-phosphate dehydrogenase (GAPDH) is a specific substrate of yeast metacaspase. *Biochim Biophys Acta.* (2011), 1813(12):2044-9.

Silva R.D., Sotoca R., Johansson B., Ludovico P., Sansonetty F., Silva M.T., Peinado J.M., Côrte-Real M. Hyperosmotic stress induces metacaspase- and mitochondria-dependent apoptosis in *Saccharomyces cerevisiae*. *Mol Microbiol*. (2005), 58(3):824-34.

Thornberry N.A. and Lazebnik Y. Caspases: enemies within. *Science.* (1998), 281(5381):1312-6. Review.

Tsiatsiani L., Van Breusegem F., Gallois P., Zavialov A., Lam E., Bozhkov P.V. Metacaspases. *Cell Death Differ.* (2011), 18(8):1279-88. Review.

Uren A.G., O'Rourke K., Aravind L.A., Pisabarro M.T., Seshagiri S., Koonin E.V., Dixit V.M. Identification of paracaspases and metacaspases: two ancient families of caspase-like proteins, one of which plays a key role in MALT lymphoma. *Mol Cell.* (2000), 6(4):961-7.

Warner J.R., Vilardell J., Sohn J.H. Economics of ribosome biosynthesis. *Cold Spring Harb Symp Quant Biol.*(2001), 66:567-74. Review.

Washburn M.P., Wolters D., Yates JR 3rd. Large-scale analysis of the yeast proteome by multidimensional protein identification technology. *Nat Biotechnol.* (2001), 19(3):242-7.

Watanabe N. and Lam E. Two Arabidopsis metacaspases AtMCP1b and AtMCP2b are arginine/lysine-specific cysteine proteases and activate apoptosis-like cell death in yeast. *J Biol Chem.* (2005), 15;280(15):14691-9.

Wehner E.P., Rao E., Brendel M. Molecular structure and genetic regulation of SFA, a gene responsible for resistance to formaldehyde in *Saccharomyces cerevisiae*, and characterization of its protein product. *Mol Gen Genet*. (1993), 237(3):351-8.

Wilkinson D. and Ramsdale M. Proteases and caspase-like activity in the yeast *Saccharomyces cerevisiae*. *Biochem Soc Trans.* (2011), 39(5):1502-8. Review.

Ždralević M., Guaragnella N., Antonacci L., Marra E., Giannattasio S. Yeast as a tool to study signaling pathways in mitochondrial stress response and cytoprotection. *ScientificWorldJournal*. (2012), 2012:912147. Review.

CHAPTER 3

Apoptotic role of Yca1p

Roles of metacaspase in yeast acetic acid-induced programmed cell death.

3.1 Introduction

Mammalian apoptosis and yeast programmed cell death (PCD) have many features in common. In both the mechanisms reactive oxygen species (ROS) production, protease activity, chromatin condensation, externalization of phosphatidylserine onto the cell surface exposure and DNA fragmentation occur (Ludovico et al., 2001; Guaragnella et al., 2012). Physical agents like UV radiation or heat and chemical agents like ethanol, hypochlorous acid, high concentration of salt and the most commonly used triggers hydrogen perodixe (H_2O_2) (Magherini et al., 2007) and acetic acid (AA) (Guaragnella et al., 2006; Almeida et al., 2009; Giannattasio et al., 2013) can induce apoptosis in yeast.

A characteristic feature of mammalian apoptosis is the activation of caspases. Caspases are endoproteases that hydrolyze peptide bonds in a reaction that depends on catalytic cysteine residues in the caspase active site and occurs only after certain aspartic acid residues in the substrate (McIlwain et al., 2013). This subgroup of proteolytic enzymes can be divided into two functional subgroups on the basis of their known or hypothetical roles. The first subgroup includes initiator or apical caspases (caspases 2, 8, 9 and 10) which are responsible for initiating caspase activation cascades, while the second subgroup composed by the downstream or effector caspases (caspases 3, 6 and 7) is responsible for the actual demolition/dismantling of the cell during apoptosis (Logue et al., 2008).

Deregulations in the caspase proteases expression or activity can lead to the development of several diseases, including cancer and neurodegenerative disorders (Pereira et al., 2012).

Unlike mammalian, yeast contains only one gene homolog of caspases, named YCA1, encoding for yeast metacaspase (Madeo et al., 2002) which has substrate specificity different from canonical caspases (Wilkinson and Ramsdale, 2011).

Recently, was identified in glyceraldehyde-3-phosphate dehydrogenase (GAPDH) the first direct yeast metacaspase substrate. Although mammalian caspases and yeast metacaspase differences, GAPDH appears as a "meeting point" for these pathways (Silva et al., 2011).

Sacchamomyces cerevisiae metacaspase exhibit arginine/lysine-specific endopeptidase activities (Watanabe et al., 2005), unlike to canonical caspases that cut after aspartic acid residues.

Numerous studies have shown that in YCA1-lacking cells, acetic acid-induced programmed cell death (AA-PCD) happen with lower rates (Guaragnella et al., 2006; Guaragnella et al., 2010). These data suggest that AA-PCD can occur via two alternative pathways, one dependent and the other independent of YCA1. As a result, the role of other proteases in yeast PCD remain to be established (Madeo et al.,2009; Wilkinson and Ramsdale et al., 2011).

Furthermore, it was demonstrated the ability of metacaspases to both promote and antagonize different cell cycle checkpoints, representing an early form of the proliferation/differentiation regulating activity exhibited by metazoan caspases (Lee et al., 2008).

Since in the last years, the concept of non-apoptotic roles of metacaspase is expanding, we have first conducted a comparative analysis between wild type and *Δyca1* cells using proteomic and metabolomic approach (Žd ralevic and Longo et al. 2015). Through these methodologies, we have shown that the deletion of YCA1 gene alters the carbon metabolism, amino acid and nucleotide metabolism and interferes with protein biosynthesis and protein transport/folding. Moreover, in knockout cells is established a stress response.

In the present section, we want to extend this analysis during the death process in order to better understanding the difference of this pathway in the two strains. In particular, the first aim (i) of the current study is to investigate the *S. cerevisiae* proteome and metabolome during apoptosis induced by acetic acid, in order to identify which pathways are more affected during this process. Since acetic acid was demonstrated to induce apoptosis in mammals as well as in yeast, we choose this kind of stimulus in order to obtain more information about the proteins and, for the first time, metabolites involved, useful to understand the apoptotic mechanism in higher

eukaryotes. The second purpose (ii) of this work was to compare strains of YCA1 cells, lacking the gene encoding for metacaspase as control versus YCA1 cells grown in presence of acetic acid in order to have finally, and this was the last objective (iii), a direct comparison between the two deaths, so we can establish definitively the role of metacaspase. To do this, we combined a proteomics and metabolomics analytical workflow to complement physiological information on the biological responses to PCD in both cases (**Scheme 1**). All analysis were carried out using cell treated with acetic acid for 150 min, because it represents the time in which the maximum release of cytochrome c happens and it represents one of the main apoptotic event as described by Giannattasio and coworkers (Giannattasio at al., 2008).

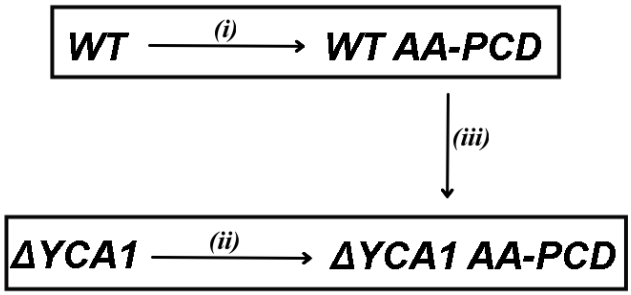

Scheme 1. Representation of the proteomic workflow

3.2. Materials and methods

3.2.1. Yeast strains, growth condition and protein extraction

Wild type (MATα ade2 leu2 his3 trp1 ura3) and Δyca1 W303-1B yeast cells (W303-1B yca1Δ::KanMX4) (Guaragnella et al, 2006) were grown at 26 °C in 1 % yeast extract, 2 % peptone, 2 % glucose (YPD) medium up to the exponential phase (OD_{600} about 0.7). An aliquot (Ctrl) ($2x10^7$ cells) was collected and used for proteomic analysis as a control before acetic acid treatment and the remainder was harvested, washed once and incubated in the same medium set to pH 3.00 in the presence of 80 mM acetic acid for AA-PCD induction (Guaragnella et al, 2006). Cells ($2x10^7$) were harvested after 150 min for further analysis.

Cycloheximide (Sigma–Aldrich) dissolved in water was added to yeast cell cultures grown to OD_{600} = 0.5–0.6 at a final concentration of 100 μg/ml and the culture

incubated for 30 min before acetic acid treatment which was then carried out in the presence of the same concentration of cycloheximide. Cell viability was determined by measuring colony-forming units (cfu) after 2 days of growth on YPD plates at 30 °C.
Proteins were extracted from either control or AA-PCD cells using YPX™ Yeast Protein Extraction Kit (Expedeon). Briefly, cells were harvested (5000× g, at 4 ºC for 5 min), and proteins were solubilized with extraction buffers provided in the kit, which contain SDS and reducing agents, providing unbiased extraction of proteins from cells. The buffers are designed to maximize the protein extraction and are compatible with downstream proteomics applications. Protease Inhibitor Cocktail (Sigma) was added to the cell lysate to improve the yield of intact proteins. The samples were denaturated at 100 ºC for 3 min, cooled down at 4 ºC for 10 min, harvested at 20000 × g for 10 min to pellet the cellular debris and the supernatant was collected for the analysis. For accurate determination of total protein concentration Bradford Ultra (Expedeon) assay, compatible with the presence of detergents, was used.

3.2.2 TUNEL assay

DNA fragmentation was detected in yeast cells by TUNEL assay (In Situ Cell Death Detection kit, fluorescein, Roche). AA-treated and control cells ($2x10^7$) were harvested at 150 min and before acetic acid treatment, respectively. Briefly, cells were fixed in 3.7% formaldehyde solution in PBS, digested with zymolyase and incubated in permeabilization solution (0.1 % Triton-X- 100, 0.1 % sodium citrate) for 2 min on ice, and then with 30 µl TUNEL reaction mixture for 1 h at 37 °C. After incubation, cells were washed, resuspended in PBS and applied to microscopic slides and observed using a Leica TCS SP5 II microscope equipped with a laser-scanning confocal unit containing a He–Ne argon laser (Leica). Specimens were viewed through a Planapo 63X/1.25 oil immersion objective and images were acquired by LAS-AF version 2.2.1 build 4842 software.

3.2.3. 2D-SDS-PAGE

600 µg of proteins of each sample (Wt, *Δyca1* and Wt and *Δyca1* after acetic acid-induction) were precipitated adding a cold mix of tri-n-butyl

phosphate/acetone/methanol (1:12:1) in ratio 1:4, in agitation for 90 min at 4°C. Also, in this step lipid component of the samples was removed.

After high-speed centrifugation for 20 min, the pellets were dried and solubilized in the buffer containing 7 M urea, 2 M thiourea, 4% (w/v) CHAPS, 40 mM Tris-HCl and were reduced and alkylated, with 1,4-dithiothreitol (DTT) and iodoacetamide (IAA) respectively.

After precipitation, the pellets were solubilized and used to carry out passive rehydration of IPG strips (pH 3-10, non linear, 17 cm; Bio-Rad, CA, USA) over night.

Isoelectrofocusing (IEF) was performed on an Protean IEF Cell (Bio-Rad, CA, USA) at 20 °C constant temperature and the total product time×voltage applied was 80,000 V-h.

SDS-PAGE was done in polyacrylamide gels (12% T, 2.6% C) at 35 mA per gel. The spots resulting by two dimensional separation, were stained by sensitive Coomassie brilliant blue G-250 stain. For each sample, three technical replicates were performed.

3.2.4. Image analysis and statistics

Gels were imaged with ChemiDoc XRS+ imaging system (Bio-Rad, CA, USA) and elaborated with ImageLab software (Bio-Rad, CA, USA).

Image analysis was carried out with computer software (Progenesis SameSpots, Version 2.0, Nonlinear Dynamics, Newcastle upon Tyne, UK). After manually and automatically alignment of twelve gels, the software generated a master list of detected spots and corresponding spot boundaries. For each protein spot, the average spot quantity value and its variance coefficient in each group was determined. One-way analysis of variance (ANOVA) was carried out at $p < 0.05$ to assess for absolute protein changes among the different treatments.

The statistically significant spots with fold ≥ 2 were cut by EXQuest Spot Cutter (Bio-Rad, CA, USA) and subjected to in-gel trypsin digestion.

3.2.5. Tryptic digestion

Protein bands observed in SDS-PAGE were carefully excised from Comassie-stained polyacrylamide gels and subjected to in-gel trypsin digestion according to Shevchenko (Shevchenko et al., 1996) with minor modifications. The supernatant containing tryptic peptides was dried by vacuum centrifugation. Prior to mass

spectrometric analysis, the peptide mixtures were redissolved in 10μL of 5% formic acid (FA).

3.2.6. LC-ESI-CID-MS/MS (proteomic analysis)

Samples were analyzed using a split-free nano-flow liquid chromatography system (EASY-nLC II, Proxeon, Odense, Denmark) coupled with a 3D-ion trap (model AmaZon ETD, Bruker Daltonik, Germany) equipped with an online ESI nanosprayer (the spray capillary was a fused silica capillary, 0.090 mm O.D., 0.020 mm I.D.). For all experiments a sample volume of 15 μL was loaded by the autosampler onto a homemade 2 cm fused silica precolumn (100 mm I.D.; 375 mm O.D.; Reprosil C18-AQ, 5 mm, Dr Maisch GmbH, Ammerbuch-Entringen,Germany). Sequential elution of peptides was accomplished using a flow rate of 300 nL min 1 and a linear gradient from solution A (2% acetonitrile; 0.1% formic acid) to 50% of solution B (98% acetonitrile; 0.1% formic acid) in 40 min over the precolumn on-line with a homemade 15 cm resolving column (75 mm I.D.; 375 mm O.D.; Reprosil C18-AQ, 3 mm, Dr Maisch GmbH, Ammerbuch-Entringen, Germany). The acquisition parameters for the mass spectrometer were as follows: dry gas temperature, 220 °C; dry gas, 4.0 L min^{-1}; nebulizer gas, 10 psi; electrospray voltage, 4000 V; high-voltage end-plate offset, 200 V; capillary exit, 140 V; trap drive: 63.2; funnel 1 in, 100 V out 35 V and funnel 2 in, 12 V out 10 V; ICC target, 200 000; maximum accumulation time, 50 ms. The sample was measured with the ‘‘Enhanced ResolutionMode at 8100 *m/z* per second (which allows mono isotopic resolution up to four charge stages) polarity positive, a scan range from *m/z* 300 to 1500, 5 spectra averaged, and rolling average of 1. The ‘‘Smart Decomposition’’ was set to ‘‘auto’’. Acquired CID spectra were processed in DataAnalysis 4.0, and deconvoluted spectra were further analyzed with BioTools 3.2 software and submitted to Mascot search program (in-house version 2.2, Matrix Science, London, UK). The following parameters were adopted for database searches: NCBInr database (release date 22/09/2012; 20 543 454 sequences; 7 050 788 919 residues); taxonomy = all entries; peptide and fragment mass tolerance of 0.3 Da; enzyme specificity trypsin with 2 missed cleavages considered; fixed modifications: carbamidomethyl (C); variable modifications: oxidation (M).

3.2.7. Sample preparation for metabolomic analysis

For metabolomic analysis wild type and Δyca1 W303-1B yeast cells, grown in YPD medium up to the exponential phase (OD600 about 0.7) before (ctrl) and after 150 min AA-PCD (see section 3.2.1) were collected ($2x10^7$ cells) and resuspended in 100 µl of ice cold ultra-pure water (18 MΩ) to lyse the cells and then the tubes were plunged alternatively into a water bath at 37 °C for 0.5 minutes and at 4 °C for 0.5 minutes. To be sure that the cells are lysed, the samples were sonicated for 10 minutes. Samples were mixed with 400 µl of -20°C methanol and then with 600 µL of -20 °C chloroform. The tubes were stored at -20 °C over night. After centrifugation, we have taken the top fraction (methanol fraction) which contained metabolites and the bottom fraction (chloroform fraction) which contained lipids.

3.2.8. Rapid resolution reversed-phase HPLC

An Ultimate 3000 Rapid Resolution HPLC system (DIONEX, Sunnyvale, USA) was used to perform metabolite separation. The system featured a binary pump and vacuum degasser, well plate autosampler with a six-port micro-switching valve, and a thermostated column compartment. A Phenomenex Luna 3 µm HILIC 200A (150 x 2.0 mm) protected by a guard column HILIC 4 x 2.0 mm ID (Phenomenex) was used to perform metabolite separation over a phase B to phase A gradient lasting 35 minutes. For HILIC separation, 50mM ammonium acetate was prepared bydissolving ammonium acetate in deionized water. The aqueous ammonium acetate was mixed with acetonitrile (95 : 5, v/v). This was used for the mobile phase 'A'. Eluent 'B' was composed of amixture of 50 mM aqueous ammonium acetate : water and acetonitrile (95 : 5, v/v).

Samples were loaded onto a Reprosil C18 column (2.0 mm x 150 mm, 2.5 mm—Dr Maisch, Germany) for metabolite separation.

Chromatographic separations were achieved at a column temperature of 30 °C; and a flow rate of 0.2 mL min-1. For downstream positive ion mode (+) MS analyses, a 0–100% linear gradient of solvent A (ddH2O, 0.1% formic acid) to B (acetonitrile, 0.1% formic acid) was employed over 30 min, returning to 100% A in 2 min and a 6 min post-time solvent A hold. Acetonitrile, formic acid, and HPLC-grade water and standards (Ω 98% chemical purity) were purchased from Sigma Aldrich.

3.2.9 Mass spectrometry: Q-TOF settings

Due to the use of linear ion counting for direct comparisons against naturally expected isotopic ratios, time-of-flight instruments are most often the best choice for molecular formula determination. Thus, mass spectrmetry analysis was carried out on an electrospray hybrid quadrupole time-of flight mass spectrometer MicroTOF-Q (Bruker-Daltonik, Bremen, Germany) equipped with an ESI-ion source. Mass spectra for metabolite extracted samples were acquired both in positive and negative ion modes. ESI capillary voltage was set at 4500 V (+) (-) ion mode. The liquid nebulizer was set to 27 psi and the nitrogen drying gas was set to a flow rate of 6 L min^{-1}. Dry gas temperature was maintained at 200 °C. Data were stored in a centroid mode. Data were acquired with a stored mass range of *m/z* 50–1200. Calibration of the mass analyzer is essential in order to maintain a high level of mass accuracy. Instrument calibration was performed externally every day with a sodium formate solution consisting of 10 mM sodium hydroxide in 50% isopropanol: water, 0.1% formic acid. Automated internal mass scale calibration was performed through direct automated injection of the calibration solution at the beginning and at the end of each run by a 6-port divert-valve.

3.9. 10. Data elaboration and statistical analysis

In order to reduce the number of possible hits in molecular formula generation, we exploited the SmartFormula3D TM software (Bruker Daltonics, Bremen, Germany), which directly calculates molecular formulae based upon the MS spectrum (isotopic patterns) and transition fingerprints (fragmentation patterns). This software generates a confidence based list of chemical formulae on the basis of the precursor ions and all fragment ions, and the significance of their deviations to the predicted intact mass and fragmentation pattern. Triplicate runs for each one of the three biologicalreplicates were exported as mzXML files and processed through MAVEN.52. Mass spectrometry chromatograms were elaborated for peak alignment, matching and comparison of parent and fragment ions, and tentative metabolite identification (within a 20 ppm mass-deviation range between observed and expected results against the imported KEGG database53) MAVEN is an open-source software that could be freely downloaded from the official project websites (http://genomics-pubs.princeton.edu/mzroll/index.php?show=download). Metabolite assignment was

further elaborated in the light of the hydrophobicity/hydrophilicity of the compound and its relative retention time in the RP-HPLC run (as gleaned through database information and preliminary calibration with commercially-available ultra-pure standards, as previously described). Relative quantitative variations of intact mass peak areas for each metabolite assigned through MS were normalized against internal standard.

3. 3. Results

3.3.1 Effect of acetic acid on apoptosis in WT and ΔYCA1 cells.

Before starting the differential proteome and metabolome analysis which are the main purposes of this work, we measured cell viability at 150 min after the treatment with 80 mM acetic acid in WT and *Δyca1* cells grown in glucose. In WT it was about 10 %, with respect to 30 % found for *Δyca1* (**Figure 15 panel A**). The percentage of TUNEL positive cells at 150 min was about 50 % for WT and 55 % for ΔYCA1, confirming the apoptotic nature of this loss of viability (**Figure 15 panel B**). **Figure 15 panel C** shows cell viability in presence of cycloheximide, an inhibitor of protein synthesises. The presence of it attenuated the toxic effects of acetic acid and enhanced the survival percentage.

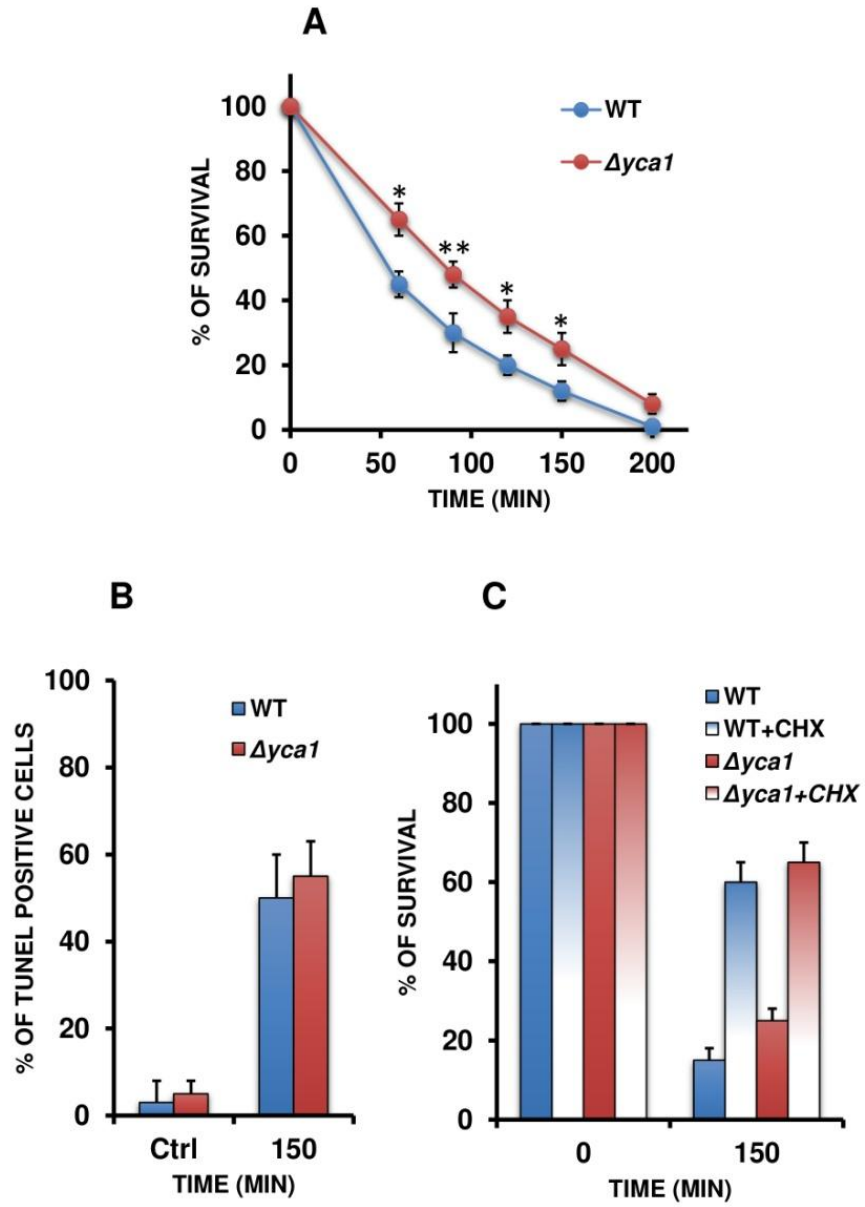

Figure 15. Occurrence of AA-PCD in WT and *Δyca1* cells. WT and Δyca1 cells were treated with 80 mM AA. Cell viability was analyzed at indicated times by measuring colony-forming units (cfu) (panel A). Percentage of TUNEL-positive WT, WT AA-treated, *Δyca1* and *Δyca1* AA-treated cells at indicated times (panel B). At least 400 cells were evaluated for each sample and for each time analyzed in four independent experiments. In panel C, was reported cell viability of four samples with or without cycloheximide in exponential cells exposed to acetic acid.

3.3.2. Identification of differentially expressed proteins in WT and Δyca1 cells undergoing AA-PCD and related metabolites.

The analysis of protein expression in WT and *Δyca1* cells before and after 150 min of AA-PCD induction was performed by the extraction of total yeast soluble proteins and their subsequent resolution by 2-DE. The resulting Comassie stained electropherograms were analyzed using Progenesis SameSpots software. **Figure 16** shows a typical image of 2-DE Comassie-stained gel of WT (**Figure 16A**) and *Δyca1* (**Figure 16B**) cells where the spots affected by acetic acid treatment, are marked by a symbol (+).

Comparison made between the total cellular proteome separated by 2-DE from WT cells undergoing AA-PCD at 150 min after the AA-treatment and the control cells shifted to acidic medium, but without AA addition, resulted in the identification of 51 spots with altered expression (**Figure 16A**). Only 8 spots (16%) were up-regulated; remaining 43 spots (84%) showed decreased expression caused by AA-treatment. These spots corresponded to the total of 45 proteins, that were classified into functional groups, as shown in **Table 3**.

Comparison made between the total cellular proteome separated by 2-DE from *Δyca1* cells undergoing AA-PCD at 150 min after the AA-treatment and the *Δyca1* cells shifted to acidic medium, but without AA addition, resulted in the identification of 52 spots with altered expression see **Figure 16B**.

Only 10 spots (24%) were up-regulated; remaining 42 spots (76%) showed decreased expression caused by AA-treatment. These spots corresponded to the total of 47 proteins, that were classified into functional groups, as shown in **Table 4**.

Total tandem mass spectrometry identified proteins listed in **Table 3** and **Table 4**, were grouped in **Figure 17** which represent a Venn diagram.

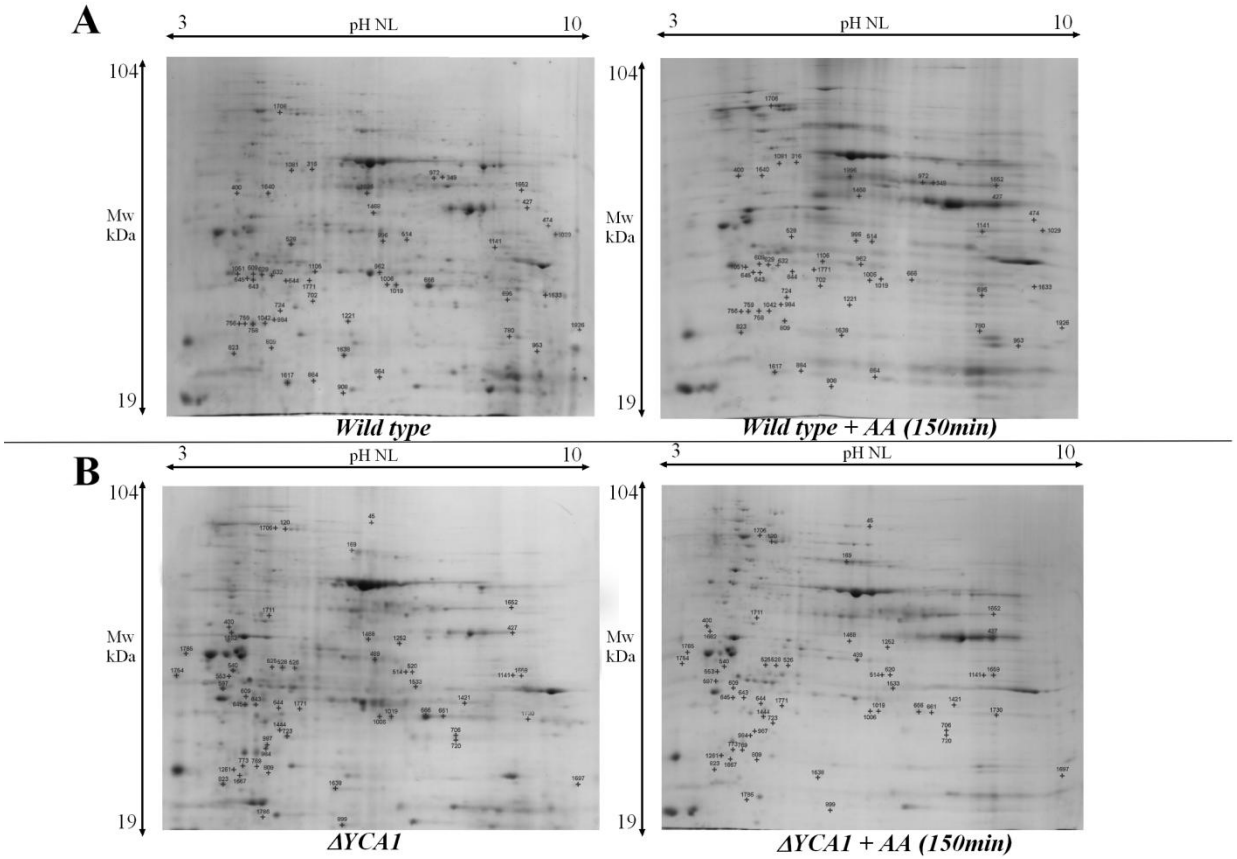

Figure 16. Representative 2-DE Coomasie-stained gels of total protein extract of W303-1B wild type, wild type AA-induced, *Δyca1* and *Δyca1* AA-induced *S. cerevisiae* cells. Statistically significant differential spots (p value < 0.05 and fold change > 2) for WT vs WT AA-induced cells (panel A) and *Δyca1* vs *Δyca1* AA-induced cells (panel B) analysis are reported in both panels. Molecular weight (MW) and pI range of the first dimension strips (3-10 NL) are indicated on the appropriate axis. Numbers identify proteins with altered expression between the four gels, given as in Table 3 and Table 4. All experiments were performed in triplicate.

Table 3. Relative proteomic changes between WT and WT AA-treated

Proteins identified	Function	NCBI accession number	Theoretical Mr (Da)	Theoretical pI	Spot number	Matches	Mascot score	Fold change	Expression level
Carbohydrate metabolism									
Eno1	Enolase I (phosphopyruvate hydratase)	gi|171455	46830	6.16	*1468*	11	232	2.6	Down
Eno2	Enolase II	gi|6321968	46942	5.67	*528*	68	957	3.6	Down
Hxk2	Hexokinase isoenzyme 2	gi|3710	27525	5.19	*1019*	9	261	2.5	Down
Tdh3	Glyceraldehyde-3-phosphate dehydrogenase, isozyme 3	gi|45269553	35780	6.72	*1006*	11	453	2.0	Down
					666	89	683	4.4	Down
Adh1	Alcohol dehydrogenase I	gi|223142	31954	6.38	*514*	19	419	2.0	Down
		gi|6324486	37282	6.21	*349*	46	827	2.6	Down
					972	55	943	2.6	Down
					996	30	589	2.7	Down
Fba1	Fructose 1,6-bisphosphate aldolase	gi|6322790	39881	5.51	*1896*	7	120	2.7	Down
					1221 (fragment)	11	199	3.0	Down
Tpi1	Triose-phosphate	gi|6320255	26893	5.74	*1051*	31	463	2.0	Down

	isomerase								
Pdc1	Pyruvate DeCarboxylase	gi|871533	61840	5.99	*908 (fragment)*	8	128	2.4	Down
		gi|256270485	46909	5.74	*1638 (fragment)*	17	264	2.9	Down
		gi|259148033	61719	5.71	*702 (fragment)*	11	177	2.1	Down
Pgk1	phosphoglycerate kinase	gi|10383781	44768	7.11	*1771*	39	667	2.0	Down
Amino acid metabolism									
Bat1	Mitochondrial branched-chain amino acid (BCAA) aminotransferase	gi|151944153	43798	8.80	*1652*	3	97	2.3	Up
Ilv5	IsoLeucine-plus-Valine requiring	gi|323347291	44510	9.1	*1633*	22	502	3.4	Down
Sam2	S-adenosylmethionine synthetase	gi|51013823	42489	5.24	*1081*	14	284	2.2	Down
Nucleic acid metabolism									
Adk1	Adenylate kinase	gi|6320432	24297	5.98	*962*	3	153	2.4	Down
Ura5	URAcil requiring	gi|6323530	24763	5.80	*962*	3	127	2.4	Down
Ado1	Adenosine kinase	gi|6322565	36521	4.99	*1640*	4	130	3.1	Down
Fur1	Uracil phosphoribosyltransferase	gi|171529	29015	5.83	*1105*	38	736	2.7	Down
Prs3	5-phospho-ribosyl-1(alpha)-pyrophosphate	gi|6321776	35387	8.51	*474*	5	133	3.5	Down

	synthetase								
Transcription/translation machinery									
Eft2	Elongation factor 2 (EF-2)	gi|6320593	93686	5.92	*609 (fragment)*	18	352	2.1	Down
Tef1	translation elongation factor EF-1 alpha	gi|6319594	50400	9.14	*1926 (fragment)*	7	149	2.9	Down
Tef1/2	Translation elongation factor	gi|32693297	41545	8.36	*1029*	33	505	2.0	Down
Yef3	Yeast Elongation Factor	gi|173214	116775	5.73	*629 (fragment)*	10	200	2.7	Down
Tif2	Translation initiation factor eIF4A	gi|6322323	44840	5.02	*1081*	12	340	2.2	Down
Rpl12a	Ribosomal 60S subunit protein L12A	gi|6320781	17869	9.43	*953*	44	341	2.6	Up
Rpl11b	Ribosomal 60S subunit protein L11B	gi|6321522	19794	9.92	*780*	15	236	2.2	Up
Rps7a	Ribosomal Protein of the Small subunit	gi|6324670	21609	9.83	*695*	22	498	2.3	Up
Rps7b	Ribosomal Protein of the Small subunit	gi|71064104	21720	9.92	*695*	18	465	2.3	Up
Rpl8b	Ribosomal 60S subunit protein L8B	gi|6322984	28151	10.02	*1141*	7	178	2.5	Up
Protein folding/degradation									
Ubc4	Ubiquitin-conjugating enzyme (E2)	gi|6319556	16616	6.04	*864*	4	60	2.3	Up

Egd2	Enhancer of Gal4 DNA binding	gi|172043	18295	4.84	*756*	6	141	2.2	Down
Stress response									
Ssa1	Stress-Seventy subfamily A Hsp70 family ATPase	gi|151941387	69772	5.00	*884 (fragment)*	31	695	2.1	Down
Ssa2	Stress-Seventy subfamily A	gi|151941146	69772	5.00	*645 (fragment)*	37	760	3.2	Down
		gi|151941387	69772	5.00	*643 (fragment)*	35	710	2.8	Down
		gi|6323004	69599	4.95	*809 (fragment)*	5	115	2.5	Down
					644 (fragment)	15	215	2.4	Down
Ssb1	Stress-Seventy subfamily B Hsp70 family ATPase	gi|6319972	66732	5.32	*632 (fragment)*	11	296	2.1	Down
					1706	41	967	2.4	Up
Ssb2	Stress-Seventy subfamily B Hsp70 family ATPase SSB2	gi|151944335	66669	5.32	*632 (fragment)*	11	296	2.1	Down
Sse1	ATPase component of the heat shock protein Hsp90 chaperone	gi|533365	77647	5.12	*400 (fragment)*	10	260	2.2	Down

	complex								
Zeo1	ZEOcin resistance protein	gi|6324463	12582	5.43	*1617*	23	376	2.3	down
Hsp82	Hsp90 chaperone	gi|2624655	24831	4.86	*823*	4	109	3.1	Down
Ahp1	Alkyl HydroPeroxide reductase	gi|6323138	19274	5.01	*1042*	16	353	2.2	Down
					759	9	174	2.3	Down
					984	18	329	2.4	Down
					758	15	248	2.3	Down
Tsa1	Thioredoxin peroxidase	gi|6323613	21690	5.03	*984*	5	95	2.4	Down
Hch1	High-Copy Hsp90 suppressor	gi|6324048	17293	4.56	*756*	3	72	2.2	Down
Sis1	Type II HSP40 co-chaperone that interacts with the HSP70 protein Ssa1p	gi|6324321	37567	9.02	*427*	1	33		
Cell signalling									
Bmh1	Brain Modulosignalin Homologue 14-3-3 protein, major isoform	gi|671634	30272	4.87	*629*	2	86	2.7	Down
Others									
Act1	actin	gi|3328	41907	5.53	*316*	29	558	2.0	Down
Vma1	Vacuolar Membrane Atp-ase	gi|3417405	68023	5.17	*1706*	29	691	2.4	Up

Tub1	alpha tubulin	gi|173058	50297	4.92	*724 (fragment)*	1	61	2.3	Down
Unknown									
Hmf1	Homologous Mmf1p Factor	gi|398364461	14011	5.28	*1638*	2	105	2.9	Down
Unidentified proteins									
682 604 1035 1016 913 1713 1157									

Table 3. Relative proteomic changes between *Δyca1* and *Δyca1* AA-treated

Proteins identified	Function	NCBI accession number	Theoretical Mr (Da)	Theoretical pI	Spot number	Matches	Mascot score	Fold change	Expression level
Carbohydrate metabolism									
Eno1	Enolase I (phosphopyruvate hydratase)	gi|171455	46830	6.16	*1468*	11	232	2.4	Down
Eno2	Enolase II	gi|6321968	46942	5.67	*899 (fragment)*	25	276	2.2	Down
					528	68	957	3.1	Down
					525	17	497	2.5	Down
					526	39	740	3.2	Down
Tdh3	Glyceraldehyde-3-phosphate dehydrogenase, isozyme 3	gi|45269553	35780	6.72	*1421*	26	437	2.0	Down
					720 (fragment)	49	638	2.9	Down
					666	89	683	2.4	Down
					661	37	594	2.1	Down
					1006	10	335	3.0	Down
Hxk2	Hexokinase isoenzyme 2	gi|3710	27525	5.19	*1019*	9	261	3.6	Down
Pgi1	Phosphoglucose isomerase (Glucose-6-phosphate isomerase)	gi|6319673	61261	6.00	*169*	9	231	3.4	Up

Adh2	Alcohol dehydrogenase II	gi|171029	37162	6.31	*1252*	4	114	2.7	Down
Adh1	Alcohol dehydrogenase I	gi|223142	31954	6.38	*520*	17	492	2.3	Down
					514	19	419	2.3	Down
Fba1	Fructose 1,6-bisphosphate aldolase	gi|6322790	39881	5.51	*644*	11	199	2.5	Down
Pdc1	Pyruvate DeCarboxylase	gi|256270485	46909	5.74	*1638 (fragment)*	17	264	2.6	Down
		gi|6323073	61685	5.80	*45*	7	250	2.3	Up
Pgk1	phosphoglycerate kinase	gi|10383781	44768	7.11	*1771*	39	667	2.3	Down
Amino acid metabolism									
Bat1	Mitochondrial branched-chain amino acid (BCAA) aminotransferase	gi|151944153	43798	8.80	*1652*	3	97	2.0	Up
Cys3	Cystathionine gamma-lyase	gi|6319307	42516	6.06	*706 (fragment)*	10	210	3.3	Down
Nucleic acid metabolism									
Ado1	Adenosine kinase	gi|365764754	36501	4.99	*1711*	10	476	2.3	Down
Transcription/translation machinery									
Eft2	Elongation factor 2	gi|6320593	93686	5.92	*609*	18	352	2.0	Down

	(EF-2)				*(fragment)*				
Hef3	Translational elongation factor EF-3	gi|173214	116775	5.73	*1444 (fragment)*	3	97	2.1	Down
Tif6	Translation initiation factor 6	gi|6325273	26669	4.54	*553*	3	105	2.0	Down
Rpl1a	Ribosomal 60S subunit protein L1A	gi|6325036	24189	9.72	*1730*	8	130	3.4	Up
Rpl7a	Ribosomal 60S subunit protein L7A	gi|6321362	27621	10.15	*1730*	7	185	3.4	Up
Rpl12a	Ribosomal 60S subunit protein L12A	gi|6320781	17869	9.43	*1697*	51	581	3.1	Down
Rpl8b	Ribosomal 60S subunit protein L8B	gi|6322984	28151	10.02	*1141*	7	178	2.0	Up
Rpl13b	Ribosomal 60S subunit protein L13B (YMR142Cp-like protein)	gi|207342264	22511	11.08	*1730*	14	318	3.4	Up
Rpl22a	Ribosomal 60S subunit protein L22A	gi|6323090	13685	5.91	*1786*	2	61	2.0	Down
Rps0a	Ribosomal 40S subunit protein S0A	gi|6321653	28064	4.65	*1754*	3	60	2.6	Down
Rps1b	Ribosomal protein	gi|6323577	28852	10.02	*1659*	11	249	4.0	Up

	10 (rp10) of the small (40S) subunit								
Rps4b	Protein component of the small (40S) ribosomal subunit	gi|6321997	29449	10.09	*1659*	32	653	4.0	Up
Ssz1	Hsp70 protein that interacts with Zuo1p	gi|37362658	58316	4.94	*1662 (fragment)*	8	136	2.9	Down
Ses1	seryl-tRNA synthetase	gi|6320226	53732	5.80	*169*	8	179	3.4	Up
Protein folding/turnover/transport									
Cct2	Chaperonin Containing TCP-1 Subunit beta of the cytosolic chaperonin Cct ring complex	gi|6322049	57510	5.80	*169*	10	394	3.4	Up
Pam16	Presequence translocase-Associated Motor	gi|6322357	16263	9.43	*1697*	8	229	3.1	Down
Sar1	Secretion-Associated, Ras-related GTP-binding protein of the ARF family	gi|6325038	21494	5.21	*1444*	4	114	2.1	Down
Smt3	Suppressor of Mif Two	gi|6320718	11590	4.92	*1667*	3	114	2.1	Down

	Ubiquitin-like protein of the SUMO family								
Stress response									
Ssa1	Stress-Seventy subfamily A Hsp70 family ATPase	gi|6323371	33696	4.75	*1662*	5	168	2.9	Down
Ssa2	Stress-Seventy subfamily A	gi|6323004	69599	4.95	*540 (fragment)*	16	416	2.0	Down
					1261 (fragment)	15	285	2.3	Up
		gi|151941146	69772	5.00	*645 (fragment)*	37	760	2.8	Down
		gi|151941387	69772	5.00	*643 (fragment)*	36	741	2.6	Down
Ssb1	Stress-Seventy subfamily B Hsp70 family ATPase	gi|6319972	66732	5.32	*1706*	41	967	2.0	Up
					723 (frammento)	19	460	2.7	Down
Ssb2	Stress-Seventy subfamily B Hsp70 family ATPase SSB2	gi|151944335	66669	5.32	*120*	127	2015	3.4	Up
Sse1	ATPase component of the heat shock protein Hsp90	gi|533365	77647	5.12	*400 (fragment)*	10	260	2.9	Down

	chaperone complex								
Zeo1	ZEOcin resistance protein	gi|6324463	12582	5.43	*809*	4	127	2.2	Down
Ahp1	Alkyl HydroPeroxide reductase	gi|6323138	19274	5.01	*769*	20	336	2.1	Down
					987	16	292	3.4	Down
					984	18	329	4.0	Down
					773	30	396	2.0	Down
Tsa1	Thioredoxin peroxidase	gi|6323613	21690	5.03	*984*	5	95	4.0	Down
Hsp82	Hsp90 chaperone	gi|2624655	24831	4.86	*823*	4	109	2.3	Down
Sba1	increased Sensitivity to Benzoquinone Ansamycins	gi|6322732	24123	4.46	*1754*	4	77	2.6	Down
Sis1	Type II HSP40 co-chaperone that interacts with the HSP70 protein Ssa1p	gi|6324321	37567	9.02	*427*	1	33	3.6	Up
Fatty acid biosynthesis									
Fas2	Alpha subunit of fatty acid synthetase	gi|2326840	34921	6.12	*1533*	2	82	2.3	Down

Cell signalling									
Bmh1	Brain Modulosignalin Homologue 14-3-3 protein, major isoform	gi|671634	30272	4.87	*1765*	35	681	2.7	Down
Asc1 (Chain A)	G-protein beta subunit; core component of the small (40S) ribosomal subunit	gi|223674073	34757	5.64	*489*	33	653	2.2	Down
Others									
Vma1	Vacuolar Membrane Atp-ase	gi|3417405	68023	5.17	*1706*	29	691	2.0	Up
Unknown									
Hmf1	Homologous Mmf1p Factor	gi|398364461	14011	5.28	*1638*	2	105	2.6	Down
Unidentified proteins									
1035									

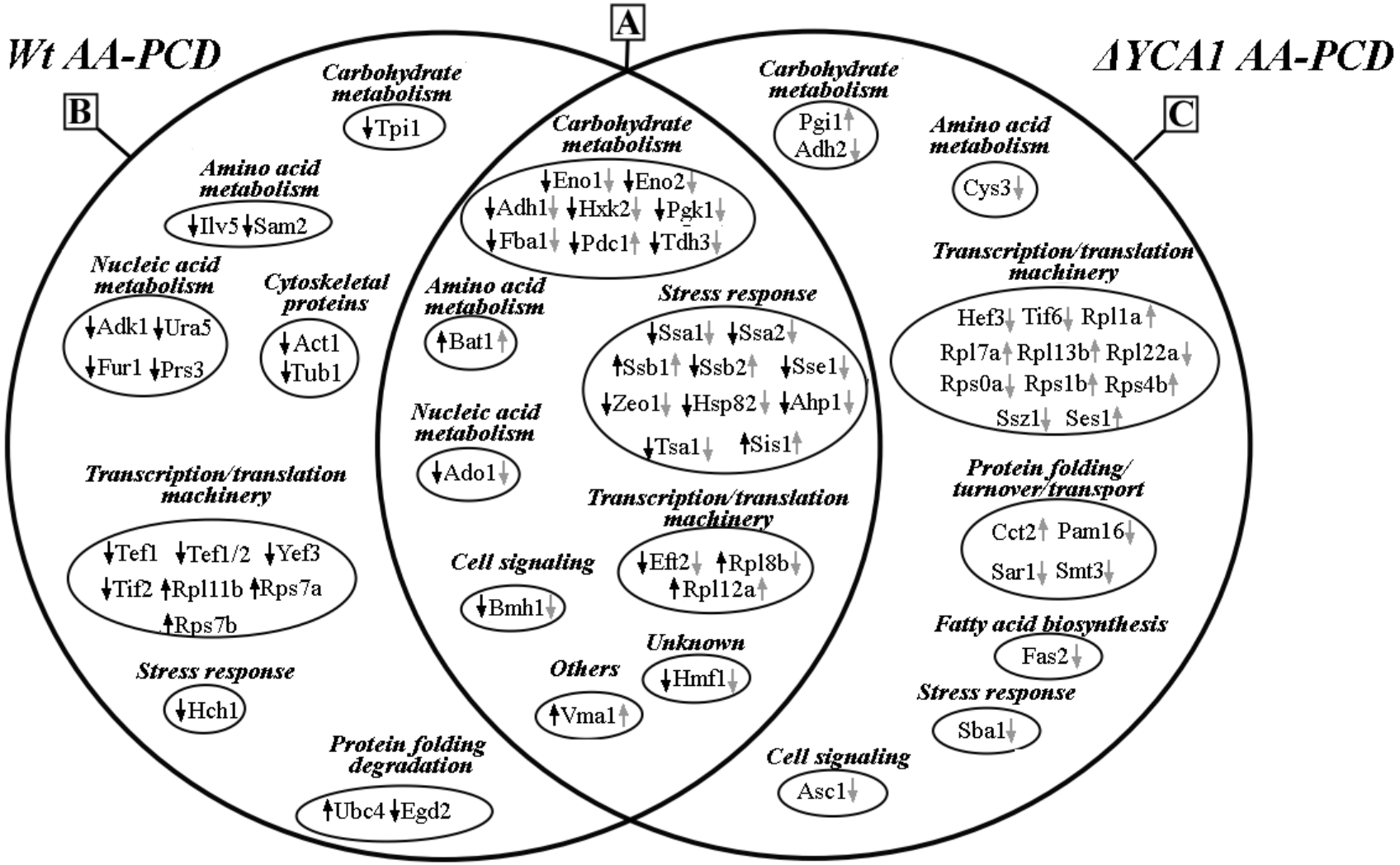

Figure 17. Venn diagram of identified differentially expressed in the WT and Δyca1 death.

The intersection (A) of **Figure 17** contains the differentially expressed proteins found in both analysis (WT AA-PCD and *Δyca1* AA-PCD).

The proteins found altered in both analysis are involved in several processes as consequences of response to AA-PCD.

Carbohydrate metabolism (Hxk2p, Fba1p, Tdh3p, Pgk1p, Eno1p, Eno2p, Pdc1p, Adh1p). Except for pyruvate decarboxylase (Pdc1p), that showed increased expression only in *Δyca1* cells, all other enzymes involved in glycolysis/gluconeogenesis had a decreased expression upon AA-PCD. Pyruvate decarboxylase is identified in WT analysis in three different spots, all of which corresponds to protein fragments, while in knock-out cells it was more abundant in its integral form.

Main glucose phosphorylating enzyme, hexokinase isoenzyme 2 (Hxk2p) was found to be down-regulated. Adh1p, an enzyme catalyzing acetaldehyde reduction to ethanol, the last step in the glycolytic pathway, was found in WT cells in two different spots with the same MW, but slightly different pI, suggesting that there could be the involvement of additional post-translational modifications (PTMs), while in *Δyca1* AA-PCD it present other two isoforms. Alcohol dehydrogenase II (Adh2p), an enzyme that catalyzes the reverse reaction of ethanol conversion to acetaldehyde was also down-regulated.

Thus, there is a strong down-regulation of glycolytic enzymes in *Δyca1* cells en route to AA-PCD, but, similar to what we have shown occurs in WT cells, metabolomic analysis reveals higher levels of several glycolytic intermediates. In particular, glucose-6-phosphate levels increase dramatically in *Δyca1* A150 cells. Fructose 1,6-bisphosphate aldolase (Fba1p) and pyruvte decarboxylase (Pdc1p) were found to be fragmented. Fba1p was detected in two spots; spot 1896 indicate the presence of the complete protein, whereas spot 1221 represents putative protein fragment. Glyceraldehyde-3-phosphate dehydrogenase, isozyme 3 (Tdh3p) in wild type was found in two different spots, 1006 and 666, that have similar Mr but different pI values, representing probably some PTM, while in *Δyca1*, isozyme 3 of the glyceraldehyde-3-phosphate dehydrogenase (Tdh3p) was identified in five different spots; spots 1421, 666, 661 and 1006 represent putative PTM, whereas spot 720 is a putative protein fragment. Phosphopyruvate hydratase, Eno2p, that in wild type cells was identified in

only one spot, in *Δyca1* was found in four spots; spots 528, 525 and 526 have the same MW and a slightly different pI values, so we can hypothesise that they correspond to PTMs, whereas spot 899 has a significantly lower MW and represents a putative protein fragment. These results are in agreement with proteomic data in (Almeida et al, 2009), who also showed decreased expression of glycolytic enzymes in *S. cerevisiae* BY4742 cells upon AA-treatment.

Our metabolomic analysis shows that the levels of glycolytic intermediates, fructose-6-phosphate, fructose-1,6-bisphosphate, glyceraldehydes-3-phosphate, 2-phosphoglycerate and pyruvate decrease en route to AA-PCD. On the contrary, our metabolic data indicate an increase of pentose phosphate pathway intermediates (ribose 5-phophate, sedoheptulose-7-phosphate and erytrose-4-phophate) (**Figure 18**).

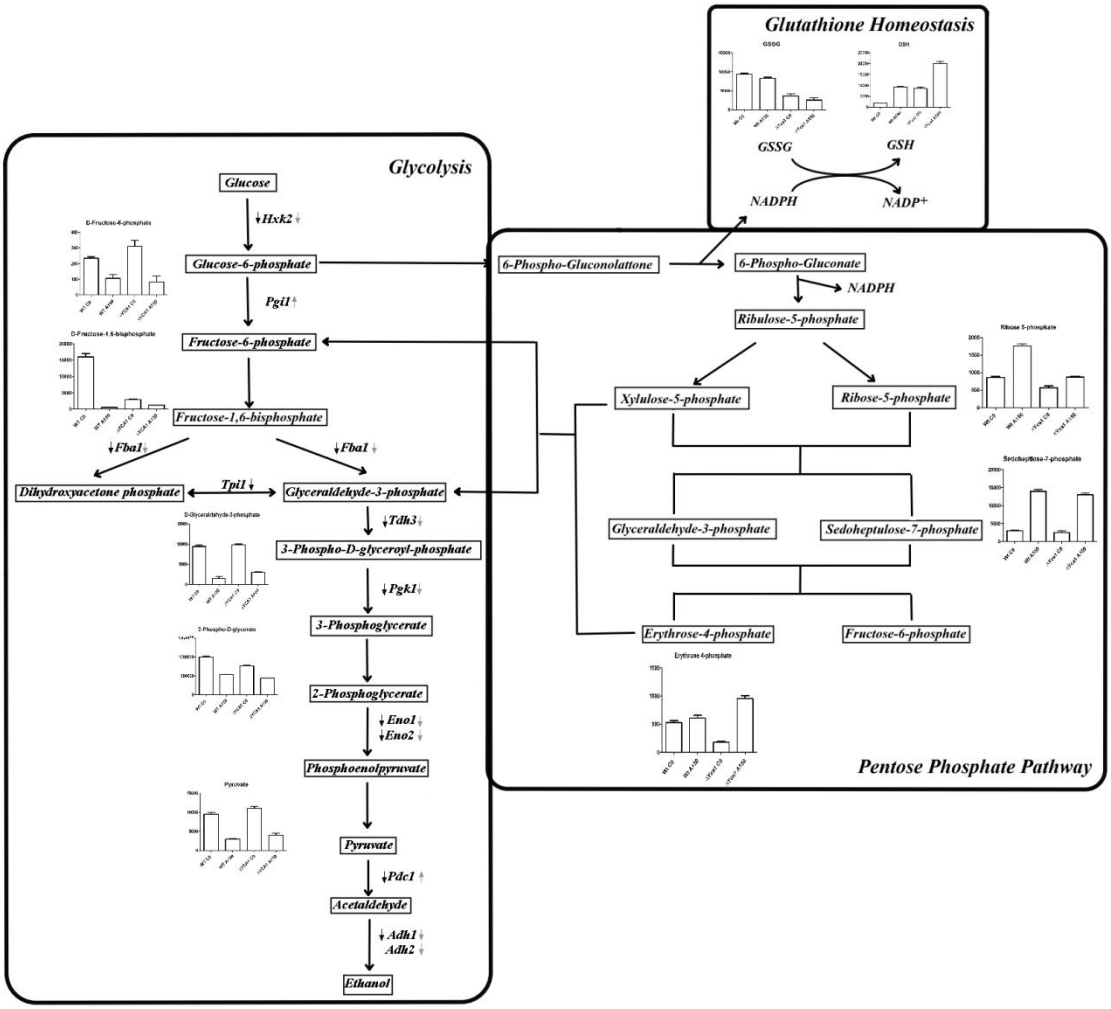

Figure 18. Overview of carbohydrate metabolism during wild type and *Δyca1* AA-PCD, obtained by proteomics and metabolimics integrated analysis.

Amino acid metabolism (Bat1p). Branched-chain-amino-acid transaminase is a protein involved in leucine, isoleucine and valine synthesis, increased expression upon treatment.

Nucleotide metabolism (Ado1p). Adenosine kinase catalyzes ATP dependent phosphorylation of purine nucleosides to monophosphate derivatives and, together with adenylate kinase (Adk1p), which catalyzes the reversible transfer of the terminal phosphate group between ATP and AMP, is involved in purine biosynthesis and salvage pathways. Ado1p is strictly required for the utilization of AdoMet and consequently adenosine, as a purine source (Lecoq et al, 2001). In yeast, Ado1p does not seem to play a major role in adenine utilization, it is rather involved in recycling the adenosine produced through the methyl cycle (Lecoq et al, 2001).

Cell signaling (Bmh1p). Brain modulosignalin homologue is the only protein involved in cell signaling found to be affected upon AA-PCD induction in both apoptotic analysis. Major isoform of 14-3-3 protein, BMH1, that has a role in exocytosis, vesicle transport, Ras/MAPK signaling and rapamycin-sensitive signaling, showed decreased expression upon AA-PCD. 14-3-3 proteins are highly conserved chaperone-like proteins that can counteract cell death in response to multiple stresses; yeast cells expressing human 14-3-3b/a are able to complement deletion of the endogenous yeast 14-3-3 and confer resistance to a variety of different stresses (Clapp et al, 2012). Deletion of the yeast Bmh1p was shown to extend chronological life span (CLS) by activating the stress response, protecting the cells from ROS-induced damages during chronological aging (Wang et al, 2009). Thus, decreased expression of Bmh1p during *Δyca1* AA-PCD could contribute to the overall higher susceptibility to oxidative stress en route to AA-PCD.

Vacuolar membrane Atp-ase (Vma1p). Vma1p is the A subunit of the vacuolar ATP-ase and contains the catalytic nucleotide binding site and it was found to be up-regulated both in WT and in *Δyca1* cells. Vacuolar ATP-ases are ATP-dependent proton pumps that acidify intracellular vacuolar compartments, important for many cellular processes, such as endocytosis, targeting of newly synthesized lysosomal enzymes, and other molecular targeting processes.

Stress response (Ssa1p, Ssa2p, Ssb1p, Ssb2p, Sse1p, Zeo1p, Hsp82p, Ahp1p, Tsa1p, Sis1p). Proteins involved in stress response consist of Hsp70 and Hsp90 family proteins, as well as proteins involved in cell redox homeostasis (Ahp1p, Tsa1p) and cell wall stress response (Zeo1p). Four members of the Hsp70 family (Ssa1p, Ssa2p, Ssb1p, Ssb2p) showed decreased expression and fragmentation induced by AA-treatment, with the exception of Ssb1p, which was identified in both analysis, but while the intact form is showed in spot 1706 and increased expression upon AA-treatment the putative protein fragment, found to be down-regulated, was detected in two different spots in the two proteome. Ssa1p and Ssb2p were identified in spot 884 and 632, respectively, that both might represent a protein fragment. In *Δyca1* cells, these protein were found in their integral form, but Ssa1p was less abundant during AA-PCD, while Ssb2 was more expressed. Ssa2p was found in four different spots, showing that extensive fragmentation of Hsp70 family proteins has occurred in AA-treated WT cells. All spots were down-regulated, except for 1261 in *Δyca1* analysis which was more abundant.

The expression of Hsp90 chaperone family member, Hsp82p, a co-chaperone that regulates the activity of members of HSP90 family, was found to decrease upon AA-treatment. Alkyl hydroperoxide reductase (Ahp1p) was identified in four different spots with similar Mr but different pI values, suggesting some post-translational modifications occurred; all of which down-regulated. Zeo1p, mitochondrial phosphoprotein involved in signalling cell wall stress to the PKC1-MPK1 cell integrity pathway (Reinders et al, 2007; Green et al, 2003), was found with decreased expression upon AA-treatment. Sis1p was the only ones found to be up-regulated in either proteomes. Sse1p, Sba1p and Hsp82p and thioredoxin peroxidase (TSA1) were also found to be down-regulated.

Transcription/translation machinery (Eft2p, Rpl8bp, Rpl12ap). Elongation factor Eft2p was found like protein fragments and was down expressed. 40S and 60S ribosomal subunits, Rpl12ap and Rpl8bp, were altered. But while Rpl12ap was up-regulated in either the samples, Rpl8bp was up-regulated in WT cells and down-regulated in *Δyca1*.

Unknown function (Hmf1). Hmf1p, member of the highly conserved p14.5 protein family was found to be down-regulated both in WT and in *Δyca1* cells

undergoing AA-PCD. HMF1 has a paralog, MMF1 (mitochondrial matrix factor 1) that arose from the whole genome duplication. Mmf1p is involved in maintenance of mitochondrial genome (Oxelmark et al, 2000), it is required for transamination of isoleucine but not of valine or leucine and may regulate specificity of branched-chain transaminases Bat1p and Bat2p (Kim et al, 2001).

3.3.3. Identification of differentially expressed proteins exclusively detected in WT cells undergoing AA-PCD and related metabolites.

Figure 17 part B shows proteins altered only in WT AA-PCD. In addition, in this case we grouped proteins in basis of their function.

Carbohydrate metabolism (Tpi1p). Triose phosphate isomerase it was down-regulated only in WT cells, while in *Δyca1* cells did not show a statistically difference.

Amino acid metabolism (Ilv5p, Sam1p). Ketol-acid reductoisomerase (Ilv5) and S-adenosylmethionine synthase 1 (Sam1) showed decreased expression. Ilv5p is involved in branched-chain amino acid biosynthetic process, as well as in mitochondrial genome maintenance. Sam1p catalyzes transfer of the adenosyl group of ATP to the sulfur atom of methionine to form S-adenosyl-L-methionine (AdoMet), a major constituent of intermediary metabolism. AdoMet is a cofactor involved in methylation of organic molecules, polyamine and biotin synthesis, as well in the synthesis of queuine, a modified base of tRNAs of prokaryotes and eukaryotes (Thomas and Surdin-Kerjan, 1997). Metabolomic analysis of amino acid content of apoptotic WT versus (WT control cells versus AA-induced WT) revealed higher levels of leucine, isoleucine, valine, tryptophane, methionine, threonine, phenylalanine and homoserine.

Nucleotide metabolism (Adk1p, Ura5p, Fur1p, Prs3p). Ura5p and Fur1p are involved in pyrimidine biosynthesis and salvage pathways. Ura5p is a major orotate phosphoribosyltransferase isozyme that catalyzes the conversion of orotate into orotidine-5'-phosphate in pyridine biosynthesis pathway. Fur1p is uracil phosphoribosyltransferase that catalyzes the conversion of uracil into uridine 5'-monophosphate (UMP) in the pyrimidine salvage pathway. Finally, Prs3p, 5-phosphoribosyl-1(a)-pyrophosphate synthetase that catalyzes the reaction at a key

junction in intermediary metabolism, biosynthesis of phosphoribosyl-pyrophosphate (PRPP) is also found to be down-regulated upon AA-treatment. PRPP is a precursor for the production of purine, pyrimidine, and pyridine nucleotides and the amino acids histidine and tryptophan (Hove-Jensen, 1988); it is required for both biosynthetic and salvage pathways of nucleotide metabolism (Switzer, 1969). Thus, overall down-regulation of major enzymes of nucleotide metabolism indicate that both de novo biosynthesis as well as nucleotide salvage pathways are compromised in WT cells following AA-treatment.

Protein folding/degradation (Ubc4p, Egd2p). The expression of Ubc4p, ubiquitin-conjugating enzyme that mediates selective degradation of short-lived and abnormal proteins, was found to be up regulated upon AA-treatment. Ubc4p is a central component of the cellular stress response (Seufert and Jentsch, 1991), interacts with many SCF ubiquitin protein ligases (Kus et al., 2004) and also promotes efficient and accurate DNA replication by regulating steady-state DNA polymerase-α levels (Haworth et al., 2010). The expression of Egd2p, alpha subunit of the heteromeric nascent polypeptide-associated complex (NAC) was found to decrease in WT cells en route to AA-PCD.

Stress response (Hch1p). High-Copy Hsp90 suppressor is down regulated, like the other stress response proteins.

Transcription/translation machinery (Tef1/2p, Yef3p, Tif2p, Rpl11bp, Rps7ap, Rps7bp). Different elongation factors were found to be down-regulated, whereas 40S and 60S ribosomal subunits were found to be up-regulated en route to AA-PCD. Translation elongation factors Tef1p and Yef3p were found as protein fragments.

Cytoskeletal proteins (Act1p, Tub1p). Actin, a structural protein involved in cell polarization, endocytosis and other cytoskeletal functions, was found to be down-regulated en route to AA-PCD in WT cells. Actin is shown to be involved in yeast cell stress response and the control of signalling through the RAS/cAMP/PKA pathway, pheromone and cell wall integrity MAPK pathways and TOR pathways (Smethurst et al., 2013). The corruption of actin leads to the induction of apoptosis via the hyperactivation of RAS signalling. This combination leads us to suggest that actin-

mediated apoptosis serves as a mechanisms by which yeast cells that are unable to respond to a number of stresses can be removed from a population. Furthermore, alpha-tubulin (TUB1), which polymerizes into microtubules with beta-tubulin, was found to be down-regulated in WT cells undergoing AA-PCD. Microtubules are conserved cytoskeletal elements known to be involved in chromosome segregation during mitosis and meiosis, spindle orientation and nuclear migration during mitosis and mating.

3.3.4 Identification of differentially expressed proteins exclusively detected in Δyca1 cells undergoing AA-PCD and related metabolites.

Other proteins were differentially expressed only in *Δyca1* AA-PCD and were grouped in section C of **Figure 17**. These proteins are involved in:

Carbohydrate metabolism (Pgi1p, Adh2p). Alcohol dehydrogenase II (Adh2p), an enzyme that catalyzes the reverse reaction of ethanol conversion to acetaldehyde was also down-regulated. Phosphoglucose isomerase (Pgi1p), with Pdc1, were the only glycolytic enzymes increased in *Δyca1* apoptosis. Thus, there is a strong down-regulation of glycolytic enzymes in *Δyca1* cells en route to AA-PCD, but the fold-change of differential protein were smaller than WT cells. In fact, in general, glycolytic intermediates were more abundant, while those of pentose phosphate pathway were higher in YCA1-knock-out AA-PCD (**Figure 18**).

Amino acid metabolism (Cys3p). Cys3p expression (detected only as a protein fragment) was decreased upon AA-PCD. Cystathionine gamma-lyase (Cys3p) catalyzes one of the two reactions involved in transsulfuration pathway that yields cysteine from homocysteine, as well as a reaction in threonine degradation pathway that yields cystathionine.

Protein folding/degradation/transport (Cct2p, Pam16p, Sar1p, Smt3p). A subunit of cytosolic chaperonin Cct ring complex, Cct2p, was found to be up-regulated upon AA-PCD. These chaperones assists the folding of proteins upon ATP hydrolysis and are known to play a role, in vitro, in the actin and tubulin folding, and may play a role in mitotic spindle formation. Smt3p protein involved in protein sumoylation is found to be down-regulated in *Δyca1* AA-PCD. Smt3p is ubiquitin-like protein of the

SUMO family involved in the regulation of chromatid cohesion, chromosome segregation, APC-mediated proteolysis, DNA replication and septin ring dynamics. Two other proteins, Pam16p and Sar1p, involved in intracellular protein transport, are also found to be down-regulated. Pam16p is the constituent of the import motor (PAM complex) component of the Translocase of the Inner Mitochondrial membrane (TIM23 complex) involved in protein import into mitochondrial matrix. Sar1p is Secretion-Associated, Ras-related GTP-binding protein of the ARF family involved in coat protein complex II (COPII) vesicles-mediated transport of proteins from the endoplasmic reticulum (ER) to the Golgi. Sar1p is a COPII vesicle core component involved in the regulation of COPII vesicle coating (Hughes and Stephens, 2007).

Cell segnaling (Asc1p). Asc1p was also found to be down-regulated en route to AA-PCD. Asc1p is yeast ortholog of RACK1 (receptor for activated protein kinase C1) that has an inhibitory effect on glucose signaling and cAMP production (Zeller et al., 2007). As a core conserved ribosomal protein, Asc1p also has a role in transcriptional repression (Gerbasi et al., 2004).

Stress response (Sba1p). Sba1p was found to be down expressed, such as the other proteins with the same function. Sba1p is a co-chaperone that binds and regulates Hsp90 family chaperons; it is homologous to human p23 proteins, responsible for the reconstitution of human telomerase activity in vitro.

Transcription/translation machinery (Hef3p, Tif6p, Rpl1ap, Rpl7ap, Rpl13bp, Rpl22ap, Rps0ap, Rps1bp, Rps4bp, Ssz1p, Ses1p). It is interesting to note that the proteins involved in cytoplasmic transcription and translation and ribosomal biogenesis are quantitatively the biggest group of proteins affected by acetic acid-induced apoptosis in *Δyca1* cells and that 11 out of the total 14 proteins (79%) affected, were identified only in *Δyca1* cells. Out of 14 proteins affected, 7 were up- and 7 down-regulated. Structural constituents of ribosome, Rpl1ap, Rpl7ap, Rpl8bp, Rpl13bp, Rps1bp and Rps4bp, involved in cytoplasmic translation, were found to be up-regulated, whereas Rpl12ap, Rpl22ap, Rps0ap and Ssz1p (a fragment) were down-regulated. Ses1p, seryl-tRNA synthetase, was found to be up-regulated, whereas Ssz1p, also involved in cytoplasmic translation, was found to be down-regulated. It is

important to note that Ssz1p is also involved in pleiotropic drug resistance by post-translational activation of transcription factor Pdr1p. Translation initiation factor 6 (TIF6) was found to be down-regulated, as well as translational elongation factor EF-3 (HEF3) and elongation factor 2 (EF-2). Hef3p and Eft2p were identified as protein fragments.

Fatty acid biosynthesis (Fas2p). Exclusively in *Δyca1* cells undergoing AA-PCD the expression of fatty acid synthetase (Fas2p, alpha subunit) was found to be decreased while it remains unaffected in WT (data not shown). Fas2p catalyzes the formation of long-chain saturated fatty acids from acetyl-CoA, malonyl-CoA and NADPH. In *S.cerevisiae* fatty acid biosynthesis, only the acetyl-CoA carboxylase activity (Acc1p) is separate, all other activities are distributed between two proteins, Fas1p and Fas2p, the beta and alpha subunits of a large, barrel-shaped complex containing 6 copies of each protein (Wieland et al., 1978; Kolodziej et al., 1996). Together, the six Fas1p and six Fas2p subunits form six independent reaction centers, each containing all enzyme activities required for synthesizing long chain fatty acids from acetyl- and malonyl-CoA (Leibundgut et al., 2007; Lomakin et al., 2007 and references therein). FAS2 encodes the acyl-carrier protein domain and three independent enzymatic functions: 3-ketoreductase, 3-ketosynthase and phosphopantetheinyl transferase. A corroboration of the decrease of fatty acid synthesis could be the malonyl-CoA accumulation.

3.3.5. Comparative metabolomic analysis of WT and Δyca1 cells undergoing AA-PCD

Metabolomics analyses were performed to integrate and expand the physiological and protoemics observations. Also in this case we compere WT and *Δyca1* cells before and after 150 min of AA-PCD induction. Due to the massive amount of output data, only significant results displaying absolute values for fold-change variations higher than 1.5. Along with feature number, feature name, p-value, mass to charge ratio (*m/z*), chromatographic retention times, day specific intensities and tentative identification (with isotope description, molecular weight deviation in ppm from database top hit reports, name, presence of K+ , Na+ , NH4 + adducts and

MAVEN identifier), as identified by XCMS. (Tautenhahn et al., 2011; Melamud et al., 2010; C. Smith et al., 2005).

S. cerevisiae cells inherit a unique glucose repression system that upon growth on glucose drastically suppresses respiration independently of oxygen availability (Haussmann P and Zimmermann FK, 1976) for this reason we have not found metabolites belonging to the Krebs cycle.

In order to report the main results in a more readable layout, metabolites accounting for the most relevant catabolic pathways were grouped and plotted as follows: metabolites involved in glycolysis and pentose phosphate pathway (PPP) and glutathione homeostasis (**Figure 18**), amino acid transport (**Figure 19**) and ceramides/lipid metabolism (**Figure 20**).

.

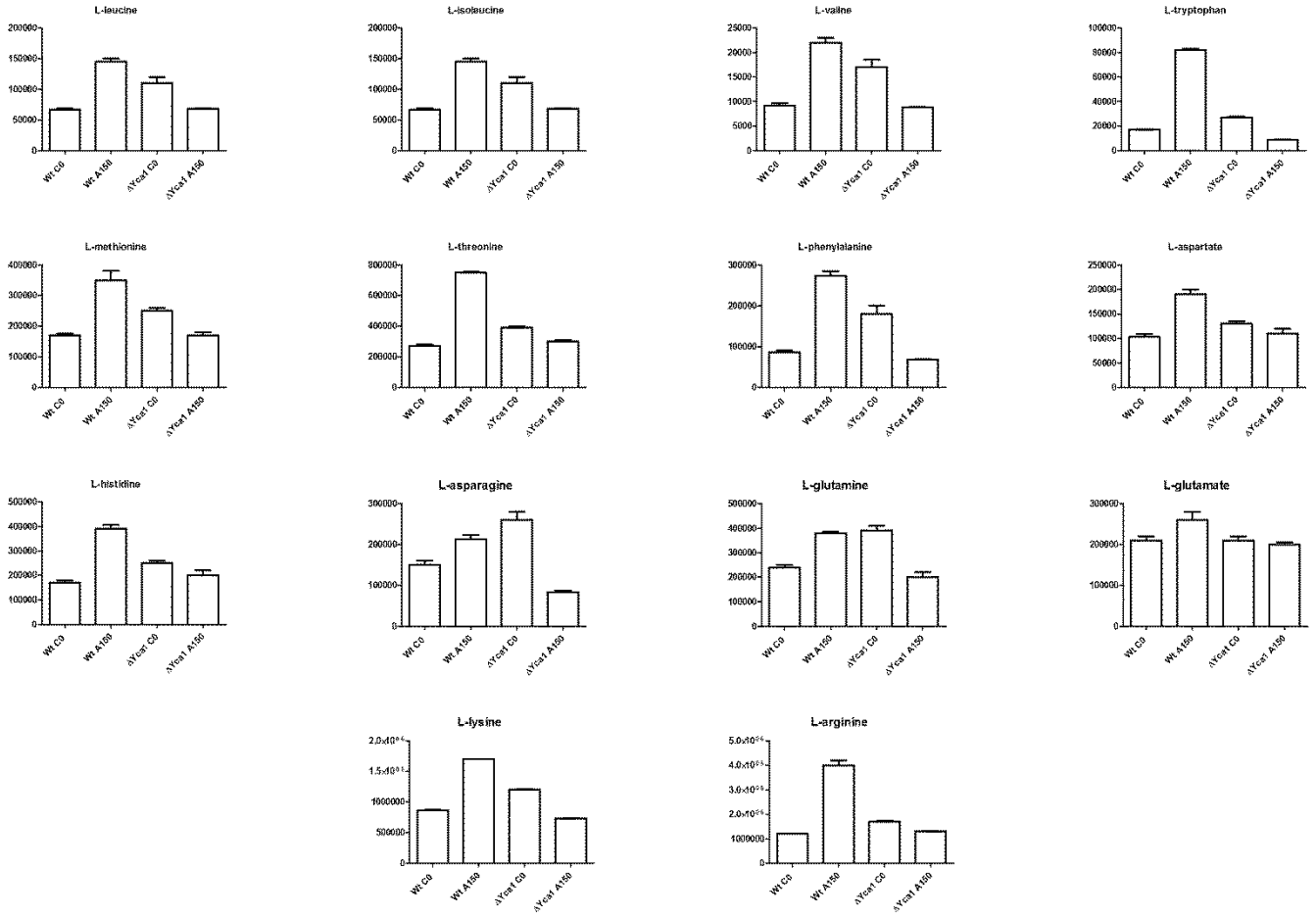

Figure 19. Metabolomic analysis of amino acidic levels in Wt, WT AA-treated, *Δyca1* and *Δyca1* AA-treated

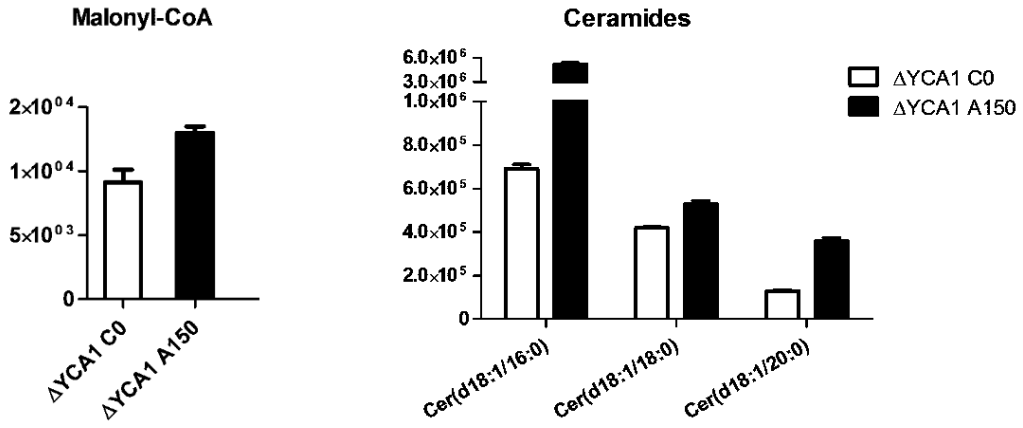

Figure 20. Analysis of lipid metabolism in Δ*yca1* death

3.4.Discussion

The yeast model could help to understand the complicated hierarchy between different apoptotic pathways and be able to elucidate the protein and metabolomic pathways involved in apoptosis.

Yeast AA-PCD occurs both in wild type cells that in *Δyca1* cells, although in the second case the rate of death was reduced (Guaragnella et al., 2006). The nuclear ultrastructural changes were significantly reduced when the treatment was carried out in the presence of cycloheximide, strengthening our interpretation about the active nature of cell death induced by the lower concentration of acetic acid. Since AA-PCD is dependent on *de novo* protein synthesis (Ludovico et al., 2001), cycloheximide prevent cell death both in WT that in knock-out cells, also that even in this case the rate of survival of the latter is higher. Indeed, TUNEL assay, commonly used to identify death via apoptosis, detects also necrotic death (Leist et Jaattela., 2001, Galluzzi et al., 2009, ludovico). In fact, in spite of similar percentage of TUNEL-positive cells, the survival of mutant cells is higher. This data confirmed the model of Guaragnella and co-workers (Guaragnella et al., 2012) that have hypothesized a different pathway of PCD in *Δyca1* cells.

Assuming that both strains WT and *Δyca1* undergo cell death in the presence of acetic acid, our interest has been orientated to the role of metacaspases gene during cell death.

To do this we focused our attention and discussed those groups which have differentially expressed proteins connected with the most important metabolisms, so that we can deduce the main mechanisms in which the metacaspase is involved (see **Figure 17**).

3.4.1. Analysis of differential proteins in AA-PCD of WT and Δyca1 cells.

Our findings enable us to state that the presence or absence of the metacaspases gene does not influence the cell fate. **Figure 17** sector A, which represents the proteins differentially expressed in Wt and *Δyca1*, clearly highlights what previously asserted. Two categories of molecules seemed have most influence on cell death, corroborated by metabolites: carbohydrate metabolism and stress response.

A general down regulation of expression level of enzyme involved in glycolysis, fermentation and other metabolic functions were observed (**Figure 17A**). The decrease of glycolytic rate can be correlated to growth arrest that occurs to save energy to induce apoptosis phenotype, as reported also by Almeida (Almeida et al., 2009).

Through an integrated proteomics and metabolomics approach it emerged that *Δyca1* and WT cells while undertaking an apoptotic fate, decreased glycolytic rate. Furthermore, through metabolomics we could detect a diversion from the main glycolytic pathway towards the pentose phosphate pathway. This shift resulted in accumulation of NADPH, an essential coenzyme in oxidized-glutathione (GSSG) reduction to GSH. Since NADPH is needed to reduce the disulfide form of glutathione (GSSG) to the sulfhydryl form (GSH), an oxidative stress modulated increase in the PPP rate and it was considered a natural self-defensive mechanism of cells to cope with oxidative injury, as also deducible from widespread hereditary anomalies to rate limiting enzymes of this pathways (Efferth et al., 2004; Fico et al., 2004)

Consequently to this, GSH was higher in cells after 150 minutes of grown in acetic acid for both cells, GSH plays an essential role in maintaining the intracellular redox environment that is critical for function of various cellular proteins. Cellular GSH is predominantly present in the reduced thiol form, GSH, which is also the biologically active form (Circu and Aw, 2008).

In addition, we noted a dramatically decrease of stress response proteins. Like in Almeida's work (Almeida et al, 2009)., numerous members of Hsp70 family showed a reduced intensity upon acetic acid-induced apoptosis. Is known that in mammalian cells chaperones present anti-apoptotic activity, by preventing caspase activation or by neutralizing the apoptosis-inducing factor (AIF) function through direct interaction (Wissing et al., 2004). This suggest that acetic acid-induced PCD can be enhanced by the absence of this anti-apoptotic action. Furthermore, despite the ROS and H_2O_2 production occurs in PCD pathway (Guaragnella et al., 2010), after 150 minutes of acetic acid-induction cells showed a reduction of their antioxidant defence induced a down-regulation of Ahp1 and Tsa1, probably to be more prone to apoptosis (Magherini et al., 2007).

A down regulation of Bmh1 occurs. Bmh1 is an homolog of human 14-3-3 protein. This protein is known for its capacity to protect cells against stress-induced apoptosis (Clapp et al., 2012). The minor abundance of this protein reflect the apoptotic state of cells undergo AA-treatment.

Vacuolar acidity was found to modulate mitochondrial function and yeast life span (Hughes and Gottschling, 2012). Prevention of decline of vacuolar acidity, which occurs during replicative ageing, was found to suppress mitochondrial dysfunction and extend lifespan in yeast. Furthermore, vacuolar protease Pep4p, was found to be involved in mitochondrial degradation and is released into the cytosol upon AA-treatment (Pereira et al., 2010). Finally, Ca^{2+}-sensitive Pet^- mutants have been reported to have mutations in the family of *VMA* genes, including *VMA1*, which affected Ca^{2+} homeostasis, glycerol metabolism and phospholipid metabolism in these cells (Ohya et al., 1991). All of these Pet^- mutants have lost vacuolar membrane H^+-ATP-ase activity, vacuolar Ca^{2+} uptake activity and the ability to acidify the vacuole *in vivo.*

3.4.2. Analysis of differential proteins exclusively in wild type AA-PCD

This section is dedicated to comment proteins and metabolites differentially expressed between Wt and Wt growth in the presence of acetic acid (**Figure 17B**). These proteins could be correlated to cell death induced by acetic acid and to presence of metacaspase.

Another important glycolytic enzyme, triose phosphate isomerise (Tpi1) decreases during AA-PCD only in wild type cells (**Figure 17B**). Tpi1 is known to be a potent inhibitor of pentose phosphate pathway, in fact Ralser and co-workers (Ralser et al., 2007) have demonstrated that reduced activity of TPI causes a re-configuration of central metabolism, leading to increased flux of the PPP and increased stress resistance in yeast. This evidence would explain why the PPP intermediate metabolite in AA-PCD increase more respect YCA1-knock-out cells. To corroborate the hypothesis, the fold-change of differential expressed glycolytic enzyme, in general, is higher in WT cells.

Except for Ado1p, which we have already seen that was altered in both PCD pathways, the proteins involved in nucleic acid metabolism were dramatically down regulated only in wild type cells. This aspect can induce to think that Yca1p influence strongly this metabolism.

In fact, adenylate kinase 1 (Adk1p) which catalyze phosphate group transfer from ATP to AMP, orotate phosphoribosyltransferase (Ura5p) which represent the fifth enzyme in *de novo* biosynthesis of pyrimidines, uracil phosphoribosyltransferase (Fur1p) involved in UMP synthesis and phosphoribosylpyrophosphate (PRPP) synthetase (Prs3p) which synthesize PRPP, were all down-regulated. The decreased glucose metabolism resulting in AA-PCD leads to decreased ATP generation as well as loss in generation of many biosynthetic precursor molecules, including nucleic acids (Altman and Rathmell, 2012). All energy available in the cell is used in order that PCD occurs, consequently all biosynthetic pathways appear to be down regulated.

In agreement to this, also amino acid synthesis enzymes were less abundant.

In this view, can be explained transcription and translation machinery slowdown. Cells do not misspend energy for biosynthesis of new proteins, rather seek to obtain from their degradation.

In fact, in wild type cells, Ubc4p, the ubiquitin-conjugating enzyme (E2) was up-regulated. Ubc4p, as well as Ubc1p and Ubc5p, was found to mediate selective degradation of short-lived and abnormal proteins (Seufert et al., 1991). Ubc4p generates high molecular weight ubiquitin-protein conjugates and comprise a major ubiquitin-conjugation activity in yeast cells. Moreover, this enzyme is a central component of the cellular stress response. Furthermore, Chuang and co-workers (Chuang et al., 2005)

have demonstrated that Ubc4p has a specific role in degradation of cotranslationally damage proteins and this can be explained by the failure of translationally machinery.

The abundance of this enzyme is correlated with the increase of proteome activity that is needed for AA-PCD occurs (Valenti et al., 2008). In fact, unlike certain mammalian and plant cells in which proteosome inhibition was found during PCD, in yeast there is a transient increased in proteosome activity from 60 up to 150 minutes after AA-induction because of increased efficiency of catalytic activity. To corroborate this, Egd2p, alpha subunit of the nascent polypeptide-associated complex, which appears to less abundant, is known to be degraded via the proteasome pathway in stress condition. In addition, protein degradation by the ubiquitin-proteosoma pathway, determine accumulation of aminoacids , as reported by Lecker (Lecker et al.,2006) protein degradation is an irreversible process, destruction of a protein can lead to a compete, rapid unsustain termination of the process involving the protein as well as in cell composition. The rapid degradation of specific protein permits adaptation to new physiologic condition.

3.4.3. Analysis of differential proteins exclusively in Δyca1 AA-PCD

Finally, the third part of this work concerns and describes those molecules that could be regulated by the metacaspases gene (**Figure 17C**).

In *Δyca1* AA-PCD, the situation is very similar to wild type death: glycolysis pathway is slowed, with the increase of phosphate pentose pathway, although with a lower rate than in WT cells; transcription and translation of news proteins was blocked, stress response protein were down regulated to allow the cells to die (**Figure 17C**). Noteworthy is the presence of the protein Fas2 in the mutant only, which means a probable involvement of the gene *Δyca1* in fatty acid biosynthesis, which appear to be altered in AA-PCD. Fas2 is alpha subunit of fatty acid synthetase which catalyzes the synthesis of long-chain saturated fatty acids. This enzyme was decreased undergo AA-treatment only in knock-out cells. In mammal, the inhibition of fatty acid synthase induce apoptosis. On the contrary, its overexpression occurs in a wide range of tumors, including breast, prostate, and ovaries cancers. The inhibition of Fas2 elicits cell cycle arrest and apoptosis, so it is considered a potential drug target for oncology (Knowles et

al., 2008). Bandyopadhyay and collaborators (Bandyopadhyay at al., 2006) have proposed a model for the apoptotic pathway induced by FAS inhibition, whereby inhibition of FAS leads to accumulation of malonyl-CoA, which in turn inhibits carnitine palmitoyltransferase I, resulting in up-regulation of ceramide followed by induction of the proapoptotic genes BNIP3, TRAIL, and DAPK2. Regarding ceramides, they are bioactive sphingolipids that mediate antiproliferative and pro-apoptotic signalling in response to various stress stimuli (Ogretmen and Hannun, 2004). More recently Aflaki (Aflaki et al., 2012) have written a work about the role of ceramide C16 in inducing apoptosis in macrophages. The authors provide evidence that increased ceramides synthesis triggers the mitochondrial apoptosis pathway resulting in mitochondrial dysfunction. Koybasi and collaborators (Koybasi et al., 2004) emphasized the role of C18 in the regulation of growth of neck squamous cell carcinoma. The authors suggest that decreased levels of C18 ceramide may impart a growth advantage to cancer cells, whereas increased generation/accumulation of C18-ceramide may lead to inhibition of growth of cells, which involves the modulation of telomerase activity and induction of apoptosis in cancer cells. Furthermore, the role of ceramide in yeast PCD is confirmed by Carmona-Gutierrez and co-workers (Carmona-Gutierrez et al., 2011) demonstrating *S.cereviasiae* death ceramide-induced, through a mechanism ROS-dipendent. Their experiments, conduced also in *Δyca1* cells, shown that yeast metacaspase does not contribute to ceramide cell killing in yeast in perfect agreement to our findings. Because the relevance of endogenous ceramide and its roles in the regulation of cell growth in yeast has not been established previously, this study suggests an important and novelty role of ceramides in PCD progression.

Above all, it can be assumed and inferred from our results, that a relevant importance is due to the gene that would control the synthesis of fatty acids through the FAS2 protein.

Thus, considered the decrease in the expression of Fas2 protein involved in fatty acid synthesis, considered the increase of malonyl-CoA and ceramides, established the role of the ceramides in apoptosis, we can speculated a new or an alternative apoptotic YCA1-indipendent via-ceramides pathway that induce PCD in absence of metacaspase (**Figure 20**).

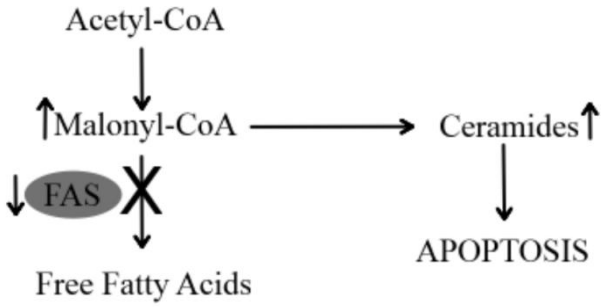

Figure 20. Hypothetical mechanism involved in yeast death in absence of metacaspase

Although a transient proteasome activation is needed for AA-PCD to occur (Valenti et al., 2008), we noted in *Δyca1* a general decrease of some proteins belong to protein folding degradation which is also reflected in reduced degradation of protein and amino acids.

Less abundance in *Δyca1* cells undergo AA-PCD of Smt3, an ubiquitin-like protein of the SUMO family, and also of Sar1, a GTP-binding protein involved in transport vesicle formation during ER to Golgi protein transport and related to proteolytic process, suggest that the absence of MCA1 affect the proteolysis. Since is well known that proteasome levels and the proteolytic capacity of cells are unaffected in YCA1-knock-out cells (Khan et al., 2005), Mca1 can be involved in regulation of ubiquitination pathways. In fact, H_2O_2-mediated stress leads to up-regulation of the 20S proteasome, but suppression of ubiquitinylation activities (Khan et al., 2005).

3.5. Conclusion

Recent advances in various 'omics' technologies enable quantitative monitoring of the abundance of various biological molecules in a high-throughput manner, and thus allow determination of their variation between different biological states. In this study the integration of proteomics and metabolomics, has proved a potent tool of investigation on acetic acid-induced programmed cell death dependent and independent-YCA1, and it will be pivotal for understanding how the individual components in the system interact and influence overall cell metabolism.

Although a common decrease in glycolytic cycle enzymes and shift towards the pentose phosphate pathway happened in both cases, WT cells seem to be more affected. Moreover, it could be in relation to the presence of metacaspases and its biochemical function, this allowed us to conclude that metacaspase could has a key role for the shift from glycolysis to pentose phosphate pathway during death.

We have also discussed a pro-apoptotic mechanism YCA1-indipendent that involve FAS2 protein.

The activation of Ceramides (C18, C16, and 20), in our opinion, can trigger apoptosis. It is likely that the gene has a role on FAS2 regulation.

Furthermore, this study emphasized the central role of metacaspase gene in proteolysis, because its presence or absence influence the expression of ubiquitin proteasome pathway through the modulation of crucial proteins.

REFERENCES

Aflaki E., Doddapattar P., Radović B., Povoden S., Kolb D., Vujić N., Wegscheider M., Koefeler H., Hornemann T., Graier W.F., Malli R., Madeo F., Kratky D. C16 ceramide is crucial for triacylglycerol-induced apoptosis in macrophages. *Cell Death Dis*. (2012) doi: 10.1038/cddis.2012.17.

Almeida B., Ohlmeier S., Almeida A.J., MadeoF., Leao C.,Rodrigues F., Ludovico P. Yeast protein expression profile during acetic acid-induced apoptosis indicates causal involvement of the TOR pathway. *Proteomics*.(2009), 9:720–732.

Altman B.J., Rathmell J.C. Metabolic stress in autophagy and cell death pathways. *Cold Spring Harb Perspect Biol*. (2012), doi:10.1101/cshperspect.a008763. Review.

Bandyopadhyay S., Zhan R., Wang Y., Pai S.K., Hirota S., Hosobe S., Takano Y., Saito K., Furuta E., Iiizumi M., Mohinta S., Watabe M., Chalfant C., Watabe K. Mechanism of apoptosis induced by the inhibition of fatty acid synthase in breast cancer cells. *Cancer Res*. (2006), 66(11):5934-40.

Carmona-Gutierrez D., Reisenbichler A., Heimbucher P., Bauer M.A., Braun R.J., Ruckenstuhl C., Büttner S., Eisenberg T., Rockenfeller P., Fröhlich K.U., Kroemer G., Madeo F. Ceramide triggers metacaspase-independent mitochondrial cell death in yeast. *Cell Cycle*. (2011), 10(22):3973-8.

Chuang S.M., Madura K. *Saccharomyces cerevisiae* Ub-conjugating enzyme Ubc4 binds the proteasome in the presence of translationally damaged proteins. *Genetics.* (2005), 171(4):1477-84.

Circu M.L., Aw T.Y. Glutathione and apoptosis. *Free Radic Res*. (2008) , 42(8):689-706.

Clapp C., Portt L., Khoury C., Sheibani S., EidR., Greenwood M., Vali H., Mandato C. A., Greenwood M. T. Untangling the Roles of Anti-Apoptosis in Regulating Programmed Cell Death using Humanized Yeast Cells. *Front Oncol*. (2012), 2: 59.

Efferth T., Bachli E. B., Schwarzl S. M., Goede J. S., West C., Smith J. C., Beutler E. Glucose-6-phosphate dehydrogenase(G6PD) deficiency-type Zurich: a splice site mutation as an uncommon mechanism producing enzyme deficiency. *Blood.* (2004), 104: 2608.

Fico A., Paglialunga F., Cigliano L., Abrescia P., Verde P., Martini G., Iaccarino I., Filosa S. Glucose-6-phosphate dehydrogenase plays a crucial role in protection from redox-stress-induced apoptosis. *Cell Death Differ*. (2004), 11:823–831.

Galluzzi L., Kepp O., Kroemer G. RIP kinases initiate programmed necrosis. *J Mol Cell Biol.* (2009), 1(1):8-10.

Gerbasi V.R., Weaver C.M., Hill S., Friedman D.B., Link A.J. Yeast Asc1p and mammalian RACK1 are functionally orthologous core 40S ribosomal proteins that repress gene expression. *Mol Cell Biol.* (2004), 24(18):8276-87.

Giannattasio S., Atlante A., Antonacci L., Guaragnella N., Lattanzio P., Passarella S., Marra E. Cytochrome c is released from coupled mitochondria of yeast en route to acetic acid-induced programmed cell death and can work as an electron donor and a ROS scavenger. *FEBS Lett*.(2008), 582(10): 1519-1525.

Giannattasio S., Guaragnella N., Arbini A.A., Moro L. Stress-related mitochondrial components and mitochondrial genome as targets of anticancer therapy. *Chem Biol Drug Des.* (2013), 81(1):102-12.

Green R., Lesage G., Sdicu A.M., Ménard P., Bussey H. A synthetic analysis of the *Saccharomyces cerevisiae* stress sensor Mid2p, and identification of a Mid2p-interacting protein, Zeo1p, that modulates the PKC1-MPK1 cell integrity pathway. *Microbiology.* (2003), 149(Pt 9):2487-99.

Guaragnella N., Bobba A., Passarella S., Marra E., Giannattasio S. Yeast acetic acid-induced programmed cell death can occur without cytochrome c release which requires metacaspase YCA1. *FEBS Lett*. (2010), 584(1): 224-228.

Guaragnella N., Pereira C., Sousa M. J., Antonacci L., Passarella S., Corte-Real M., Marra E., Giannattasio S. YCA1 participates in the acetic acid induced yeast programmed cell death also in a manner unrelated to its caspase like activity. *FEBS Lett.* (2006), 580(30):6880-6884.

Guaragnella, N., Ždralević, M., Antonacci, L., Passarella, S., Marra, E. and Giannattasio, S. The role of mitochondria in yeast programmed cell death. *Front Oncol.*(2012), 2: 70.

Haussmann P., Zimmermann F.K. The role of mitochondria in carbon catabolite repression in yeast. *Mol Gen Genet*. (1976), 148(2):205-11.

Haworth J., Alver R.C., Anderson M., Bielinsky A.K. Ubc4 and Not4 regulate steady-state levels of DNA polymerase-α to promote efficient and accurate DNA replication. *Mol Biol Cell*. (2010), 21(18):3205-19.

Hove-Jensen B. Mutation in the phosphoribosylpyrophosphate synthetase gene (prs) that results in simultaneous requirements for purine and pyrimidine nucleosides, nicotinamide nucleotide, histidine, and tryptophan in Escherichia coli. *J Bacteriol.* (1988), 170(3):1148-52.

Hughes A.L. and Gottschling D.E. An early age increase in vacuolar pH limits mitochondrial function and lifespan in yeast. *Nature*. (2012), 492(7428):261-5.

Hughes H. and Stephens D.J. Assembly, organization, and function of the COPII coat. *Histochem Cell Biol.* (2008), 129(2):129-51. Epub 2007 Dec 4. Review.

Khan M.A., Chock P.B., Stadtman E.R. Knockout of caspase-like gene, YCA1, abrogates apoptosis and elevates oxidized proteins in *Saccharomyces cerevisiae*. *Proc Natl Acad Sci U S A.* (2005), 102(48):17326-31.

Kim J.M., Yoshikawa H., Shirahige K. A member of the YER057c/yjgf/Uk114 family links isoleucine biosynthesis and intact mitochondria maintenance in *Saccharomyces cerevisiae. Genes Cells.* (2001), 6(6):507-17.

Knowles L.M., Yang C., Osterman A., Smith J.W. Inhibition of fatty-acid synthase induces caspase-8-mediated tumor cell apoptosis by up-regulating DDIT4. *J Biol Chem.* (2008), 283(46):31378-84.

Koybasi S., Senkal C.E., Sundararaj K., Spassieva S., Bielawski J., Osta W., Day T.A., Jiang J.C., Jazwinski S.M., Hannun Y.A., Obeid L.M., Ogretmen B. Defects in cell growth regulation by C18:0-ceramide and longevity assurance gene 1 in human head and neck squamous cell carcinomas. *J Biol Chem.* (2004), 279(43):44311-9.

Kolodziej S.J., Penczek P.A., Schroeter J.P., Stoops J.K. Structure-function relationships of the *Saccharomyces cerevisiae* fatty acid synthase. Three-dimensional structure. *J Biol Chem*. (1996), 271(45):28422-9.

Kus B.M., Caldon C.E., Andorn-Broza R., Edwards A.M. Functional interaction of 13 yeast SCF complexes with a set of yeast E2 enzymes in vitro. *Proteins*. (2004), 54(3):455-67.

Lecker S.H., Goldberg A.L., Mitch W.E. Protein degradation by the ubiquitin-proteasome pathway in normal and disease states. *J Am Soc Nephrol.* (2006), 17(7):1807-19.

Lecoq K., Belloc I., Desgranges C., Konrad M., Daignan-Fornier B. YLR209c encodes *Saccharomyces cerevisiae* purine nucleoside phosphorylase. *J Bacteriol.* (2001), 183(16):4910-3.

Lee R.E., Puente L.G., Kaern M., Megeney L.A. A non-death role of the yeast metacaspase: Yca1p alters cell cycle dynamics. *PLoS One.* (2008), 3;3(8):e2956.

Leibundgut M., Jenni S., Frick C., Ban N. Structural basis for substrate delivery by acyl carrier protein in the yeast fatty acid synthase. *Science.* (2007), 316(5822):288-90.

Leist M. and Jaattela M. Four deaths and a funeral: fromcaspases to alternative mechanisms. *Nat. Rev. Mol. Cell Biol*. (2001) 2, 589–598.

Logue S.E., Martin S.J. Caspase activation cascades in apoptosis. *Biochem Soc Trans*. (2008), 36(Pt 1):1-9.

Lomakin I.B., Xiong Y., Steitz T.A. The crystal structure of yeast fatty acid synthase, a cellular machine with eight active sites working together. *Cell.* (2007), 129(2):319-32.

Ludovico P., Sousa M.J., Silva M.T., Leão C., Côrte-Real M. *Saccharomyces cerevisiae* commits to a programmed cell death process in response to acetic acid. *Microbiology* (2001), 147: 2409-2415.

Madeo F., Carmona-Gutierrez D., Ring J., Büttner S., Eisenberg T., Kroemer G.. Caspase-dependent and caspase- independent cell death pathways in yeast. *Biochem.Biophys.Res.Commun.* (2009), 382:227–231.

Madeo F., Herker E., Maldener C., Wissing S., Lachelt S., Herlan M., Fehr M., Lauber K., Sigrist S.J., Wesselborg S., Frohlich K.U. A caspase-related protease regulates apoptosis in yeast. *Mol.Cell* (2002), 9: 911–917.

Magherini F., Tani C., Gamberi T., Caselli A., Bianchi L., Bini L., Modesti A. Protein expression profiles in *Saccharomyces cerevisiae* during apoptosis induced by H_2O_2. *Proteomics.* (2007), 7(9):1434-45.

McIlwain D.R., Berger T., Mak T.W. Caspase functions in cell death and disease. *Cold Spring Harb Perspect Biol.* (2013), 5(4):a008656.

Melamud E., Vastag L. ,. Rabinowitz J. D. Metabolomic analysis and visualization engine for LC-MS data. *Anal. Chem.* (2010) , 82(23), 9818–9826.

Ogretmen B., Hannun Y.A. Biologically active sphingolipids in cancer pathogenesis and treatment. *Nat Rev Cancer.* (2004), 4(8):604-16. Review.

Ohya Y., Umemoto N., Tanida I., Ohta A., Iida H., Anraku Y. Calcium-sensitive cls mutants of *Saccharomyces cerevisiae* showing a Pet- phenotype are ascribable to defects of vacuolar membrane H(+)-ATPase activity. *J Biol Chem*. (1991), 266(21):13971-7.

Oxelmark E., Marchini A., Malanchi I., Magherini F., Jaquet L., Hajibagheri M.A., Blight K.J., Jauniaux J.C., Tommasino M. Mmf1p, a novel yeast

mitochondrial protein conserved throughout evolution and involved in maintenance of the mitochondrial genome. *Mol Cell Biol*. (2000), ;20(20):7784-97.

Pereira C., Chaves S., Alves S., Salin B., Camougrand N., Manon S., Sousa M. J., Corte-Real M. Mitochondrial degradation in acetic acid-induced yeast apoptosis: the role of Pep4 and the ADP/ATP carrier. *Mol Microbiol*. (2010), 76(6): 1398-1410.

Pereira C., Coutinho I., Soares J., Bessa C., Leão M., Saraiva L. New insights into cancer-related proteins provided by the yeast model. *FEBS J.* (2012), 279(5):697-712.

Ralser M., Wamelink M.M., Kowald A., Gerisch B., Heeren G., Struys E.A., Klipp E., Jakobs C., Breitenbach M., Lehrach H., Krobitsch S. Dynamic rerouting of the carbohydrate flux is key to counteracting oxidative stress. *J Biol.* (2007), 21;6(4):10.

Reinders J., Sickmann A. Proteomics of yeast mitochondria. *Methods Mol Biol.* (2007), 372:543-57.

Seufert W., Jentsch S. Yeast ubiquitin-conjugating enzymes involved in selective protein degradation are essential for cell viability. *Acta Biol Hung*. (1991), 42(1-3):27-37. Review.

Shevchenko A., Wilm M., Vorm O., Mann M. Mass spectrometric sequencing of proteins silver-stained polyacrylamide gels. *Anal Chem.* (1996), 68(5):850-8.

Silva R.D., Manon S., Gonçalves J., Saraiva L., Côrte-Real M. The importance of humanized yeast to better understand the role of bcl-2 family in apoptosis: finding of novel therapeutic opportunities. *Curr Pharm Des*. (2011), 17(3):246-55. Review.

Smethurst D.G., Dawes I.W., Gourlay C.W. Actin - a biosensor that determines cell fate in yeasts. *FEMS Yeast Res*. (2014), 14(1):89-95.

Smith C.A., O'Maille G., Want E.J., Qin C., Trauger S.A., Brandon T.R., Custodio D.E., Abagyan R., Siuzdak G. METLIN: a metabolite mass spectral database. *Ther Drug Monit.* (2005), 27(6):747-51.

Switzer R.L. Regulation and mechanism of phosphoribosylpyrophosphate synthetase. I. Purification and properties of the enzyme from Salmonella typhimurium. *J Biol Chem.* (1969), 244(11):2854-63.

Tautenhahn R., Patti G. J., Kalisiak E., Miyamoto T., Schmidt M., Lo F. Y., McBee J., Baliga N. S., Siuzdak G.. MetaXCMS: second-order analysis of untargeted metabolomics data, *Anal. Chem*. (2011), 83(3): 696–700.

Thomas D., Surdin-Kerjan Y. Metabolism of sulfur amino acids in *Saccharomyces cerevisiae. Microbiol Mol Biol Rev.* (1997), 61(4):503-32. Review.

Valenti D., Vacca R.A., Guaragnella N., Passarella S., Marra E., Giannattasio S. A transient proteasome activation is needed for acetic acid-induced programmed cell death to occur in *Saccharomyces cerevisiae*. *FEMS Yeast Res.* (2008), 8(3):400-4.

Wang C. and Youle R. J. The role of mitochondria in apoptosis. *Annu Rev Genet.* (2009), 43: 95-118.

Watanabe N. and Lam E. Two Arabidopsis metacaspases AtMCP1b and AtMCP2b are arginine/lysine-specific cysteine proteases and activate apoptosis-like cell death in yeast. *J. Biol. Chem.* (2005), 280:14691–14699.

Wieland F., Siess E.A., Renner L., Verfürth C., Lynen F. Distribution of yeast fatty acid synthetase subunits: three-dimensional model of the enzyme. *Proc Natl Acad Sci U S A.* (1978), 75(12):5792-6.

Wilkinson D., Ramsdale M. Proteases and caspase-like activity in the yeast *Saccharomyces cerevisiae*. *Biochem.Soc.Trans.* (2011), 39: 1502–1508.

Wissing S., Ludovico P., Herker E., Büttner S., Engelhardt S.M., Decker T., Link A., Proksch A., Rodrigues F., Corte-Real M., Fröhlich K.U., Manns J., Candé C., Sigrist S.J., Kroemer G., Madeo F. An AIF orthologue regulates apoptosis in yeast. *J Cell Biol.* (2004), 166(7):969-74.

Ždralević M., Longo V., Guaragnella N., Giannattasio S., Timperio A.M., Zolla L. Differential proteome-metabolome profiling of YCA1-knock-out and wild type cells

reveals novel metabolic pathways and cellular processes dependent on the yeast metacaspase. *Mol Biosyst.* (2015).

Zeller C.E., Parnell S.C., Dohlman H.G. The RACK1 ortholog Asc1 functions as a G-protein beta subunit coupled to glucose responsiveness in yeast. *J Biol Chem.* (2007), 282(34):25168-76.

Supplementary table . Detailed MS/MS peptide sequence analysis of successfully identified proteins of 2D-SDS-PAGE

Spot No.	NCBI GI Number	Protein ID	*Matches*[a]	*no of peptides identified*[a]	*Sequence coverage*	Peptides identified by MS/MS					
						m/z	charge state	Mass error observed	start-end	sequence	Mascot Ion Score
1468	gi|171455	Enolase	11 (4)	5 (3)	14%	708.82	2+	-0.0855	16–28	GNPTVEVELTTEK	33
						789.85	2+	-0.0970	89–103	AVDDFLISLDGTANK	71
						749.40	2+	-0.0440	127–139	NVPLYKHLADLSK	11
						580.31	2+	0.0036	186–195	IGSEVYHNLK	58
						687.29	2+	-0.0654	244–255	IGLDCASSEFFK	60
899	gi|6321968	Phosphopyruvate hydratase ENO2	25(4)	7 (2)	11%	437.23	2+	-0.0693	331–338	IATAIEKK	39
						471.76	2+	-0.0704	338–346	KAADALLLK	27
						407.69	2+	-0.1203	339–346	AADALLLK	52
						644.80	2+	-0.1072	347–358	VNQIGTLSESIK	65
						466.69	2+	-0.0779	416–423	IEEELGDK	36
						482.18	3+	-0.1206	424–436	AVYAGENFHHGDK	16
						779.29	2+	-0.1677	424–437	AVYAGENFHHGDKL	40
528	gi|6321968	Phosphopyruvate hydratase ENO2	68(12)	19(5)	43%	421.17	2+	-0.0411	179–185	TFAEAMR + Oxid (M)	41
						580.27	2+	-0.0639	186–195	IGSEVYHNLK	74
						534.22	3+	-0.1308	242–255	VKIGLDCASSEFFK	31
						687.26	2+	-0.1146	244–255	IGLDCASSEFFK	50
						837.32	2+	-0.1327	244–258	IGLDCASSEFFKDGK	45
						367.50	3+	-0.0126	256–264	DGKYDLDFK	23
						490.86	3+	-0.1038	259–270	YDLDFKNPESDK	39
						637.28	3+	-0.0897	273–288	WLTGVELADMYHSLMK + Oxid (M)	33
						521.26	4+	0.0118	273–289	WLTGVELADMYHSLMKR + 2 Oxid (M)	36
						943.33	3+	-0.2927	290–312	YPIVSIEDPFAEDDWEAWSHFFK	33

						927.89	2+	-0.2171	313–330	TAGIQIVADDLTVTNPAR	76
						437.26	2+	-0.0201	331–338	IATAIEKK	46
						471.79	2+	-0.0240	338–346	KAADALLLK	45
						407.74	2+	-0.0196	339–346	AADALLLK	69
						644.82	2+	-0.0601	347–358	VNQIGTLSESIK	93
						621.58	3+	-0.1193	359–375	AAQDSFAANWGVMVSHR + Oxid (M)	23
						911.38	2+	-0.1608	376–392	SGETEDTFIADLVVGLR	93
						466.71	2+	-0.0353	416	IEEELGDK	53
						779.29	2+	-0.1593	424	AVYAGENFHHGDKL	52
525	gi|6321968	Phosphopyruvate hydratase ENO2	17(9)	7(4)	17%	580.30	2+	-0.0041	186–195	IGSEVYHNLK	53
						687.29	2+	-0.0600	244–255	IGLDCASSEFFK	72
						927.95	2+	-0.0844	313–330	TAGIQIVADDLTVTNPAR	96
						437.25	2+	-0.0371	331–338	IATAIEKK	53
						407.74	2+	-0.0137	339–346	AADALLLK	72
						644.83	2+	-0.0499	347–358	VNQIGTLSESIK	98
						466.72	2+	-0.0226	416–423	IEEELGDK	54
526	gi|6321968	Phosphopyruvate hydratase ENO2	39(13)	13(6)	31%	421.18	2+	-0.0267	179–185	TFAEAMR + Oxid (M)	47
						580.27	2+	-0.0638	186–195	IGSEVYHNLK	75
						687.27	2+	-0.1040	244–255	IGLDCASSEFFK	87
						558.58	3+	-0.0506	244–258	IGLDCASSEFFKDGK	14
						490.86	3+	-0.1008	259–270	YDLDFKNPESDK	36
						927.88	2+	-0.2200	313–330	TAGIQIVADDLTVTNPAR	86
						437.27	2+	0.0026	331–338	IATAIEKK	54
						471.79	2+	-0.0086	338–346	KAADALLLK	55
						407.74	2+	-0.0283	339–346	AADALLLK	72
						644.81	2+	-0.0931	347–358	VNQIGTLSESIK	80
						621.55	3+	-0.1951	359–375	AAQDSFAANWGVMVSHR + Oxid (M)	16
						911.41	2+	-0.1084	376–392	SGETEDTFIADLVVGLR	98
						519.88	3+	-0.0974	424–437	AVYAGENFHHGDKL	19

1421	gi|45269553	YGR192C	26(6)	10(4)	34%	746.96	3+	-0.2166	117–137	VVITAPSSTAPMFVMGVNEEK + 2 Oxid (M)	28
						910.38	2+	-0.1476	144–160	IVSNASCTTNCLAPLAK	63
						687.80	2+	-0.1246	199–213	TASGNIIPSSTGAAK	37
						442.24	2+	-0.0387	218-225	VLPELQGK	19
						406.21	2+	0.0054	226–232	LTGMAFR + Oxid (M)	21
						735.89	2+	-0.0651	233–246	VPTVDVSVVDLTVK	91
						376.17	3+	-0.0428	250–258	ETTYDEIKK	15
						876.80	2+	-0.1794	308–321	LVSWYDNEYGYSTR	61
						370.19	3+	-0.0545	322–331	VVDLVEHVAK	25
						590.31	2+	-0.0434	322–332	VVDLVEHVAKA	78
720	gi|45269553	YGR192C	49(9)	11(4)	34%	607.26	3+	-0.1295	144–160	IVSNASCTTNCLAPLAK	53
						864.39	4+	-0.1433	161–184	VINDAFGIEEGLMTTVHSLTATQK+ Oxid (M)	69
						687.81	2+	-0.1042	199–213	TASGNIIPSSTGAAK	49
						406.20	2+	-0.0099	226–232	LTGMAFR.V + Oxid (M)	46
						735.90	2+	-0.0331	233–246	VPTVDVSVVDLTVK.L	79
						677.30	2+	-0.0882	247–257	LNKETTYDEIK.K	45
						499.73	2+	-0.0047	250–257	ETTYDEIK.K	38
						563.78	2+	-0.0003	250–258	ETTYDEIKK.V	51
						876.83	2+	-0.1292	308–321	LVSWYDNEYGYSTR.V	90
						554.80	2+	-0.0292	322–331	VVDLVEHVAK.A	48
						590.34	2+	0.0029	322–332	VVDLVEHVAKA	71
666	gi|45269553	YGR192C	89(16)	12(6)	37%	910.37	2+	-0.1586	144–160	IVSNASCTTNCLAPLAK	61
						864.37	3+	-0.1853	161–184	VINDAFGIEEGLMTTVHSLTATQK + Oxid (M)	71
						433.20	3+	-0.0293	185–195	TVDGPSHKDWR	16
						687.81	2+	-0.1047	199–213	TASGNIIPSSTGAAK	52
						406.20	2+	-0.0177	226–232	LTGMAFR + Oxid (M)	38
						735.90	2+	-0.0423	233–246	VPTVDVSVVDLTVK	87
						677.30	2+	-0.0966	247–257	LNKETTYDEIK	53
						499.73	2+	-0.0139	250–257	ETTYDEIK	39

						563.76	2+	-0.0465	250–258	ETTYDEIKK	58
						876.84	2+	-0.0988	308–321	LVSWYDNEYGYSTR	68
						554.82	2+	-0.0034	322–331	VVDLVEHVAK	67
						590.29	2+	-0.0951	322–332	VVDLVEHVAKA	67
661	gi|45269553	YGR192C	37(5)	12(3)	36%	363.69	2+	0.0058	138–143	YTSDLK	20
						910.38	2+	-0.1388	144–160	IVSNASCTTNCLAPLAK	52
						864.39	4+	-0.1400	161–184	VINDAFGIEEGLMTTVHSLTATQK + Oxid (M)	23
						687.82	2+	-0.0802	199–213	TASGNIIPSSTGAAK	63
						406.22	2+	0.0227	226–232	LTGMAFR + Oxid (M)	44
						735.88	2+	-0.0859	233–246	VPTVDVSVVDLTVK	117
						451.89	3+	-0.0129	247–257	LNKETTYDEIK	30
						499.71	2+	-0.0406	250–257	ETTYDEIK	23
						563.77	2+	-0.0236	250–258	ETTYDEIKK	52
						876.84	2+	-0.1127	308–321	LVSWYDNEYGYSTR	50
						554.81	2+	-0.0079	322–331	VVDLVEHVAK	48
						590.33	2+	-0.0062	322–332	VVDLVEHVAKA	71
1006	gi|229428	glyceraldehydephosphate dehydrogenase	10(6)	5(3)	12%	687.79	2+	-0.1300	198–212	TASGNIIPSSTGAAK	36
						735.88	2+	-0.0803	232–245	VPTVDVSVVDLTVK	94
						876.83	2+	-0.1215	307–320	LVSWYDNEYGYSTR	85
1019	gi|3710	hexokinase PII	9(3)	5(2)	27%	712.80	2+	-0.0725	22–32	ELMQQIENFEK + Oxid (M)	46
						774.35	2+	-0.1606	33–46	IFTVPTETLQAVTK	44
						839.35	2+	-0.1408	78–93	ESGDFLAIDLGGTNLR	73
						471.74	2+	-0.0514	166–173	INEGILQR	66
						694.62	3+	-0.1821	177–194	GFDIPNIENHDVVPMLQK + Oxid (M)	31
169	gi|6319673	glucose-6-phosphate isomerase	9(2)	5(1)	10%	558.29	2+	-0.0324	11–20	LATELPAWSK	24
						516.72	2+	-0.0278	51–59	TFTNYDGSK	31
						430.20	2+	-0.0539	83–90	EANVTGLR	46
						792.37	2+	-0.0418	220–234	TFTTAETITNANTAK	78
						759.39	2+	0.0220	251–264	HFAALSTNETEVAK	52

	gi|6320226	serine-tRNA ligase SES1	8(2)	5(1)	12%	475.70	2+	-0.0102	161–168	LDGYDPDR	34
						747.32	2+	-0.1148	203–215	GYIPLQAPVMMNK + 2 Oxid (M)	23
						786.82	2+	-0.1014	221–233	TAQLSEFDEELYK	21
						656.76	2+	-0.0462	319–328	MISYSEEFYK + Oxid (M)	23
						728.35	2+	-0.1085	336–350	IVGIVSGELNNAAAK	80
	gi|6322049	Cct2p	10(4)	7(3)	14%	572.79	2+	-0.0758	126–137	LASAAALDALTK	92
						545.25	2+	-0.0729	361–370	AGEACTIVLR	62
						653.27	2+	-0.0424	371–382	GATDQTLDEAER	93
						736.29	2+	-0.0736	400–413	TVLGGGCAEMVMSK + 2 Oxid (M)	61
						463.55	3+	-0.0440	414-426	AVDTEAQNIDGKK	20
						482.25	2+	-0.0267	427–435	SLAVEAFAR	55
						518.77	2+	-0.0336	484–492	QLGIVESYK	11
1252	gi|171029	alcohol dehydrogenase	4(2)	2(1)	4%	507.31	2+	0.0286	31-39	ANELLINVK	65
						484.72	2+	-0.0397	304-311	EALDFFAR	49
520	gi|223142	dehydrogenase isozyme I,alcohol	17(6)	9(3)	31%	507.29	2+	-0.0100	20–28	ANELLINVK	50
						809.91	2+	-0.0261	171–185	VLGIDGGEGKEELFR	87
						701.83	2+	-0.0765	212–226	ANGTTVLVGMPAGAK + Oxid (M)	58
						678.28	2+	-0.0423	227–237	CCSDVFNQVVK	75
						626.29	2+	-0.0842	238–249	SISIVGSYVGNR	74
						484.74	2+	0.0013	254–261	EALDFFAR	47
						724.35	2+	-0.0964	270–282	VVGLSTLPEIYEK	55
						617.98	3+	-0.0391	270–285	VVGLSTLPEIYEKMEK + Oxid (M)	22
						406.21	2+	0.0106	292–298	YVVDTSK	24
514	gi|223142	dehydrogenase isozyme I,alcohol	19(8)	10(5)	32%	507.29	2+	-0.0139	20–28	ANELLINVK	59
						809.86	2+	-0.1199	171–185	VLGIDGGEGKEELFR	71
						407.72	2+	-0.0579	188–195	DIVGAVLK	44
						701.82	2+	-0.1026	212–226	ANGTTVLVGMPAGAK + Oxid (M)	59
						678.25	2+	-0.1014	227–237	CCSDVFNQVVK	82
						626.28	2+	-0.1133	238–249	SISIVGSYVGNR	61

644						484.73	2+	-0.0275	254–261	EALDFFAR	43
						724.33	2+	-0.1320	270–282	VVGLSTLPEIYEK	36
						406.20	2+	-0.0175	292–298	YVVDTSK	21
	gi|6322790	fructose-bisphosphate aldolase FBA1	11(1)	6(1)	23%	621.63	3+	-0.0686	11–27	TGVIVGEDVHNLFTYAK	14
						709.00	3+	-0.0924	53–73	DSKSPIILQTSNGGAAYFAGK	27
						609.26	2+	-0.0846	74–85	GISNEGQNASIK	50
						521.77	2+	-0.0306	86–95	GAIAAAHYIR	61
						705.95	3+	-0.1749	309–327	DYIMSPVGNPEGPEKPNKK + Oxid (M)	21
						341.16	2+	-0.0105	328–332	FFDPR	27
	gi|6323004	Hsp70 family chaperone SSA2	14(2)	7(1)	15%	729.29	2+	-0.1065	35-47	TTPSFVGFTDTER	54
						804.31	2+	-0.1340	55-69	NQAAMNPANTVFDAK + Oxid (M)	39
						783.84	2+	-0.0963	111-124	NFTPEQISSMVLGK + Oxid (M)	14
						448.52	3+	-0.0822	125-136	MKETAESYLGAK + Oxid (M)	34
						632.25	3+	-0.1777	137-153	VNDAVVTVPAYFNDSQR	45
						600.31	2+	-0.0524	158-169	DAGTIAGLNVLR	80
						596.64	3+	-0.0714	170-186	IINEPTAAAIAYGLDKK	19
1638	gi|256270485	Pdc1p	17(2)	6(1)	11%	332.71	2+	0.0126	342–347	LIHGPK	24
						503.73	2+	-0.0184	375–383	VATTGEWDK	47
						796.34	2+	-0.1123	375–388	VATTGEWDKLTQDK	55
						773.35	3+	-0.1355	398–417	MIEIMLPVFDAPQNLVEQAK + 2 Oxid (M)	33
						395.22	2+	-0.0088	418–425	LTAATNAK	35
						459.24	2+	-0.0297	418–426	LTAATNAKQ	69
	gi|398364461	Hmf1p	2(2)	1(1)	9%	652.77	2+	-0.1110	62-73	NVLEASNSSLDR	105
45	gi|6323073	indolepyruvate decarboxylase 1	7(1)	7(1)	12%	364.19	2+	0.0070	9–13	YLFER	17
						563.90	3+	-0.1057	210–224	DAKNPVILADACCSR	52
						688.27	2+	-0.0962	213–224	NPVILADACCSR	58
						532.94	3+	-0.0391	259–273	YGGVYVGTLSKPEVK	23
						554.75	2+	-0.0331	318–327	NATFPGVQMK + Oxid (M)	21
						508.81	2+	0.0153	333–342	LLTTIADAAK	41

						669.33	2+	-0.0876	353–366	TPANAAVPASTPLK	38
1771	gi|10383781	phosphoglycerate kinase	39(19)	14(9)	30%	569.94	3+	-0.0614	244–258	KVLENTEIGDSIFDK	47
						790.32	2+	-0.1442	245–258	VLENTEIGDSIFDK	81
						782.33	3+	-0.2465	245–266	VLENTEIGDSIFDKAGAEIVPK	68
						776.29	3+	-0.2621	298–319	TVTDKEGIPAGWQGLDNGPESR	25
						594.88	3+	-0.1872	303–319	EGIPAGWQGLDNGPESR	27
						474.76	2+	-0.0626	320–328	KLFAATVAK	54
						410.75	2+	0.0105	321–328	LFAATVAK	7
						860.36	2+	-0.1567	331–345	TIVWNGPPGVFEFEK	37
						443.76	2+	-0.0020	352–359	ALLDEVVK	51
						895.35	2+	-0.2215	360–379	SSAAGNTVIIGGGDTATVAK	113
						639.96	3+	-0.1574	360–380	SSAAGNTVIIGGGDTATVAKK	37
						585.60	3+	-0.1140	387–404	ISHVSTGGGASLELLEGK	28
						595.29	2+	-0.0720	405–415	ELPGVAFLSEK	68
						659.34	2+	-0.0601	405–416	ELPGVAFLSEKK	16
1652	gi|151944153	branched-chain amino acid transaminase	3(0)	2(0)	4%	520.25	2+	-0.0039	201–209	LEATDYATR	41
						608.80	2+	-0.0233	311–320	YYTITEVATR	56
706	gi|6319307	cystathionine gamma-lyase CYS3	10(6)	3(2)	8%	395.85	3+	-0.0861	289–298	THPNYDVVLK	43
						570.26	2+	-0.0265	302–312	DALGGGMISFR + Oxid (M)	88
						604.26	2+	-0.0664	360–370	EASGVFDDLVR	79
1711	gi|365764754	Ado1p	47(9)	10(3)	27%	526.94	3+	-0.0073	27–40	YSLKENDAILVDAK	8
						544.21	2+	-0.1343	31–40	ENDAILVDAK	37
						566.57	3+	-0.1063	46–59	MAIFDELLQMPETK + 2 Oxid (M)	52
						564.75	2+	-0.1009	60–71	LVAGGAAQNTAR	92
						430.21	2+	-0.0287	97–103	LLNENEK	46
						728.79	2+	-0.1223	108–120	SFYQVQNDIGTGK	78
						556.74	2+	-0.0734	121–130	CAALITGHNR	39
						338.85	3+	-0.0281	245–253	IVKDSPVEK	35

						740.34	2+	-0.0803	271–284	GTSTYPVKPLDSSK	23
609	gi|6320593	Eft2p	18(5)	6(3)	6%	533.73	2+	-0.0788	2–10	VAFTVDQMR	66
						560.27	2+	-0.0488	33–42	STLTDSLVQR	62
						365.71	2+	-0.0259	43–50	AGIISAAK	56
						895.80	2+	-0.1988	72–87	STAISLYSEMSDEDVK + Oxid (M)	75
						720.94	3+	-0.2061	72–90	STAISLYSEMSDEDVKEIK + Oxid (M)	35
						571.72	2+	-0.1082	172–180	EDLYQTFAR	52
1444	gi|173214	elongation factor 3	3(0)	2(0)	1%	503.27	2+	-0.0111	10–17	VLEELFQK	46
						473.72	2+	-0.0595	18–26	LSVATADNR	51
	gi|6325038	Sar1p	4(0)	3(0)	19%	580.82	2+	-0.0150	26–36	LLFLGLDNAGK	38
						692.83	2+	-0.0453	134–146	IDAPNAVSEAELR	34
						659.30	2+	-0.1014	147–159	SALGLLNTTGSQR	42
553	gi|6325273	Tif6p	3(0)	2(0)	11%	800.31	2+	-0.1515	5–18	TQFENSNEIGVFSK	52
						764.33	2+	-0.1102	224–237	LQDAQPESISGNLR	53
1730	gi|6325036	ribosomal 60S subunit protein L1A	8(1)	4(1)	16%	395.70	2+	-0.0408	4–10	ITSSQVR	33
						706.75	2+	-0.0992	79–91	SCGVDAMSVDDLK + Oxid (M)	61
						514.20	3+	-0.0918	79–92	SCGVDAMSVDDLKK + Oxid(M)	26
						530.56	3+	-0.0836	134–147	FPTPVSHNDDLYGK	10
	gi|6321362	ribosomal 60S subunit protein L7A	7(2)	5(1)	22%	487.73	2+	-0.0264	22–30	TAEQVAAER	76
						357.72	2+	-0.0082	42–47	AIILER	16
						524.89	3+	-0.0659	48–60	NAAYQKEYETAER	24
						777.38	2+	-0.0867	161–175	VPLSDNAIIEANLGK	37
						613.77	2+	-0.0836	207–218	LSNPSGGWGVPR	31
	gi|207342264	YMR142Cp-like protein	14(4)	6(2)	30%	432.72	2+	-0.0369	104–111	GFTLAEVK	58
						482.72	2+	-0.0708	112–121	AAGLTAAYAR	53
						577.91	3+	-0.1097	132–145	QNRNQEIFDANVQR	24
						667.27	2+	-0.0986	135–145	NQEIFDANVQR	86
						885.02	3+	-0.2784	162–187	APEAEQVLSAAATFPIAQPATDVEAR	22
						597.24	2+	-0.0713	188–198	AVQDNGESAFR	75

1697	gi|6320781	ribosomal 60S subunit protein L12A	51(5)	12(4)	65%	364.20	2+	-0.0103	12–16	YLYLR	27
						649.32	2+	-0.0748	17–31	AVGGEVGASAALAPK	63
						441.27	2+	-0.0083	32–40	IGPLGLSPK	62
						430.21	2+	-0.0577	41–48	KVGEDIAK	48
						366.18	2+	-0.0313	42–48	VGEDIAK	55
						344.22	2+	-0.0061	58–63	VTVQLK	27
						605.06	3+	0.1423	68–86	QAAASVVPSASSLVITALK	54
						764.73	3+	-0.1104	68–90	QAAASVVPSASSLVITALKEPPR	14
						360.20	2+	-0.0193	124–130	TLASVTK	37
						645.77	2+	-0.0976	131–142	EILGTAQSVGCR	90
						855.00	4+	-0.2757	143–165	VDFKNPHDIIEGINAGEIEIPEN	43
						1037.4	2+	-0.1885	147–165	NPHDIIEGINAGEIEIPEN	59
	gi|6322357	Pam16p	8(3)	5(2)	29%	414.19	2+	-0.0156	20–26	AFAEAYR	41
						714.74	2+	-0.1489	48–60	GEYGGITLDESCK	64
						473.27	2+	0.0225	61–68	ILNIEESK	42
						578.86	3+	-0.2844	61–75	ILNIEESKGDLNMDK + Oxid (M)	18
						493.71	2+	-0.0656	92–100	GGSFYLQSK	65
1141	gi|6322984	ribosomal 60S subunit protein L8B	7(0)	4(0)	15%	579.81	2+	-0.0130	33–43	NFGIGQAVQPK	49
						430.22	2+	-0.0056	112–120	EAAAIAEGK	36
						559.29	2+	-0.0386	194–204	TSAVAALTEVR	55
						672.67	3+	-0.0589	194–213	TSAVAALTEVRAEDEAALAK	38
1786	gi|6323090	ribosomal 60S subunit protein L22A	2(1)	1(1)	14%	1036.33	2+	-0.1908	105-121	LAFYQVTPEEDEEEDEE	61
1754	gi|6321653	ribosomal 40S subunit protein S0A	3(0)	2(0)	8%	423.86	3+	-0.0859	89-101	FAAHTGATPIAGR	18
						456.77	2+	-0.0164	120-127	LVIVTDPR	42
	gi|6322732	Sba1p	4(0)	2(0)	9%	641.30	2+	-0.1071	5-15	VINPQVAWAQR	28
						597.75	2+	-0.0449	98-106	DLESEYWPR	49
1659	gi|6323577	ribosomal 40S	11(3)	7(2)	29%	461.22	2+	-0.0094	34–41	APSTFENR	26

		subunit protein S1B				348.56	3+	0.0907	86–94	LRVDEVQGK	27
						484.68	2+	-0.1104	129–136	TSDDYVLR	59
						465.80	2+	0.0414	167–174	VISEILTR	31
						709.85	2+	-0.0536	175–187	EVQNSTLAQLTSK	62
						621.59	3+	-0.0996	223–240	FDVGALMALHGEGSGEEK + Oxid (M)	24
						661.83	2+	-0.0303	244–255	VSGFKDEVLETV	20
	gi|6321997	ribosomal 40S subunit protein S4B	32(6)	16(4)	50%	533.25	3+	-0.0495	23–37	LSGCYAPRPSAGPHK	20
						593.85	2+	-0.0138	40–49	ESLPLIVFLR	52
						366.21	2+	0.0079	63-68	AILMQR	30
						869.99	3+	-0.2244	78–100	TDTTYPAGFMDVITLDATNENFR + Oxid (M)	31
						368.71	2+	-0.0002	101–106	LVYDVK	20
						528.20	2+	-0.0954	114–122	ITDEEASYK	79
						677.33	2+	-0.0286	114–125	ITDEEASYKLGK	60
						443.24	3+	-0.0063	134–145	KGVPYVVTHDGR	49
						600.28	2+	-0.0580	135–145	GVPYVVTHDGR	62
						453.92	3+	0.0013	156–168	VNDTVKIDLASGK	37
						352.20	2+	-0.0051	162–168	IDLASGK	43
						627.79	2+	-0.0817	169–179	ITDFIKFDAGK	16
						461.60	3+	0.0606	175–187	FDAGKLVYVTGGR	10
						432.73	2+	-0.0256	180–187	LVYVTGGR	35
						584.26	2+	-0.0415	212–221	DSLDNTFVTR	76
						409.21	2+	-0.0156	246–252	LSIAEER	34
1662	gi|37362658	Ssz1p	8(0)	4(0)	7%	623.60	3+	-0.1233	366–384	NASNNPNELAASGAALQAR	54
						398.22	2+	-0.0109	491–497	LYTLGTK	37
						315.85	3+	0.0186	527–535	DLKTGNAVK	20
						444.73	2+	-0.0242	530–538	TGNAVKGEL	26
	gi|6323371	ribosomal protein P0	5(2)	4(1)	11%	367.20	2+	-0.0279	49–55	AVVLMGK + Oxid (M)	25
						401.22	2+	-0.0065	98–104	NVIVSNR	30
						642.28	2+	-0.1060	111–122	AGAVAPEDIWVR	25

						530.76	2+	-0.0641	148–157	GTIEIVSDVK	88
1667	gi|6320718	SUMO family protein SMT3	3(1)	2(1)	17%	608.28	2+	-0.0292	28-38	VSDGSSEIFFK	43
						442.24	2+	0.0196	65-71	FLYDGIR	71
540	gi|6323004	Hsp70 family chaperone SSA2	16(5)	8(4)	17%	730.33	2+	-0.1185	326–339	SQVDEIVLVGGSTR	67
						387.21	2+	0.0035	449–455	DNNLLGK	35
						509.30	2+	0.0291	498–506	ITITNDKGR	38
						481.27	2+	0.0178	507–514	LSKEDIEK	62
						633.31	2+	-0.0547	537–547	NQLESIAYSLK	54
						875.86	2+	-0.1176	569–584	AEETIAWLDSNTTATK	58
						687.81	2+	-0.0788	593–604	ELQEVANPIMSK + Oxid (M)	75
						1088.0	3+	-0.2782	605–639	LYQAGGAPEGAAPGGFPGGAPPAPEAEGPTVEE	28
1261	gi|6323004	Hsp70 family chaperone SSA2	15(1)	7(1)	11%	449.52	3+	-0.1748	495–506	SNKITITNDKGR	26
						509.22	2+	-0.1199	498–506	ITITNDKGR	48
						481.21	2+	-0.1069	507–514	LSKEDIEK	38
						475.50	3+	-0.1736	522–532	FKEEDEKESQR	35
						633.26	2+	-0.1480	537–547	NQLESIAYSLK	68
						711.61	3+	-0.2297	548–567	NTISEAGDKLEQADKDAVTK	40
						687.80	2+	-0.0871	593–604	ELQEVANPIMSK + Oxid (M)	31
645	gi|151941387	stress-seventy subfamily A protein	37(12)	13(8)	19%	607.74	2+	-0.1281	24–34	VDIIANDQGNR	54
						736.27	2+	-0.1653	35–47	TTPSFVAFTDTER	73
						812.26	2+	-0.2183	55–69	NQAAMNPSNTVFDAK + Oxid (M)	92
						593.88	3+	-0.1975	55–70	NQAAMNPSNTVFDAKR + Oxid(M)	32
						705.22	2+	-0.1636	75–86	NFNDPEVQGDMK + Oxid(M)	64
						783.82	2+	-0.1453	111–124	NFTPEQISSMVLGK + Oxid(M)	67
						672.25	2+	-0.1465	125–136	MKETAESYLGAK + Oxid (M)	61
						534.70	2+	-0.1161	127–136	ETAESYLGAK	53
						632.24	3+	-0.2238	137–153	VNDAVVTVPAYFNDSQR	65
						600.28	2+	-0.1069	158–169	DAGTIAGLNVLR	88
						830.35	2+	-0.1968	170–185	IINEPTAAAIAYGLDK	64

643	gi|151941387	stress-seventy subfamily A protein	36(13)	12(7)	19%	607.78	2+	-0.0425	24–34	VDIIANDQGNR	65
						736.31	2+	-0.0817	35–47	TTPSFVAFTDTER	19
						812.31	2+	-0.1204	55-69	NQAAMNPSNTVFDAK + Oxid (M)	102
						593.92	3+	-0.0802	55–70	NQAAMNPSNTVFDAKR + Oxid (M)	15
						705.25	2+	-0.0967	75–86	NFNDPEVQGDMK + Oxid (M)	48
						775.83	2+	-0.1215	111–124	NFTPEQISSMVLGK	67
						672.31	2+	-0.0354	125–136	MKETAESYLGAK + Oxid (M)	67
						534.73	2+	-0.0521	127–136	ETAESYLGAK	41
						632.29	3+	-0.0610	137–153	VNDAVVTVPAYFNDSQR	58
						600.29	2+	-0.0947	158–169	DAGTIAGLNVLR	87
						830.38	2+	-0.1304	170–185	IINEPTAAAIAYGLDK	96
						894.45	2+	-0.0942	170–186	IINEPTAAAIAYGLDKK	47
1706	gi|6319972	Hsp70 family ATPase SSB1	41(8)	22(5)	32%	493.88	3+	-0.1172	39–51	VTPSFVAFTPEER	42
						442.21	2+	-0.0605	59–66	NQAALNPR	41
						397.70	2+	-0.0016	67–73	NTVFDAK	29
						484.20	2+	-0.0358	80–87	FDDESVQK	53
						453.17	3+	-0.0836	80–90	FDDESVQKDMK + Oxid(M)	23
						1080.4	2+	-0.1899	96–114	VIDVDGNPVIEVQYLEETK	84
						782.84	2+	-0.1273	144–157	AVITVPAYFNDAQR	11
						531.71	2+	-0.0881	252–261	TGLDISDDAR	79
						584.27	2+	-0.0525	305–314	FEDLNAALFK	61
						621.82	2+	-0.0560	315–325	STLEPVEQVLK	54
						778.91	2+	-0.0348	315-328	STLEPVEQVLKDAK	13
						730.31	2+	-0.1429	332–345	SQIDEVVLVGGSTR	46
						521.24	2+	-0.0466	352–360	LLSDFFDGK	43
						593.92	3+	-0.1246	452–466	VNCKENTLLGEFDLK	28
						639.82	2+	-0.0150	456–466	ENTLLGEFDLK	79
						609.78	2+	-0.0809	502–513	SSNITISNAVGR	71
						467.72	2+	-0.0263	514–521	LSSEEIEK	48

						676.31	3+	-0.0263	514–530	LSSEEIEKMVNQAEEFK + Oxid(M)	7
						556.22	2+	-0.0628	522–530	MVNQAEEFK + Oxid (M)	52
						638.93	3+	-0.1113	522–538	MVNQAEEFKAADEAFAK + Oxid (M)	32
						411.70	2+	-0.0017	531–538	AADEAFAK	48
						722.64	3+	-0.1910	546–565	LESYVASIEQTVTDPVLSSK	23
	gi|3417405	TFP1	29(8)	15(4)	24%	479.24	2+	-0.0161	128–136	GIDTPALDR	42
						932.88	2+	-0.1653	181–197	GTITWIAPAGEYTLDEK	32
						525.25	2+	-0.0489	198–206	ILEVEFDGK	45
						667.32	2+	-0.0745	228–239	LSADYPLLTGQR.	63
						481.75	2+	-0.0507	264–272	TVISQSLSK	53
						781.33	2+	-0.1381	316–330	TTLVANTSNMPVAAR + Oxid (M)	69
						537.55	3+	-0.0845	346–360	DQGKNVSMIADSSSR + Oxid (M)	32
						583.74	2+	-0.0688	350–360	NVSMIADSSSR	86
						890.82	2+	-0.2058	372–388	LGEMPADQGFPAYLGAK + Oxid (M)	42
						443.21	2+	-0.0194	389–395	LASFYER	35
						443.23	2+	-0.0134	399–407	AVALGSPDR	37
						426.21	2+	-0.0356	464–470	YTNVLNK	43
						436.86	3+	-0.0316	550–560	AFISYHDEAQK	17
						453.21	2+	-0.0394	571–579	LADSTGDVK	64
						489.22	2+	-0.0589	604–611	LLSTMQER	32
723	gi|6319972	Hsp70 family ATPase SSB1	19(3)	9(2)	11%	593.93	3+	-0.1107	452–466	VNCKENTLLGEFDLK	38
						639.79	2+	-0.0812	456–466	ENTLLGEFDLK	53
						609.77	2+	-0.1010	502–513	SSNITISNAVGR	92
						467.73	2+	-0.0125	514–521	LSSEEIEK	33
						556.22	2+	-0.0600	522–530	MVNQAEEFK + Oxid(M)	51
						638.92	3+	-0.1296	522–538	MVNQAEEFKAADEAFAK + Oxid (M)	51
						411.70	2+	-0.0011	531–538	AADEAFAK	57
						1083.4	2+	-0.1956	546–565	LESYVASIEQTVTDPVLSSK	60
120	gi|151944335	stress-seventy	127(29)	34(13)	48%	740.31	2+	-0.1232	39–51	VTPSFVAFTPEER	50

		subfamily B protein				442.22	2+	-0.0242	59–66	NQAALNPR	64
						475.74	2+	-0.0188	67–74	NTVFDAKR	41
						562.26	2+	-0.0130	79–87	RFDDESVQK	54
						484.22	2+	0.0006	80–87	FDDESVQK	55
						679.28	2+	-0.0362	80–90	FDDESVQKDMK + Oxid(M)	33
						1080.4	2+	-0.1212	96–114	VIDVDGNPVIEVQYLEETK	93
						776.38	2+	-0.0480	115–128	TFSPQEISAMVLTK	59
						460.25	2+	0.0020	129–136	MKEIAEAK	56
						522.25	3+	-0.0720	144–157	AVITVPAYFNDAQR	49
						538.72	3+	0.2693	158–173	QATKDAGAISGLNVLR	43
						593.30	2+	-0.0611	162–173	DAGAISGLNVLR	110
						865.44	2+	-0.0755	174–191	IINEPTAAAIAYGLGAGK	99
						595.75	2+	-0.1013	251–261	KTGLDISDDAR	57
						531.74	2+	-0.0142	252–261	TGLDISDDAR	78
						465.55	3+	-0.1058	303–314	ARFEDLNAALFK	45
						584.27	2+	-0.0521	305–314	FEDLNAALFK	80
						621.83	2+	-0.0316	315–325	STLEPVEQVLK	59
						778.89	2+	-0.0697	315–328	STLEPVEQVLKDAK	47
						596.64	3+	-0.0598	329–345	ISKSQIDEVVLVGGSTR	48
						730.36	2+	-0.0538	332–345	SQIDEVVLVGGSTR	111
						521.25	2+	-0.0172	352–360	LLSDFFDGK	56
						770.40	2+	-0.0001	352–364	LLSDFFDGKQLEK	57
						437.25	2+	-0.0097	421–428	NTTVPTIK	26
						515.29	2+	-0.0175	421–429	NTTVPTIKR	23
						806.69	3+	-0.0946	431–451	TFTTVSDNQTTVQFPVYQGER	50
						639.80	2+	-0.0585	456–466	ENTLLGEFDLK	71
						609.79	2+	-0.0629	502–513	SSNITISNAVGR	79
						467.71	2+	-0.0547	514–521	LSSEEIEK	48
						676.29	3+	-0.0990	514–530	LSSEEIEKMVNQAEEFK + Oxid (M)	33

						556.23	2+	-0.0501	522–530	MVNQAEEFK + Oxid (M)	72
						633.61	3+	-0.0771	522–538	MVNQAEEFKAADEAFAK	50
						411.70	2+	0.0028	531–538	AADEAFAK	73
						1083.50	2+	-0.1198	546–565	LESYVASIEQTVTDPVLSSK	52
400	gi|533365	SSE1 protein	10(4)	4(3)	8%	595.24	3+	-0.1173	583–598	KLEEEYAPFASDAEK	37
						851.31	2+	-0.1344	608–621	AEEWLYDEGFDSIK	91
						689.33	2+	-0.0804	628–639	YEELASLGNIIR	73
						514.56	3+	-0.0225	655–668	SKQEASQMAAMAEK + 2 Oxid(M)	59
809	gi|6324463	Zeo1p	4(2)	3(1)	21%	594.76	2+	-0.0604	8-18	AETAAQDVQQK	79
						496.54	2+	-0.1200	57-68	KEEQNIADGVEQK	25
						680.26	2+	-0.1230	58-69	EEQNIADGVEQK	24
	gi|6323004	Hsp70 family chaperone SSA2	5(0)	3(0)	5%	729.28	2+	-0.1182	35-47	TTPSFVGFTDTER	49
						448.54	3+	-0.0377	125-136	MKETAESYLGAK + Oxid (M)	16
						600.32	2+	-0.0316	158-169	DAGTIAGLNVLR	49
769	gi|6323138	Ahp1p	20(5)	6(2)	36%	309.17	3+	0.0406	8–15	KFPAGDYK	28
						399.18	2+	-0.0276	9–15	FPAGDYK	25
						974.85	2+	-0.1488	16–32	FQYIAISQSDADSESCK	113
						561.25	2+	-0.0246	33–41	MPQTVEWSK + Oxid (M)	57
						600.74	2+	-0.0463	114–124	FASDPGCAFTK	73
						1027.9	2+	-0.1104	157–176	ETNPGTDVTVSSVESVLAHL	39
987	gi|6323138	Ahp1p	16(8)	5(3)	36%	399.19	2+	-0.0033	9–15	FPAGDYK	25
						974.88	2+	-0.0953	16–32	FQYIAISQSDADSESCK	109
						561.22	2+	-0.0859	33–41	MPQTVEWSK + Oxid(M)	59
						600.73	2+	-0.0756	114–124	FASDPGCAFTK	69
						1027.9	2+	-0.0782	157–176	ETNPGTDVTVSSVESVLAHL	30
984	gi|6323138	Ahp1p	18(7)	6(3)	34%	463.23	2+	-0.0099	8–15	KFPAGDYK	30
						399.17	2+	-0.0343	9–15	FPAGDYK	25
						974.88	2+	-0.0962	16–32	FQYIAISQSDADSESCK	106
						561.25	2+	-0.0337	33–41	MPQTVEWSK + Oxid (M)	58

						600.73	2+	-0.0692	114–124	FASDPGCAFTK	81
						834.31	2+	-0.2292	142–156	WAMVVENGIVTYAAK + Oxid (M)	29
	gi|6323613	Tsa1p	5(0)	3(0)	11%	451.77	2+	0.0076	125–132	GLFIIDPK	41
						408.71	2+	-0.0043	148–154	NVDEALR	31
						486.21	2+	-0.0196	189–196	EYFEAANK	23
773	gi|6323138	Ahp1p	30(5)	8(3)	51%	309.15	3+	-0.0127	8–15	KFPAGDYK	32
						399.19	2+	0.0014	9–15	FPAGDYK	31
						974.81	2+	-0.2275	16–32	FQYIAISQSDADSESCK	110
						553.23	2+	-0.0674	33–41	MPQTVEWSK	64
						400.23	3+	-0.0036	103–113	SLGVKDTTHIK	19
						600.72	2+	-0.0920	114–124	FASDPGCAFTK	31
						826.36	2+	-0.1371	142–156	WAMVVENGIVTYAAK	50
						1027.9	2+	-0.1535	157–176	ETNPGTDVTVSSVESVLAHL	59
823	gi|2624655	Chain A, Yeast Hsp90 Chaperone	4(0)	3(0)	12%	638.29	2+	-0.0613	33-44	ELISNASDALDK	48
						680.85	2+	-0.0123	55-65	QLETEPDLFIR	33
						315.21	2+	0.0284	74-78	VLEIR	28
427	gi|6324321	Sis1p	1(0)	1(0)	3%	714.29	2+	-0.0931	62-73	EIYDQYGLEAAR	33
1533	gi|2326840	Fas2	2(0)	2(0)	7%	637.79	2+	-0.0937	1-12	SEGNPVIGVFQK	43
						621.30	2+	-0.0549	72-83	AVSITSFGFGQK	38
1765	gi|671634	BMH1	35(6)	14(3)	46%	462.70	2+	-0.0583	6–13	EDSVYLAK	35
						667.93	3+	-0.0903	14–29	LAEQAERYEEMVENMK + 2 Oxid (M)	39
						586.69	2+	-0.1213	21–29	YEEMVENMK	38
						746.30	2+	-0.1161	30–43	TVASSGQELSVEER	90
						454.26	2+	0.0025	44–51	NLLSVAYK	44
						452.23	2+	-0.0523	63–70	IVSSIEQK	58
						688.83	2+	-0.0581	63–74	IVSSIEQKEESK	47
						760.77	2+	-0.1777	77–88	SEHQVELICSYR	49
						524.79	2+	-0.0024	89–97	SKIETELTK	48
						360.19	2+	0.0111	121–125	VFYYK	19

						608.24	2+	-0.0791	133–143	YLAEFSSGDAR	80
						534.21	2+	-0.1121	146–155	ATNASLEAYK	76
						611.94	3+	-0.1427	156–172	TASEIATTELPPTHPIR	27
489	gi|223674073	Chain A, Crystal Structure Of The Yeast Orthologue Of Rack1, Asc1.	33(9)	11(5)	24%	337.71	2+	0.0224	54–59	FGVPVR	31
						719.79	2+	-0.1122	91–102	LWDVATGETYQR	87
						618.79	2+	-0.0370	108–118	SDVMSVDIDKK	48
						469.20	2+	-0.1056	119–127	ASFIISGSR	57
						729.62	3+	-0.2225	156–176	VVPNEKADDDSVTIISAGNDK	40
						760.78	2+	-0.1521	162–176	ADDDSVTIISAGNDK	92
						688.81	2+	-0.0679	217–228	DGEIMLWNLAAK + Oxid (M)	77
						482.70	2+	-0.0865	312–319	VWQVFTAN	61
349	gi|6324486	alcohol dehydrogenase ADH1	46(14)	18(8)	51%	568.75	2+	-0.0749	9–18	GVIFYESHGK	41
						447.25	2+	-0.0409	23–30	DIPVPKPK	21
						507.30	2+	0.0040	31–39	ANELLINVK	63
						679.00	3+	-0.0531	61–81	LPLVGGHEGAGVVVGMGENVK + Oxid (M)	54
						418.72	2+	-0.0055	85–92	IGDYAGIK	48
						472.74	2+	-0.0310	198–207	VLGIDGGEGK	63
						809.88	2+	-0.0709	198–212	VLGIDGGEGKEELFR	85
						536.30	2+	-0.0375	225–234	EKDIVGAVLK	13
						407.73	2+	-0.0432	227–234	DIVGAVLK	44
						771.32	3+	-0.1733	235–258	ATDGGAHGVINVSVSEAAIEASTR	17
						701.84	2+	-0.0493	262–276	ANGTTVLVGMPAGAK + Oxid (M)	67
						678.29	2+	-0.0207	277–287	CCSDVFNQVVK	70
						626.31	2+	-0.0451	288–299	SISIVGSYVGNR	83
						484.72	2+	-0.0408	304–311	EALDFFAR	30
						624.99	3+	-0.1019	316–332	SPIKVVGLSTLPEIYEK	29
						724.37	2+	-0.0567	320–332	VVGLSTLPEIYEK	54
						617.97	3+	-0.0562	320–335	VVGLSTLPEIYEKMEK + Oxid(M)	20
						406.18	2+	-0.0614	342–348	YVVDTSK	25

972	gi|6324486	alcohol dehydrogenase ADH1	55(9)	19(7)	52%	568.75	2+	-0.0681	9–18	GVIFYESHGK	49
						476.19	3+	-0.2512	19–30	LEYKDIPVPKPK	25
						447.24	2+	-0.0622	23–30	DIPVPKPK	22
						507.31	2+	0.0236	31–39	ANELLINVK	68
						679.00	3+	-0.0696	61–81	LPLVGGHEGAGVVVGMGENVK + Oxid(M)	59
						418.72	2+	-0.0138	85–92	IGDYAGIK	52
						472.72	2+	-0.0574	198–207	VLGIDGGEGK	55
						809.91	2+	-0.0244	198–212	VLGIDGGEGKEELFR	76
						536.31	2+	-0.0202	225–234	EKDIVGAVLK	37
						771.34	3+	-0.1204	235–258	ATDGGAHGVINVSVSEAAIEASTR	21
						693.85	2+	-0.0420	262–276	ANGTTVLVGMPAGAK	68
						678.31	2+	0.0200	277–287	CCSDVFNQVVK	72
						626.31	2+	-0.0545	288–299	SISIVGSYVGNR	69
						484.72	2+	-0.0479	304–311	EALDFFAR	33
						936.96	2+	-0.1529	316–332	SPIKVVGLSTLPEIYEK	82
						724.39	2+	-0.0203	320–332	VVGLSTLPEIYEK	65
						926.46	2+	-0.0510	320–335	VVGLSTLPEIYEKMEK + Oxid (M)	24
						406.19	2+	-0.0396	342–348	YVVDTSK	29
996	gi|6324486	alcohol dehydrogenase ADH1	30(6)	13(3)	34%	447.27	2+	-0.0098	23–30	DIPVPKPK	18
						507.30	2+	0.0036	31–39	ANELLINVK	46
						418.68	2+	-0.0863	85–92	IGDYAGIK	28
						472.70	2+	-0.1030	198–207	VLGIDGGEGK	41
						809.90	2+	-0.0436	198–212	VLGIDGGEGKEELFR	59
						536.29	2+	-0.0486	225–234	EKDIVGAVLK	22
						407.72	2+	-0.0537	227–234	DIVGAVLK	46
						701.83	2+	-0.0697	262–276	ANGTTVLVGMPAGAK + Oxid(M)	70
						678.26	2+	-0.0842	277–287	CCSDVFNQVVK	69
						626.29	2+	-0.0831	288–299	SISIVGSYVGNR	83
						484.71	2+	-0.0630	304–311	EALDFFAR	43

						617.95	3+	-0.1382	320–335	VVGLSTLPEIYEKMEK + Oxid (M)	20
						406.19	2+	-0.0421	342–348	YVVDTSK	38
1896	gi|6322790	fructose-bisphosphate aldolase FBA1	7(1)	4(1)	11%	521.78	2+	-0.0204	86-95	GAIAAAHYIR	53
						529.72	4+	-0.1719	309-327	DYIMSPVGNPEGPEKPNKK + Oxid (M)	24
						341.14	2+	-0.0572	328-332	FFDPR	16
						376.66	2+	-0.0696	349-354	SLETFR	29
1221	gi|6322790	fructose-bisphosphate aldolase FBA1	11(3)	6(2)	16%	609.24	2+	-0.1194	74–85	GISNEGQNASIK	62
						951.40	2+	-0.0990	286–301	VNLDTDCQYAYLTGIR	51
						663.23	3+	-0.2467	309–326	DYIMSPVGNPEGPEKPNK + Oxid (M)	17
						705.97	3+	-0.1310	309–327	DYIMSPVGNPEGPEKPNKK + Oxid (M)	30
						341.17	2+	0.0137	328–332	FFDPR	21
						376.68	2+	-0.0318	349–354	SLETFR	30
1051	gi|6320255	triose-phosphate isomerase TPI1	31(9)	9(5)	37%	508.74	2+	-0.0287	4–12	TFFVGGNFK	35
						551.26	2+	-0.0975	18–26	QSIKEIVER	35
						506.27	3+	-0.0478	56–69	KPQVTVGAQNAYLK	68
						762.32	2+	-0.0892	70–84	ASGAFTGENSVDQIK	58
						997.43	2+	-0.1231	70–89	ASGAFTGENSVDQIKDVGAK	61
						548.76	2+	-0.0641	90–98	WVILGHSER	39
						416.20	2+	-0.0461	139–145	TLDVVER	44
						530.28	2+	-0.0234	196–205	LGDKAASELR	52
						799.85	2+	-0.1052	206–221	ILYGGSANGSNAVTFK	72
908	gi|871533	pyruvate decarboxylase	8(1)	3(1)	4%	503.68	2+	-0.1241	512-520	VATTGEWDK	23
						796.32	2+	-0.1618	512-525	VATTGEWDKLTQDK	67
						459.20	2+	-0.1041	555-563	LTAATNAKQ	38
702	gi|259148033	Pdc1p	11(4)	4(1)	9%	364.19	2+	0.0066	9-13	YLFER	20
						506.72	2+	-0.0321	37-44	IYEVEGMR + Oxid (M)	30
						999.37	2+	-0.1684	45-63	WAGNANELNAAYAADGYAR	91
						852.00	2+	-0.1916	128-151	MSANISETTAMITDIATAPAEIDR + 2 Oxid (M)	36

1633	gi|323347291	Ilv5p	22(9)	11(5)	29%	637.63	3+	-0.1014	47–63	GLKQINFGGTVETVYER	29
						806.86	2+	-0.0793	50–63	QINFGGTVETVYER	67
						322.65	2+	-0.0217	64–68	ADWPR	18
						399.72	2+	0.0013	71–76	LLDYFK	29
						749.33	3+	-0.0495	77–97	NDTFALDGYGSQGYGQGLNLR	29
						585.30	2+	-0.0598	98–108	DNGLNVIIGVR	87
						571.76	2+	-0.0590	116–126	AAIEDGWVPGK	53
						575.31	2+	0.0108	127–136	NLFTVEDAIK	52
						435.89	3+	-0.0489	127–137	NLFTVEDAIKR	18
						700.37	3+	-0.0603	179–197	DLTHVEPPKDLDVILVAPK	45
						805.85	2+	-0.0799	212–226	GINSSYAVWNDVTGK	76
1081	gi|51013823	YDR502C	14(3)	7(2)	20%	517.73	2+	-0.1086	66-73	LDYQQIVR	41
						679.30	3+	-0.0644	171-187	TQVTVEYEDDNGRWVPK	31
						484.21	2+	-0.0728	231-238	YFIQPSGR	29
						722.85	2+	-0.0516	239-253	FVIGGPQGDAGLTGR	79
						459.74	2+	-0.0333	293-301	SLVAAGLCK	52
						434.90	3+	-0.0066	330-340	SDDEIIEIIKK	29
						419.90	3+	-0.0440	341-351	NFDLRPGVLVK	24
	gi|6322323	Tif2p	12(4)	7(2)	17%	892.86	2+	-0.1435	36–51	GVFGYGFEEPSAIQQR	40
						582.79	2+	-0.0585	73–83	TGTFSIAALQR	89
						609.96	3+	-0.1189	84–100	IDTSVKAPQALMLAPTR + Oxid (M)	19
						592.79	2+	-0.0551	90–100	APQALMLAPTR + Oxid (M)	68
						471.75	2+	-0.0595	101–108	ELALQIQK	46
						556.78	2+	-0.0509	139–149	DAQIVVGTPGR	31
						446.22	2+	-0.0189	150–156	VFDNIQR	46
962	gi|6320432	adenylate kinase ADK1	3(1)	3(1)	12%	557.23	2+	-0.1099	20-29	GTQAPNLQER	39
						458.72	2+	-0.0730	48-56	GTQLGLEAK	50
						515.23	2+	-0.0943	122-130	VDDELLVAR	63
	gi|6323530	indolepyruvate	4(0)	3(0)	6%	506.71	2+	-0.0580	37-44	IYEVEGMR + Oxid (M)	36

		decarboxylase 1				999.37	2+	-0.1708	45-63	WAGNANELNAAYAADGYAR	47
						508.80	2+	0.0035	333-342	LLTTIADAAK	19
1640	gi|6322565	adenosine kinase	4(1)	3(1)	12%	526.91	3+	-0.1121	27-40	YSLKENDAILVDAK	17
						564.77	2+	-0.0643	60-71	LVAGGAAQNTAR	81
						600.63	3+	-0.0964	254-270	TVIFTHGVEPTVVVSSK	32
1105	gi|171529	uracil phosphoribosyltransferase (FUR1)	38(12)	12(7)	44%	544.56	3+	-0.1124	64–76	NTTRPDFIFYSDR	42
						794.91	2+	-0.0812	80–93	LLVEEGLNHLPVQK	76
						1080.9	2+	-0.1458	94–112	QIVETDTNENFEGVSFMGK + Oxid (M)	123
						452.24	2+	-0.0260	113–120	ICGVSIVR	55
						539.19	2+	-0.1100	121–130	AGESMEQGLR	84
						509.26	3+	-0.0894	141–153	ILIQRDEETALPK	65
						451.70	2+	-0.0420	146-153	DEETALPK	35
						819.88	2+	-0.0714	154–166	LFYEKLPEDISER	49
						479.73	2+	-0.0210	159–166	LPEDISER	60
						545.23	2+	-0.0782	213–221	YHAAFPEVR	36
						422.71	2+	-0.0630	222–229	IVTGALDR.G	70
474	gi|6321776	ribose phosphate diphosphokinase subunit PRS3	5(0)	3(0)	9%	473.76	2+	-0.0281	25-33	LGLQLTSSK	47
						514.77	2+	-0.0225	234-242	AAEILLENR	53
						711.78	2+	-0.1290	271-282	VVCTNTVPFEEK	32
1926	gi|6319594	Tef2p	7(1)	4(1)	6%	426.86	3+	-0.0385	370-379	FDELLEKNDR	24
						380.69	2+	-0.0370	394-401	SGDAALVK	59
						444.89	3+	-0.0670	426-437	DMRQTVAVGVIK + Oxid (M)	25
						457.78	2+	-0.0049	429-437	QTVAVGVIK	41
1029	gi|32693297	translation elongation factor 1-alpha	33(8)	15(5)	38%	447.72	2+	-0.0228	35–41	YAWVLDK	45
						568.30	2+	-0.0499	35–43	YAWVLDKLK	35
						678.33	2+	-0.0426	64–75	YQVTVIDAPGHR	61
						465.49	4+	-0.0406	64–79	YQVTVIDAPGHRDFIK	24
						970.38	3+	-0.2949	80–108	NMITGTSQADCGILIIAGGVGEFEAGISK	50
						442.77	2+	-0.0205	126–133	QLIVAVNK	35

						487.58	3+	-0.0658	126–138	QLIVAVNKMDSVK + Oxid (M)	20
						382.21	2+	-0.0196	144–149	FQEIVK	26
						791.90	2+	-0.0509	144–156	FQEIVKETSNFIK	58
						788.43	3+	-0.0034	204–224	TLLEAIDAIEQPSRPTDKPLR	11
						488.28	2+	0.0063	225–232	LPLQDVYK	53
						513.62	2+	-0.0852	233–243	IGGIGTVPVGR	59
						612.31	4+	-0.0795	244–267	VETGVIKPGMVVTFAPAGVTTEVK + Oxid (M)	29
629	gi|173214	elongation factor 3	10(1)	4(1)	4%	503.26	2+	-0.0362	10-17	VLEELFQK	52
						473.72	2+	-0.0608	18-26+	LSVATADNR	65
						683.98	3+	-0.0930	168-184	MPELIPVLSETMWDTKK + 2 Oxid (M)	25
						695.79	2+	-0.1015	197-205	ATETVDNKDIER	59
	gi|671634	Bmh1	2(1)	2(1)	11%	746.32	2+	-0.0799	30-43	TVASSGQELSVEER	76
						611.95	3+	-0.1320	156-172	TASEIATTELPPTHPIR	10
953	gi|6320781	ribosomal 60S subunit protein L12A	44(15)	5(3)	29%	364.21	2+	0.0080	12-16	YLYLR	27
						649.33	2+	-0.0564	17-31	AVGGEVGASAALAPK	106
						441.25	2+	-0.0522	32-40	IGPLGLSPK	68
						430.21	2+	-0.0692	41-48	KVGEDIAK	55
						645.79	2+	-0.0629	131-142	EILGTAQSVGCR	86
780	gi|6321522	ribosomal 60S subunit protein L11B	15(3)	6(2)	28%	757.36	2+	-0.0961	36-49	VLEQLSGQTPVQSK	72
						430.20	2+	-0.0440	76-82	AEEILER	55
						468.24	2+	-0.0562	86-92	VKEYQLR	28
						671.30	2+	-0.0714	154-164	TTKEDTVSWFK	43
						506.19	2+	-0.0938	157-164	EDTVSWFK	15
						398.85	3+	-0.0559	165-174	QKYDADVLDK	23
695	gi|6324670	ribosomal 40S subunit protein S7A	22(6)	11(5)	43%	551.30	2+	-0.0326	36–44	AELRPLQFK	29
						394.69	2+	-0.0346	48–55	EIDVAGGK	34
						492.74	2+	-0.0761	89–96	HVIFLAER	28
						442.72	2+	-0.0325	117–124	TLTAVHDK	64
						786.92	2+	-0.0512	125–138	ILEDLVFPTEIVGK	87

						576.98	3+	-0.0609	125–139	ILEDLVFPTEIVGKR	27
						832.42	2+	-0.0407	152–165	VLLDSKDVQQIDYK	53
						504.74	2+	-0.0221	158–165	DVQQIDYK	50
						729.98	3+	-0.1473	158–175	DVQQIDYKLESFQAVYNK	21
						599.78	2+	-0.0443	166–175	LESFQAVYNK	55
						650.30	2+	-0.0547	180–190	QIVFEIPSETH	50
	gi|71064104	Rps7bp	18(7)	10(5)	48%	813.40	2+	-0.1051	8–22	ILSQAPSELELQVAK	68
						733.36	2+	-0.0159	23–35	TFIDLESSSPELK	82
						492.74	2+	-0.0761	90–97	HVIFLAER	28
						442.72	2+	-0.0325	118–125	TLTAVHDK	64
						796.90	2+	-0.0234	126–139	VLEDMVFPTEIVGK + Oxid (M)	23
						832.42	2+	-0.0407	153–166	VLLDSKDVQQIDYK	53
						504.74	2+	-0.0221	159–166	DVQQIDYK	50
						729.98	3+	-0.1473	159–176	DVQQIDYKLESFQAVYNK	21
						599.78	2+	-0.0443	167–176	LESFQAVYNK	55
						638.28	2+	-0.0987	181–191	QIVFEIPSQTN	22
864	gi|6319556	E2 ubiquitin-conjugating protein UBC4	4(0)	2(0)	12%	431.21	2+	-0.0043	10-16	ELSDLER	20
						623.28	2+	-0.0769	92-102	DQWSPALTLSK	40
756	gi|172043	Egd2p	6(2)	3(1)	25%	649.77	2+	-0.0855	54-66	SAGGNYVVFGEAK	66
						426.20	2+	-0.0183	67-73	VDNFTQK	40
						782.31	3+	-0.2176	74-96	LAAAQQQAQASGIMPSNEDVATK + Oxid (M)	35
	gi|6324048	Hch1p	3(1)	1(1)	7%	597.75	2+	-0.1140	28-39	LTSLSTVSSDGK	72
884	gi|151941387	stress-seventy subfamily A protein	31(10)	11(7)	19%	607.78	2+	-0.0425	24–34	VDIIANDQGNR	65
						736.31	2+	-0.0817	35–47	TTPSFVAFTDTER	19
						812.31	2+	-0.1204	55–69	NQAAMNPSNTVFDAK + Oxid (M)	102
						705.25	2+	-0.0967	75–86	NFNDPEVQGDMK + Oxid (M)	48
						775.83	2+	-0.1215	111–124	NFTPEQISSMVLGK	67

						672.31	2+	-0.0354	125–136	MKETAESYLGAK + Oxid (M)	67
						534.73	2+	-0.0521	127–136	ETAESYLGAK	41
						632.29	3+	-0.0610	137–153	VNDAVVTVPAYFNDSQR	58
						600.29	2+	-0.0947	158–169	DAGTIAGLNVLR	87
						830.38	2+	-0.1304	170–185	IINEPTAAAIAYGLDK	96
						894.45	2+	-0.0942	170–186	IINEPTAAAIAYGLDKK	47
632	gi|6319972	Hsp70 family ATPase SSB1	11(2)	7(1)	11%	740.35	2+	-0.0525	39-51	VTPSFVAFTPEER	37
						562.24	2+	-0.0606	79-87	RFDDESVQK	56
						505.21	3+	-0.0650	79-90	RFDDESVQKDMK + Oxid (M)	28
						453.16	3+	-0.0580	80-90	FDDESVQKDMK + Oxid (M)	18
						522.25	3+	-0.0699	144-157	AVITVPAYFNDAQR	38
						593.30	2+	-0.0514	162-173	DAGAISGLNVLR	88
						577.30	3+	-0.0505	174-191	IINEPTAAAIAYGLGAGK	32
1617	gi|6324463	Zeo1p	23(7)	9(4)	67%	594.75	2+	-0.0867	8–18	AETAAQDVQQK	80
						659.80	2+	-0.0839	19–29	LEETKESLQNK	65
						609.26	2+	-0.0774	35–45	EQAEASIDNLK	44
						608.26	2+	-0.0600	46–56	NEATPEAEQVK	25
						744.34	2+	-0.0553	57–69	KEEQNIADGVEQK	61
						680.27	2+	-0.0931	58–69	EEQNIADGVEQK	52
						449.89	3+	-0.0335	70–81	KTEAANKVEETK	12
						396.72	2+	-0.0176	107–113	KIASIFN	24
						332.65	2+	-0.0682	108–113	IASIFN	16
1042	gi|6323138	Ahp1p	16(4)	7(3)	43%	463.20	2+	-0.0756	8-15	KFPAGDYK	38
						399.17	2+	-0.0331	9-15	FPAGDYK	25
						974.88	2+	-0.0936	16-32	FQYIAISQSDADSESCK	116
						553.26	2+	-0.0131	33-41	MPQTVEWSK	64
						400.20	3+	-0.0754	103-113	SLGVKDTTHIK	35
						600.73	2+	-0.0713	114-124	FASDPGCAFTK	65
						685.65	3+	-0.0819	157-176	ETNPGTDVTVSSVESVLAHL	10

758	gi|6323138	Ahp1p	15(4)	3(3)	21%	974.85	2+	-0.1491	16-32	FQYIAISQSDADSESCK	126
						561.24	2+	-0.0544	33-41	MPQTVEWSK + Oxid (M)	67
						600.75	2+	-0.0384	114-124	FASDPGCAFTK	55
759	gi|6323138	Ahp1p	9(1)	4(1)	22%	463.22	2+	-0.0392	8-15	KFPAGDYK	36
						561.23	2+	-0.0744 -	33-41	MPQTVEWSK	48
						599.82	2+	-0.0374	103-113	SLGVKDTTHIK	37
						600.76	2+	-0.0101	114-124	FASDPGCAFTK	53
316	gi|3328	Actin	29(3)	12(3)	33%	488.70	2+	-0.0452	19–28	AGFAGDDAPR	55
						599.85	2+	-0.0078	29–39	AVFPSIVGRPR	21
						609.25	2+	-0.0724	40–50	HQGIMVGMGQK + 2 Oxid (M)	52
						599.70	2+	-0.1112	51–61	DSYVGDEAQSK	68
						677.78	2+	-0.0616	51–62	DSYVGDEAQSKR	52
						994.48	2+	-0.0500	96–113	VAPEEHPVLLTEAPMNPK + Oxid (M)	33
						322.68	2+	-0.0038	178–183	LDLAGR	45
						507.71	2+	-0.0493	184–191	DLTDYLMK + Oxid (M)	35
						559.70	2+	-0.1061	197–206	GYSFSTTAER	68
						895.90	2+	-0.0824	239–254	SYELPDGQVITIGNER	62
						582.27	2+	-0.0564	316–326	EITALAPSSMK + Oxid (M)	49
						542.55	3+	-0.1008	360–373	QEYDESGPSIVHHK	22
724	gi|173058	alpha tubulin	1(1)	1(1)	2%	515.24	2+	-0.0731	114-122	EILGDVLDR	61

[a] Values between brackets indicate statistically significant peptides ($p<0.05$)

CURRICULUM VITAE

INFORMAZIONI PERSONALI

Nome	Valentina Longo
Indirizzo	via Sergi n. 6 - 73011 Alezio (LE)
Telefono	+39 348 3842000
E-mail	valentinalongo@email.it valentinalongo@unitus.it
Data e luogo di nascita	21/10/1987 - MAGLIE (LE)
Codice Fiscale	LNGVNT87R61E815N
Patente	B

ESPERIENZE LAVORATIVE

• Date	14 Ottobre 2010 – 1 Luglio 2011
• Datore di lavoro	Laboratorio di Genetica Medica c/o P.O. Vito Fazzi - ASL Lecce
Principali mansioni e attività	Tirocinio formativo (1547 ore). Attività svolte : Processamento e cariotipizzazione di colture cellulari di sangue periferico e midollare.
• Date	15 Aprile 2009 – 15 Ottobre 2009
• Datore di lavoro	Laboratorio di Chimica Organica - Università del Salento
Principali mansioni e attività	Tirocinio formativo. Attività svolte : reazioni di sintesi di eteri ed esteri.

ISTRUZIONE E FORMAZIONE

• Anno	1 Aprile 2012 – in corso
• Istituto di istruzione	Università della Tuscia Dottorato di ricerca in Genetica e Biologia cellulare, XXVII ciclo Tutor: Prof. Lello Zolla Laboratorio di proteomica e spettrometria di massa, Prof. Lello Zolla
• Qualifica conseguita	Da conseguire
• Anno	2011
• Istituto di istruzione	Facoltà di Scienze Matematiche, Fisiche e Naturali dell'Università del Salento.
• Qualifica conseguita	Abilitazione all'esercizio della professione di Biologo Sez.A.
• Anno	2011
• Istituto di istruzione	Facoltà di Scienze Matematiche, Fisiche e Naturali dell'Università del

	Salento; Corso di Laurea Specialistica in Biologia Umana.
• Qualifica conseguita	Laurea Specialistica in Biologia Umana, con discussione della Tesi sperimentale in Diagnostica molecolare delle malattie genetiche dal titolo "*Assetto cromosomico acquisito in un gruppo di pazienti con leucemia mieloide acuta*" – Votazione finale: 110 / 110 e lode.
• Anno	2009
• Istituto di istruzione	Facoltà di Scienze Matematiche, Fisiche e Naturali dell'Università del Salento; Corso di Laurea Triennale in Biotecnologie.
• Qualifica conseguita	Laurea Triennale in Biotecnologie, con discussione della Tesi sperimentale in Chimica Organica dal titolo "*Funzionalizzazione di composti organici naturali : esterificazione ed eterificazione*" - Votazione finale : 110 / 110 e lode.
• Anno	2006
• Istituto di istruzione	Liceo Scientifico Statale "Q.Ennio" di Gallipoli (LE).
• Qualifica conseguita	Diploma di Maturità Scientifica con votazione 100 / 100.

CAPACITÀ E COMPETENZE PERSONALI

MADRELINGUA	ITALIANO
ALTRE LINGUE	
	INGLESE
• Capacità di lettura	BUONO
• Capacità di scrittura	BUONO
• Capacità di espressione orale	BUONO
	FRANCESE
• Capacità di lettura	BUONO
• Capacità di scrittura	ELEMENTARE
• Capacità di espressione orale	ELEMENTARE

COMPETENZE TECNICHE

- **Conoscenze informatiche** : utilizzo dei principali sistemi operativi Windows (9x, ME, 2000, XP, Vista, Seven). Utilizzo del Pacchetto applicativo Microsoft Office (Word, Excel, Power Point). Utilizzo dei principali browser per la navigazione internet (Internet Explorer, Mozilla Firefox, Google Chrome) e dei principali client di posta elettronica (Outlook Express, Microsoft Outlook).
- **Software di Laboratorio :** CHEM Draw; MacKtype v. 5.5.4 della Applied Imaging; Image Lab™ Software Bio-rad; Progenesis SameSpot Nonlinear.

• **Strumentazione tecnica :** Sprettrofotometro infrarosso a trasformata di Fourier, mod. FTS 2000 serie Scimitar della Digilab; Spettrometro di massa Agilent Technologies, composto da gascromatografo mod. 6850 s. II e spettrometro di massa mod. 5973; Gascromatografo HP serie 6890; ChemiDoc Bio-rad; EXQuest Spot Cutter Bio-rad;HPLC; nano-HPLC; spettrometri di massa ESI-IT, MALDI-TOF TOF, microTOF-Q, RR-RP-HPLC.

COMPETENZE SPECIFICHE

- Tecniche separative HPLC nano-HPLC; identificazione di proteine e metaboliti attraverso spettrometria di massa (analisi metabolomica e proteomica); SDS-PAGE; IEF; 2D-SDS-PAGE; immunoblotting.

PUBBLICAZIONI SCIENTIFICHE

- Longo V, Marrocco C, Zolla L, Rinalducci S. Label-free quantitation of phosphopeptide changes in erythrocyte membranes: towards molecular mechanisms underlying deformability alterations in stored red blood cells. Haematologica. (2014) 99: 122-125

- Longo V, D'alessandro A, Zolla L. Deoxygenation of leucofiltered erythrocyte concentrates preserves proteome stability during storage in the blood bank. Blood Transfus. (2014) 19:1-6

- Lana A, Longo V, Dalmasso A, D'Alessandro A, Bottero MT, Zolla L. Omics integrating physical techniques: aged Piedmontese meat analysis. Food Chemistry. (2015) 172:731–741

- Rinalducci S, Longo V, Ceci LR, Zolla L. Targeted quantitative phosphoproteomic analysis of erythrocyte membranes during blood bank storage. Journal of Mass Spectrometry. (2015) 50(2):326-335

- Ždralević M. and Longo V., Guaragnella N., Giannattasio S., Timperio A.M., Zolla L. Differential proteome-metabolome profiling of YCA1-knock-out and wild type cells reveals novel metabolic pathways and cellular processes dependent on the yeast metacaspase. Molecular Biosystem. 2015 Feb 20. [Epub ahead of print]

- Longo V. and Lana A., Bottero M.T., Zolla L. The search for clues about the duality apoptosis/autophagy in aging meat : the "omic" witness. Journal of proteomic research. 2015 (in press)

ABSTRACT

- ItPA Padova 18-21 Giugno 2013:
  Native protein complexes in the cytoplasm of Red Blood Cells.
  Valeria Pallotta, Sara Rinalducci, Cristina Marrocco, Valentina Longo, Lello Zolla

- ItPa Napoli 24-27 Giugno 2014
  Proteomic study on the role of metacaspase YCA1 in programmed cell death in *Saccharomyces cerevisiae*.
  Valentina Longo, Maša Ždralevi´, Sergio Giannattasio, Anna Maria Timperio, Lello Zolla

Targeted label-free quantitative phosphoproteomic analysis of erythrocyte membranes during blood bank storage.
Valentina Longo, Cristina Marrocco, Lello Zolla, Rinalducci Sara

Extended aging period promotes tenderness of beef from Piedmontese cull cattles: an 'omic' view integrating classical physical studies.
Alessandro Lana, Valentina Longo, Angelo D'Alessandro, Maria Teresa Bottero, Alberto Brugiapaglia, Lello Zolla

COMUNICAZIONI ORALI

- Incontro di Scienza delle separazioni 12 Dicembre 2014
  Analisi fosfoproteomica quantitativa delle proteine di membrana di globuli rossi durante la conservazione in sacca dei concentrati eritrocitari
  Valentina Longo, Cristiana Mirasole, Sara Rinalducci e Lello Zolla

- Incontro di Scienza delle separazioni 12 Dicembre 2014
  Analisi fosfoproteomica quantitativa delle proteine di membrana di globuli rossi durante la conservazione in sacca dei concentrati eritrocitari
  Valentina Longo, Cristiana Mirasole, Sara Rinalducci e Lello Zolla

PARTECIPAZIONE A CONVEGNI

12 Giugno 2012 -15 Giugno 2012

- VII congresso nazionale ItPA (Italian Proteomic Association), Viterbo.

12 Dicembre 2014

- Incontri di Scienza delle Separazioni: Stato dell'arte e innovazioni delle tecniche separative in campo agroalimentare, biomedico e ambientale – Gruppo Interdivisionale di Scienza delle Separazioni – Società Chimica Italiana - Roma

IN OTTEMPERANZA ALLA LEGGE SULLA PRIVACY N. 675/96,
AUTORIZZO IL TRATTAMENTO DEI MIEI DATI PERSONALI